Electronic Supplementary Information

Ambient-Pressure Selective Hydrogenation of Unsaturated Aldehydes and Ketones into Unsaturated Alcohols in Water Phase

Contents

I. General information

All manipulations were carried out under a dry Ar or N_2 atmosphere by using Schlenk line and glovebox techniques. Organic solvents such as toluene, *n*-hexane and tetrahydrofuran (THF) were dried by refluxing with sodium/potassium benzophenone under N_2 prior to use. $CDCl_3$ and 1,4-dioxane was distilled from CaH_2 and kept in the glovebox for use. Ligands $(CH_2NH_2)_2$, $(CH_2NHMe)_2$ and $(CH_2NHEt)_2$ were purchased from J&K Scientific Ltd. and used as received. Compounds *o*-$PPh_2C_6H_4NHMe$[1], *o*-$PPh_2C_6H_4NMe_2$[2], $RuCl_2(DMSO)_4$[3] and (*o*-$PPh_2C_6H_4NMe_2$)(PPh_3)$RuCl_2$[4] were prepared according to the literatures. ^1H, $^{13}C\{^1H\}$, and $^{31}P\{^1H\}$ NMR spectra were measured on a Bruker AVIII-500 or a Bruker AVIII-400 spectrometer with chemical shifts (δ) referenced to the residual solvent signal. The chemical shifts for protons and carbons were reported using TMS (0.05%) as the internal reference (δ = 0 ppm). Solid state ^{31}P (162 MHz) NMR spectra were measured on a Bruker AVIII SS-400 spectrometer. Infrared (IR) spectra were recorded using a Nicolet FT-IR 330 spectrometer. Elemental analysis was performed on a Thermo Quest Italia SPA EA 1110 instrument.

II. Experimental section

General procedure for activity tests

The hydrogenation reactions were performed in a 25 mL stainless-steel autoclave equipped with a quartz lining (Anhui Kemi Machinery Technology Co., Ltd). Generally, ruthenium complex, NaOH, substrate, and dodecane (internal standard) were added into an autoclave in the glovebox. The autoclave was sealed and transferred out of the glovebox, the solvent water was injected under the protection of nitrogen. Then, the autoclave was flushed with hydrogen three times, and pressurized with hydrogen (10 atm). After stirring at 40 °C for 2 h, the autoclave was cooled to approximately 5 °C using an ice bath and slowly depressurized. The reaction solution was extracted with ether (3 × 2 mL), and the combined organic phase was dried over Na_2SO_4, passed through a short silica column, analyzed by gas chromatography (GC, SHANGHAI INSTRUMENT, 9310-VI) equipped with a KB-Wax column (30 m × 0.32 mm × 0.33 μm) and a flame ionization detector (FID). The injector and detector temperature were 250 °C. Program used: 80 °C for 5 minutes and then ramped to 200 °C at 10 °C/min, and maintained for 20 minutes. The conversion of carbonyl substrates and the yield of alcohols were calculated using dodecane as the internal standard.

Procedure for gram-scale tests

The reaction was performed as described above but with a 50 mL stainless-steel autoclave, followed by heating at 100 °C. The reaction solution was evaporated to dryness under reduced pressure at room temperature, diluted with ether, passed through a short silica column and analyzed by GC.

General procedure for isolation

For isolation and purification, the combined ether phase was dried over Na_2SO_4, concentrated , and filtered by silica gel column chromatography (hexane-ethyl acetate as eluent, 20/1 ratio). Then, the solvent was removed under reduced pressure to afford the corresponding alcohol products. The purity was verified using NMR spectroscopy.

III. Synthetic details

Synthesis of (*o*-$Ph_2PC_6H_4NHMe$)$RuCl_2(DMSO)_2$ (9) A mixture of $RuCl_2(DMSO)_4$ (0.48 g, 1.0 mmol) and *o*-$PPh_2C_6H_4NHMe$ (0.29 g, 1.0 mmol) in THF (40 mL) was added into a Schlenk flask (100 mL) in the glovebox. The flask was sealed and transferred out of the glovebox, and heated to 70 °C for 12 h. During the reaction, a brick-red solid was gradually formed. After the reaction and cooling to room temperature, the brick-red solid of compound **9** was collected by filtration and washed with *n*-hexane (2 mL). Yield: 0.40 g, 64%. During to insolubility in organic solvents, the solid state ^{31}P NMR spectrum was recorded.

^{31}P NMR (162 MHz, in solid, 298 k, ppm): δ = 66.41 (br).

IR (Nujol mull, KBr, cm^{-1}): ν = 3139 (NH).

Anal. Calcd (%) for $RuCl_2C_{23}H_{30}NPS_2O_2$ (M_r = 619.7): C 44.57, N 2.26, H 4.88, S 10.33; found: C 45.03, N 2.18, H 5.07, S 10.15.

Synthesis of (*o*-$PPh_2C_6H_4NHMe$)[$NH_2(CH_2)_2NH_2$]$RuCl_2$ (10) A mixture of **9** (185.9 mg, 0.3 mmol) and $NH_2(CH_2)_2NH_2$ (18.0 mg, 0.3 mmol) in 1,4-dioxane (30 mL) was added into a Schlenk flask (100 mL) in the glovebox. The flask was sealed and transferred out of the glovebox, and heated to 101 °C for 4 d. During the reaction, solid precipitate was gradually formed. After the reaction and cooling to room temperature, the off-white solid of compound **10** was collected by filtration and washed with *n*-hexane (2 mL). Yield: 0.14 g, 89%. During to insolubility in organic solvent, the solid state ^{31}P NMR spectrum was recorded.

^{31}P NMR (162 MHz, in solid, 298 k, ppm): δ = 63.98 (br).

IR (Nujol mull, KBr, cm^{-1}): v = 3088, 3114, 3192, 3251 (NH, NH_2).

Anal. Calcd (%) for $RuCl_2C_{21}H_{26}N_3P$ (M_r = 523.40): C 48.19, N 8.03, H 5.01; found: C 47.81, N 8.27, H 5.16.

Synthesis of (*o*-$PPh_2C_6H_4NHMe$)[$MeNH(CH_2)_2NHMe$]$RuCl_2$ (11) A mixture of **9** (185.9 mg, 0.3 mmol) and $(CH_2NHMe)_2$ (26.5 mg, 0.3 mmol) in THF (30 mL) was added into a Schlenk flask (100 mL) in the glovebox. The flask was sealed and transferred out of the glovebox, and heated to 70 °C for 4 d. During the reaction, a yellow-green solution was gradually formed. After the reaction and cooling to room temperature, the solution was concentrated to ca. 1 mL, and *n*-hexane (5 mL) was added. A yellow-green precipitate of **11** was quickly formed, which was collected and washed with *n*-hexane (2 mL). Yield: 91.0 mg, 55%.

^{1}H NMR plus ^{1}H-^{13}C HSQC (500 MHz, $CDCl_3$, 298 k, ppm): δ = 2.22 (br), 2.38 (d, J_{HH} = 5.0 Hz), 2.79 (d, J_{HH} = 5.0 Hz), 3.69 (br), 4.81 (m), 5.29 (m) (3 H, N*H*), 2.59 (d, J_{HH} = 5.0 Hz, 3 H, CH_3), 2.68 (d, J_{HH} = 15.0 Hz, 1 H, CH_2), 2.73 (d, J_{HH} = 10.0 Hz, 3 H, CH_3), 2.91 (m, 1 H, CH_2), 3.10 (d, J_{HH} = 5.0 Hz, 3 H, CH_3), 3.13-3.23 (m, 2 H, CH_2), 7.21 (t, J_{HH} = 7.5 Hz), 7.24-7.43 (m), 7.72 (br), 7.85 (t, J_{HH} = 7.5 Hz), 7.95 (t, J_{HH} = 10 Hz) (14 H, C_6H_4 and *Ph*).

^{13}C{^{1}H} NMR (125 MHz, $CDCl_3$, 298 k, ppm): δ = 36.74 (s, 1 C, *C*H_3), 44.40 (s, 1 C, *C*H_3), 47.69 (s, 1 C, *C*H_3), 53.43 (d, 1 C, *C*H_2), 54.52 (s, 1 C, *C*H_2), 123.86 (d, J_{PC} = 8.8 Hz), 127.10 (s), 127.57 (d, J_{PC} = 5.0 Hz), 127.60 (d, J_{PC} = 2.5 Hz), 127.81 (s), 128.25 (d, J_{PC} = 8.8 Hz), 128.74 (s), 129.74 (s), 130.16 (s), 132.20 (s), 132.63 (d, J_{PC} = 10.0 Hz), 134.68 (d, J_{PC} = 10.0 Hz), 136.97 (t, J_{PC} = 38.8 Hz), 157.81 (d, J_{PC} = 17.5 Hz) (*C*$_6$H$_4$ and *Ph*).

^{31}P{^{1}H} NMR (202 MHz, $CDCl_3$, 298 k, ppm): δ = 65.80 (s).

IR (Nujol mull, KBr, cm^{-1}): ν = 3142, 3192, 3212 (NH).

Anal. Calcd (%) for $RuCl_2C_{23}H_{30}N_3P$ (M_r = 551.1): C 50.13, N 7.63, H 5.49; found: C 49.87, N 7.46, H 5.63.

Synthesis of (*o*-$PPh_2C_6H_4NHMe$)[$EtNH(CH_2)_2NHEt$]$RuCl_2$ (12) A mixture of **9** (185.9 mg, 0.3 mmol) and $(CH_2NHEt)_2$ (34.9 mg, 0.3 mmol) in THF (30 mL) was added into a Schlenk flask (100 mL) in the glovebox. The flask was sealed and transferred out of the glovebox, and heated to 70 °C for 2 d. During the reaction, a yellow solution was gradually formed. After the reaction and cooling to room temperature, the solution was concentrated to ca. 1 mL, and *n*-hexane (5 mL) was added. A large amount of solid was quickly formed, which was collected and subjected to recrystallization in toluene at -20 °C, giving earthy-yellow precipitate of **12**. Yield: 80.0 mg, 46%.

^{1}H NMR plus ^{1}H-^{13}C HSQC (500 MHz, $CDCl_3$, 298 k, ppm): δ = 0.89 (t, J_{HH} = 5.0 Hz, 3 H, CH_3), 1.09 (t, J_{HH} = 5.0 Hz, 3 H, CH_3), 2.44 (m, 1 H, CH_2), 2.52 (d, J_{HH} = 5.0 Hz, 3 H, CH_3), 2.62 (m, 1 H, CH_2), 2.79 (m, 1 H, CH_2), 2.96 (m, 2 H, CH_2), 3.30 (m, 1 H, CH_2), 3.46 (m, 1 H, NH), 3.48 (m, 1 H, CH_2), 3.62 (t, J_{HH} = 10.0 Hz, 1 H, CH_2), 4.44 (br, 1 H, NH), 5.47 (d, J_{HH} = 5.0 Hz, 1 H, NH), 7.21 (m), 7.24 (br), 7.25-7.27 (m), 7.32 (m), 7.36 (m), 7.38 (s), 7.40 (m), 7.42 (m), 7.46 (m), 7.71 (t, J_{HH} = 5.0 Hz) (14 H, C_6H_4 and *Ph*).

^{13}C{^{1}H} NMR (125 MHz, $CDCl_3$, 298 k, ppm): δ = 13.69 (s, 1 C, *C*H_3), 14.32 (s, 1 C, *C*H_3), 43.66 (s, 1 C, *C*H_2), 47.57 (s, 1 C, *C*H_2), 48.48 (s, 1 C, *C*H_3), 49.67 (s, 1 C, *C*H_2), 51.80 (s, 1 C, *C*H_2), 123.60 (s), 123.76 (d, J_{PC} = 8.8 Hz), 126.54 (s), 127.04 (d, J_{PC} = 5.0 Hz), 127.60 (d, J_{PC} = 8.8 Hz), 127.65(d, J_{PC} = 16.3 Hz), 128.20 (d, J_{PC} = 8.8 Hz), 128.92 (d, J_{PC} = 5.0 Hz), 129.26 (d, J_{PC} = 120.0 Hz), 129.57 (d, J_{PC} = 133.8 Hz), 131.19 (d, J_{PC} = 256.3 Hz), 132.70 (d, J_{PC} = 8.8 Hz), 133.56 (d, J_{PC} = 123.8 Hz), 134.56 (d, J_{PC} = 11.3 Hz), 135.32 (d, J_{PC} = 32.5 Hz), 136.63 (d, J_{PC} = 43.8 Hz), 137.11 (d, J_{PC} = 36.3 Hz), 142.82 (d, J_{PC} = 18.8 Hz) (*C*$_6$H$_4$ and *Ph*).

^{31}P{^{1}H} NMR (202 MHz, $CDCl_3$, 298 k, ppm): δ = 61.96 (s).

IR (Nujol mull, KBr, cm^{-1}): ν = 3136, 3189, 3212 (NH).

Anal. Calcd (%) for $RuCl_2C_{25}H_{34}N_3P$ (M_r = 579.5): C 51.81, N 7.25, H 5.91; found: C 52.37, N 6.95, H 6.12.

Synthesis of (*o*-$PPh_2C_6H_4NMe_2$)[$EtNH(CH_2)_2NHEt$]$RuCl_2$ (13) A mixture of (*o*-$PPh_2C_6H_4NMe_2$)(PPh_3)$RuCl_2$ (147.9 mg, 0.2 mmol) and $(CH_2NHEt)_2$ (23.2 mg, 0.2 mmol) in THF (30 mL) was added into a Schlenk flask (100 mL) in the glovebox. The flask was sealed and transferred out of the glovebox, and heated to 65 °C for 2 d. During the reaction, a brown solution was gradually formed. After the reaction and cooling to room temperature, the solution was concentrated to ca. 1 mL, and *n*-hexane (5 mL) was added. A large amount of solid was quickly formed, which was collected and subjected to recrystallization in toluene/n-hexane (4 mL/2 mL) at -20 °C, giving yellow precipitate of **13**. Yield: 90.2 mg, 76%.

^{1}H NMR plus ^{1}H-^{13}C HSQC (500 MHz, $CDCl_3$, 298 k, ppm): δ = 0.77 (t, J_{HH} = 5.0 Hz, CH_3), 0.79 (t, J_{HH} = 5.0 Hz, CH_3), 1.49 (t, J_{HH} = 5.0 Hz, CH_3), 1.51 (t, J_{HH} = 5.0 Hz, CH_3), 2.51 (s, CH_3), 2.66 (s, CH_3), 3.15 (s, CH_3), 3.19 (s, CH_3), 2.74-3.07 (m), 3.42-3.53 (m), 3.74 (m), 4.11 (m), 4.45 (br) (N*H* and CH_2), 7.13-7.19 (m), 7.22-7.39 (m), 7.45 (m), 7.53 (m), 7.25-7.27 (m), 7.82 (m) (C_6H_4 and *Ph*).

^{13}C{^{1}H} NMR (125 MHz, $CDCl_3$, 298 k, ppm): δ = 14.06 (s), 14.49 (s), 14.50 (s), 14.81 (s), 45.23 (s), 45.42 (s), 47.53 (s), 47.90 (s), 48.65 (s), 49.52 (s), 51.05 (s), 51.14 (s), 51.15 (s), 52.92 (s), 60.54 (s), 60.59 (s) (*C*H_2 and *C*H_3), 118.37 (d, J_{PC} = 8.8 Hz), 119.26 (d, J_{PC} = 10.0 Hz), 125.30 (s), 125.82 (d, J_{PC} = 5.0 Hz), 126.02 (d, J_{PC} = 5.0Hz), 127.82 (d, J_{PC} = 133.8 76.3Hz), 127.58 (s), 127.66 (d, J_{PC} = 3.8 Hz), 127.75 (s), 128.16 (d, J_{PC} = 8.8 Hz), 128.22 (s), 128.96 (s), 129.03 (s), 129.31 (d, J_{PC} = 52.5 Hz), 130.39 (s), 130.80 (s), 132.60 (s), 133.15 (d, J_{PC} = 8.8 Hz), 133.38 (d, J_{PC} = 12.5 Hz), 133.65 (s), 133.75 (d, J_{PC} = 10.0 Hz), 134.12 (d, J_{PC} = 10.0 Hz), 134.30 (d, J_{PC} = 8.8 Hz), 136.08 (d, J_{PC} = 36.3 Hz), 136.19 (d, J_{PC} = 38.8Hz), 136.85 (d, J_{PC} = 38.8Hz), 137.32 (d, J_{PC} = 38.8Hz), 163.47 (d, J_{PC} = 16.3Hz), 164.53 (d, J_{PC} = 17.5Hz) (*C*$_6$H$_4$ and *Ph*).

^{31}P{^{1}H} NMR (202 MHz, $CDCl_3$, 298 k, ppm): δ = 61.75 (s), 64.32 (s).

IR (Nujol mull, KBr, cm^{-1}): ν = 3164, 3192 (NH).

Anal. Calcd (%) for $RuCl_2C_{26}H_{36}N_3P$ (M_r = 593.5): C 52.61, N 7.08, H 6.11; found: C 52.67, N 6.95, H 6.17.

IV. X-ray crystallographic analysis

X-ray crystallographic analysis of 11: Crystallographic data for **11** was collected at 173 K on an Agilent Super Nova system using Mo-K_α radiation (λ = 0.71073 Å). Intensity measurements were performed on a rapidly cooled crystal with dimensions of 0.10 × 0.05 × 0.05 mm^3 in the range 6.9° < 2θ < 49.998°. The data completeness collected was 99.8 %. Absorption correction was applied using the spherical harmonic program (multi-scan type). The structure was solved by direct method (SHELXS-96)[5] and refined against F^2 using SHELXL-97 program.[6] In general, non-hydrogen atoms were located from different Fourier synthesis and refined anisotropically, and hydrogen atoms were included using a riding mode with U_{iso} tied to the U_{iso} of the parent atom unless otherwise specified. Crystal data for **11**: $C_{24}H_{31}Cl_5N_3PRu$, M_r = 670.81, monoclinic, space group $P2(1)/n$, a = 11.8765(4), b = 11.6572(3), c = 20.7114(7) Å, α = 90°, β = 97.282(3)°, γ = 90°, V = 2844.30(16) Å^3, Z = 4, ρ_{calcd} = 1.567 g·cm^{-3}, $\mu(Mo_{K\alpha})$ = 1.096 mm^{-1}, $F(000)$ = 1360; 11354 measured reflections, 5001 independent (R_{int} = 0.0294). The final refinements converged at R_1 = 0.0312 and wR_2 = 0.0742 for $I > 2\sigma(I)$ and R_1 = 0.0370 and wR_2 = 0.0778 for all data. The goodness of fit (GOF) is 1.034. Fourier synthesis gave a min/max residual electron density –1.62/1.00 e Å^3. CCDC-2384770 contains the supplementary crystallographic data. The data can be obtained free of charge from the Cambridge Crystallographic Data Centre via www.ccdc.cam.ac.uk/data_request/cif.

X-ray crystallographic analysis of 12: Crystallographic data for **12** was collected at 125 K on an Agilent Super Nova system using graphite-monochromated Cu-K_α radiation (λ = 1.54184 Å). Intensity measurements were performed on a rapidly cooled crystal with dimensions of 0.1 × 0.05 × 0.05 mm^3 in the range 7.442° < 2θ < 129.966°. The data completeness collected was 96.6 %. Absorption correction was applied using the spherical harmonic program (multi-scan type). The structure was solved by direct method (SHELXS-96)[5] and refined against F^2 using SHELXL-97 program.[6] In general, non-hydrogen atoms were located from different Fourier synthesis and refined anisotropically, and hydrogen atoms were included using a riding mode with U_{iso} tied to the U_{iso} of the parent atom unless otherwise specified. Crystal data for **12**: $C_{54}H_{76}Cl_4N_6OP_2Ru_2$, M_r = 1231.08, triclinic, space group P-1, a = 11.2337(17), b = 11.6564(17), c = 11.8853(15) Å, α = 88.336(11)°, β = 89.350(12)°, γ = 76.815(13)°, V = 1514.6(4) Å^3, Z = 1, ρ_{calcd} = 1.350 g·cm^{-3}, $\mu(Cu_{K\alpha})$ = 6.468 mm^{-1}, $F(000)$ = 636; 8644 measured reflections, 4976 independent (R_{int} = 0.1404). The final refinements converged at R_1 = 0.1251 and wR_2 = 0.2891 for $I > 2\sigma(I)$ and R_1 = 0.1771 and wR_2 = 0.3539 for all data. The goodness of fit (GOF) is 0.979. Fourier synthesis gave a min/max residual electron density –

1.55/3.34 e Å^3. CCDC-2384771 contains the supplementary crystallographic data. The data can be obtained free of charge from the Cambridge Crystallographic Data Centre via www.ccdc.cam.ac.uk/data_request/cif.

X-ray crystallographic analysis of 13: Crystallographic data for **13** was collected at 100 K on an Agilent Super Nova system using graphite-monochromated Cu-K_α radiation (λ = 1.54178 Å). Intensity measurements were performed on a rapidly cooled crystal with dimensions of 0.02 × 0.02 × 0.02 mm^3 in the range 7.774° < 2θ < 143.772°. The data completeness collected was 96.6%. Absorption correction was applied using the spherical harmonic program (multi-scan type). The structure was solved by direct method (SHELXS-96)[5] and refined against F^2 using SHELXL-97 program.[6] In general, non-hydrogen atoms were located from different Fourier synthesis and refined anisotropically, and hydrogen atoms were included using a riding mode with U_{iso} tied to the U_{iso} of the parent atom unless otherwise specified. Crystal data for **13**: $C_{66}H_{88}Cl_4N_6P_2Ru_2$, M_r = 1371.30, triclinic, space group P-1, a = 12.2517(10), b = 15.2233(12), c = 19.4390(14) Å, α = 73.615(7)°, β = 79.904(7)°, γ = 68.630(7)°, V = 3228.5(5) Å^3, Z = 2, ρ_{calcd} = 1.411 g·cm^{-3}, $\mu(Cu_{K\alpha})$ = 6.117 mm^{-1}, F(000) = 1424; 22325 measured reflections, 12211 independent (R_{int} = 0.0671). The final refinements converged at R_1 = 0.0453 and wR_2 = 0.0981 for $I > 2\sigma(I)$ and R_1 = 0.0718 and wR_2 = 0.1107 for all data. The goodness of fit (GOF) is 1.014. Fourier synthesis gave a min/max residual electron density –0.69/1.04 e Å^3. CCDC-2384772 contains the supplementary crystallographic data. The data can be obtained free of charge from the Cambridge Crystallographic Data Centre via www.ccdc.cam.ac.uk/data_request/cif.

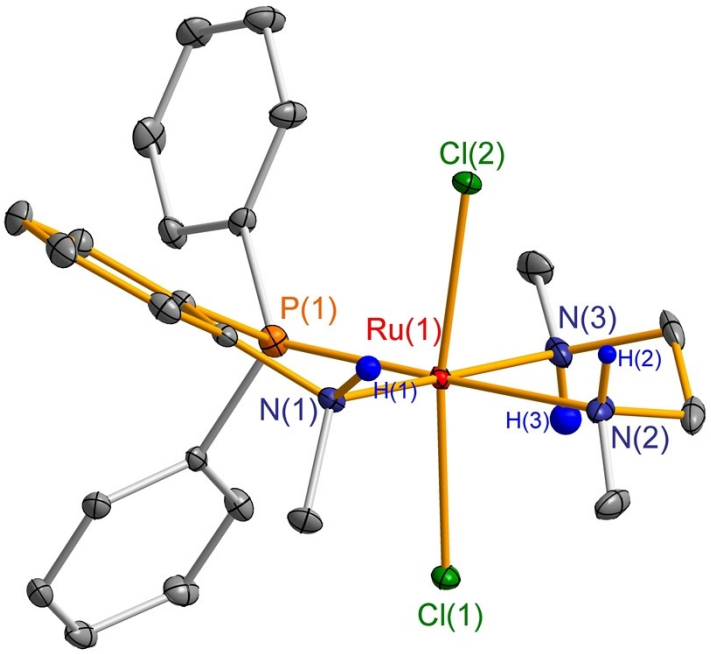

Fig. S1 X-ray crystal structure of **11** with thermal ellipsoids at 30% probability level. Hydrogen atoms except for H(1), H(2) and H(3) are omitted for clarity. Selected bond lengths [Å] and angles [°] for **11**: Ru(1)–P(1) 2.2234(7), Ru(1)–N(1) 2.164(2), Ru(1)–N(2) 2.212(3), Ru(1)−N(3) 2.115(3), Ru(1)−Cl(1) 2.4078(7), Ru(1)−Cl(2) 2.4132(7); P(1)–Ru(1)–N(1) 82.07(7), N(2)–Ru(1)–N(3) 81.30(10).

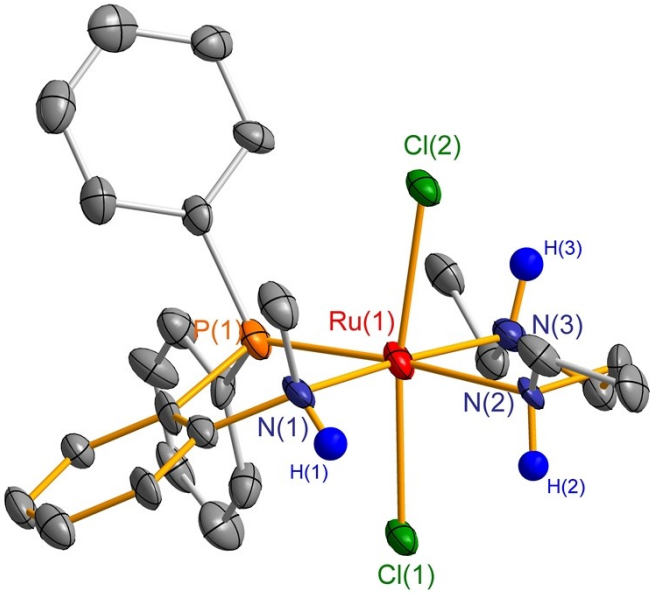

Fig. S2 X-ray crystal structure of **12** with thermal ellipsoids at 30% probability level. Hydrogen atoms except for H(1), H(2) and H(3) are omitted for clarity. Selected bond lengths [Å] and angles [°] for **12**: Ru(1)–P(1) 2.243(3), Ru(1)–N(1) 2.177(11), Ru(1)−N(2) 2.215(9), Ru(1)−N(3) 2.154(11), Ru(1)−Cl(1) 2.417(3), Ru(1)−Cl(2) 2.415(3); P(1)–Ru(1)–N(1) 82.1(3), N(2)–Ru(1)–N(3) 82.2(4).

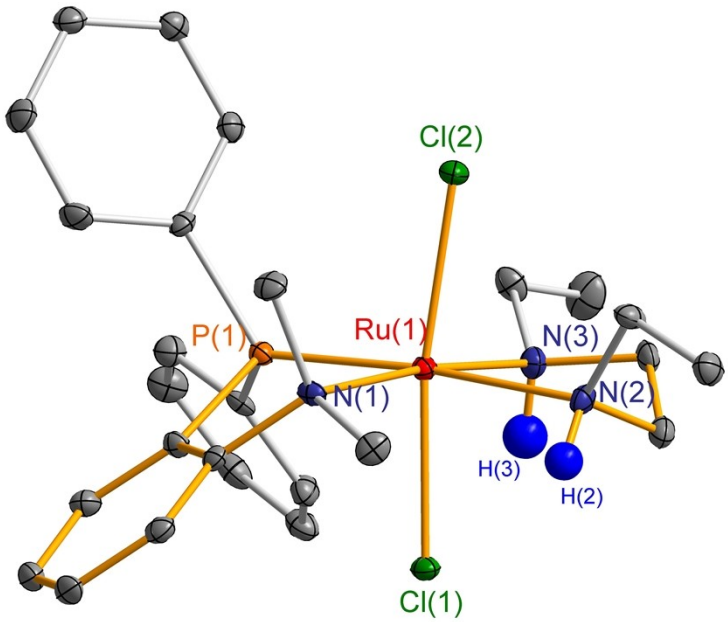

Fig. S3 X-ray crystal structure of **13** with thermal ellipsoids at 30% probability level. Hydrogen atoms except for H(2) and H(3) are omitted for clarity. Selected bond lengths [Å] and angles [°] for **13**: Ru(1)–P(1) 2.2261(11), Ru(1)–N(1) 2.246(3), Ru(1)–N(2) 2.229(3), Ru(1)−N(3) 2.143(4), Ru(1)−Cl(1) 2.4249(10), Ru(1)−Cl(2) 2.4093(10); P(1)–Ru(1)–N(1) 80.38(10), N(2)–Ru(1)–N(3) 81.29(15).

V. Activity tests

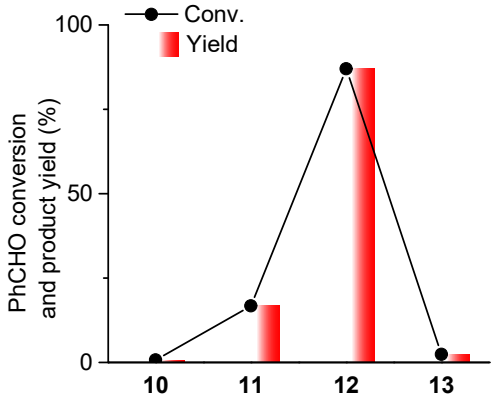

Fig. S4 Catalytic hydrogenation of benzaldehyde into benzyl alcohol by ruthenium complexes **10**-**13** in water. Reaction condition: 2.0 mmol benzaldehyde, 0.1 mol% ruthenium, 1.0 mol% NaOH, 2 mL H_2O, 10 atm H_2, 40 °C, 1 h. The conversion of benzaldehyde and the yield of benzyl alcohol were analyzed by GC.

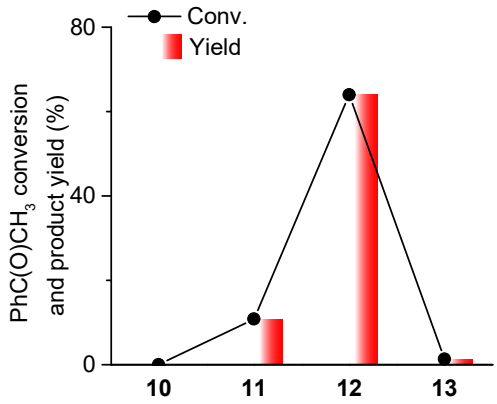

Fig. S5 Catalytic hydrogenation of acetophenone into 1-phenylethanol by ruthenium complexes **10-13** in water. Reaction condition: 2.0 mmol acetophenone, 0.1 mol% ruthenium, 1.0 mol% NaOH, 2 mL H_2O, 10 atm H_2, 40 °C, 1 h. The conversion of acetophenone and the yield of 1-phenylethanol were analyzed by GC.

Table S1 Hydrogenation of cinnamaldehyde into cinnamyl alcohol by ruthenium complex **12** in different solvents.

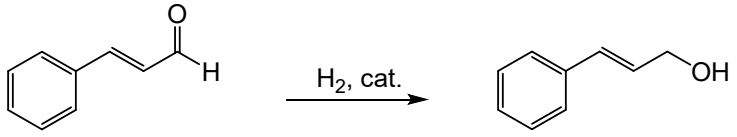

CAL COL

Entry	Solvent	Conv. of CAL (%)	Yield of COL (%)
1	*i*-PrOH	99	98
2	*n*-PrOH	97	83
3	MeOH	95	82
4	EtOH	70	58
5	Toluene	7	7
6	THF	61	61
7	1,4-dioxane	9	9
8[a]	H_2O	65	64
9	CH_3CN	2	2

Reaction conditions: 2.0 mmol cinnamyl aldehyde, 0.1 mol% **12**, 1.0 mol% NaOMe, 2 mL solvent, 10 atm H_2, 40 °C, 1 h. The conversion of CAL and the yield of COL were analyzed by GC. [a] 1.0 mol% NaOH.

Table S2 Hydrogenation of cinnamaldehyde into cinnamyl alcohol by **12** in *i*-PrOH.

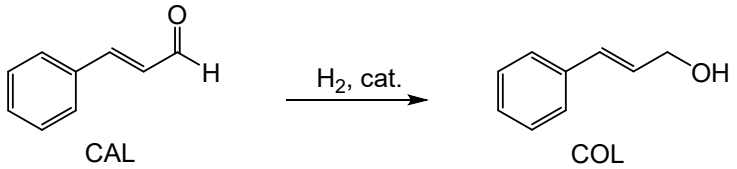

CAL COL

Entry	Ru (mol%)	T (°C)	$p(H_2)$ (atm)	Time (h)	Conv. of CAL (%)	Yield of COL (%)
1	0.1	40	10	1	99	98
2	0.1	40	1	2	96	94
3	0.1	RT	20	6	93	92
4	0.1	RT	1	10	53	51
5[a]	0.05	40	10	2	27	27
6[a]	0.05	60	10	2	98	98
7[b]	0.02	100	30	6	89	88
8[c]	0.01	100	50	16	90	89

Reaction conditions: 2.0 mmol cinnamaldehyde, 2 mL *i*-PrOH, n(NaOMe)/n(Ru) = 10. The conversion of CAL and the yield of COL were analyzed by GC. [a] 4.0 mmol cinnamaldehyde. [b] 10.0 mmol cinnamaldehyde, 4 mL *i*-PrOH. [c] 20.0 mmol cinnamaldehyde, 6 mL *i*-PrOH.

VI. NMR spectra

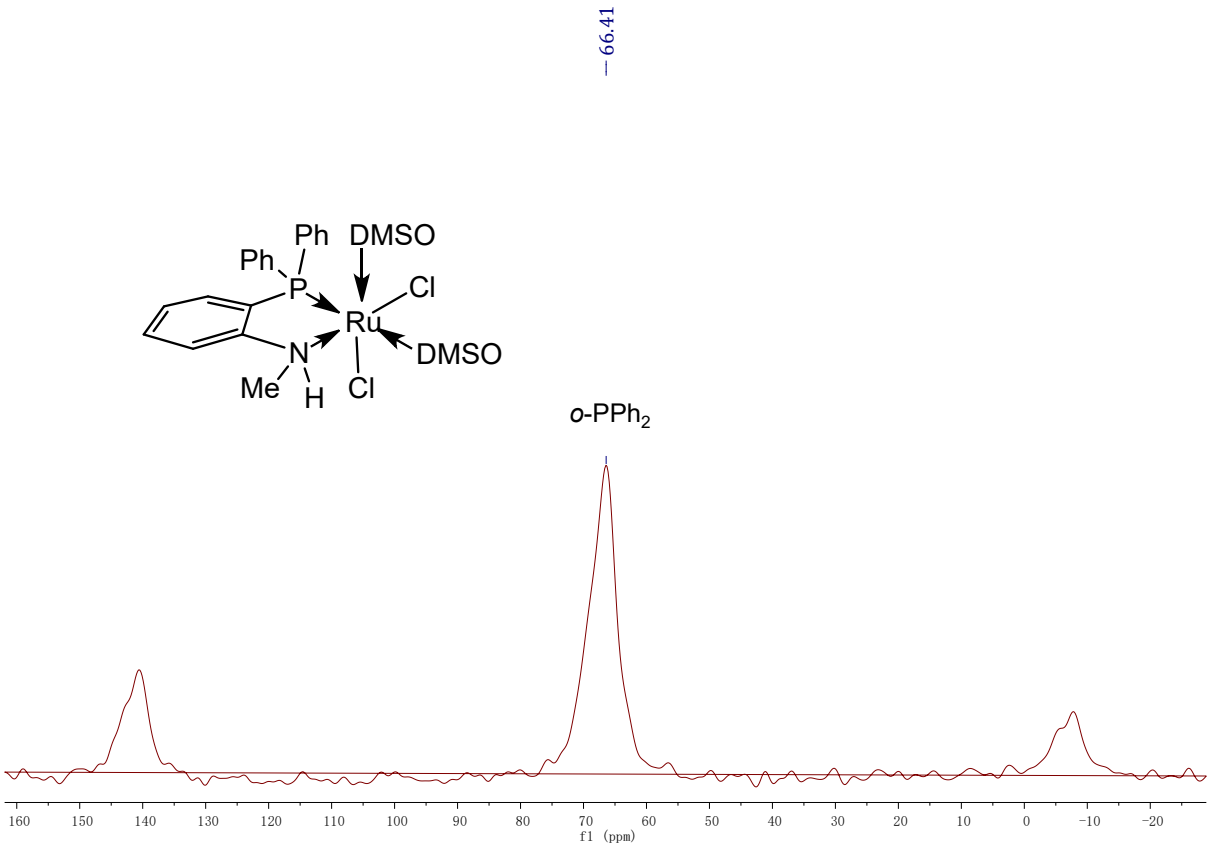

Fig. S6 Solid state ^{31}P NMR spectrum of **9**.

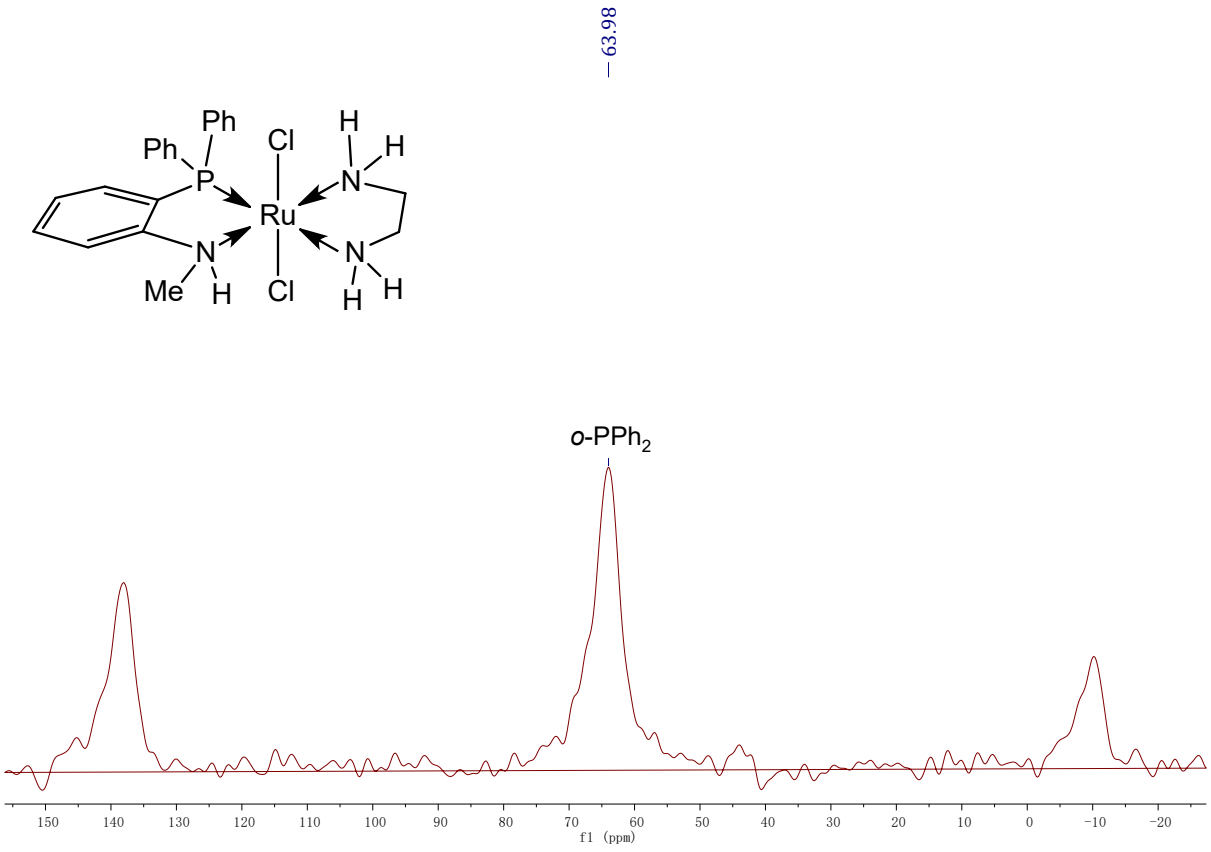

Fig. S7 Solid state ^{31}P NMR spectrum of **10**.

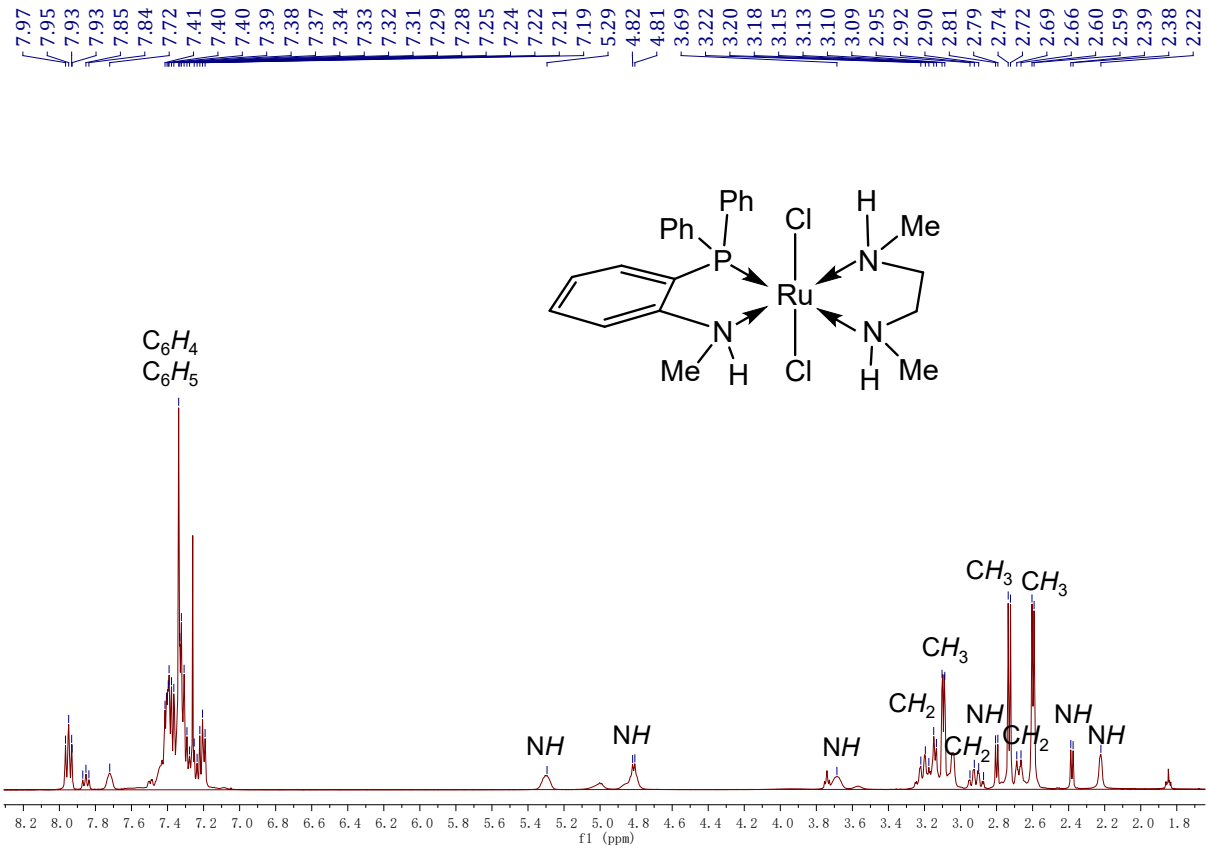

Fig. S8 ^{1}H NMR spectrum of **11** in $CDCl_3$.

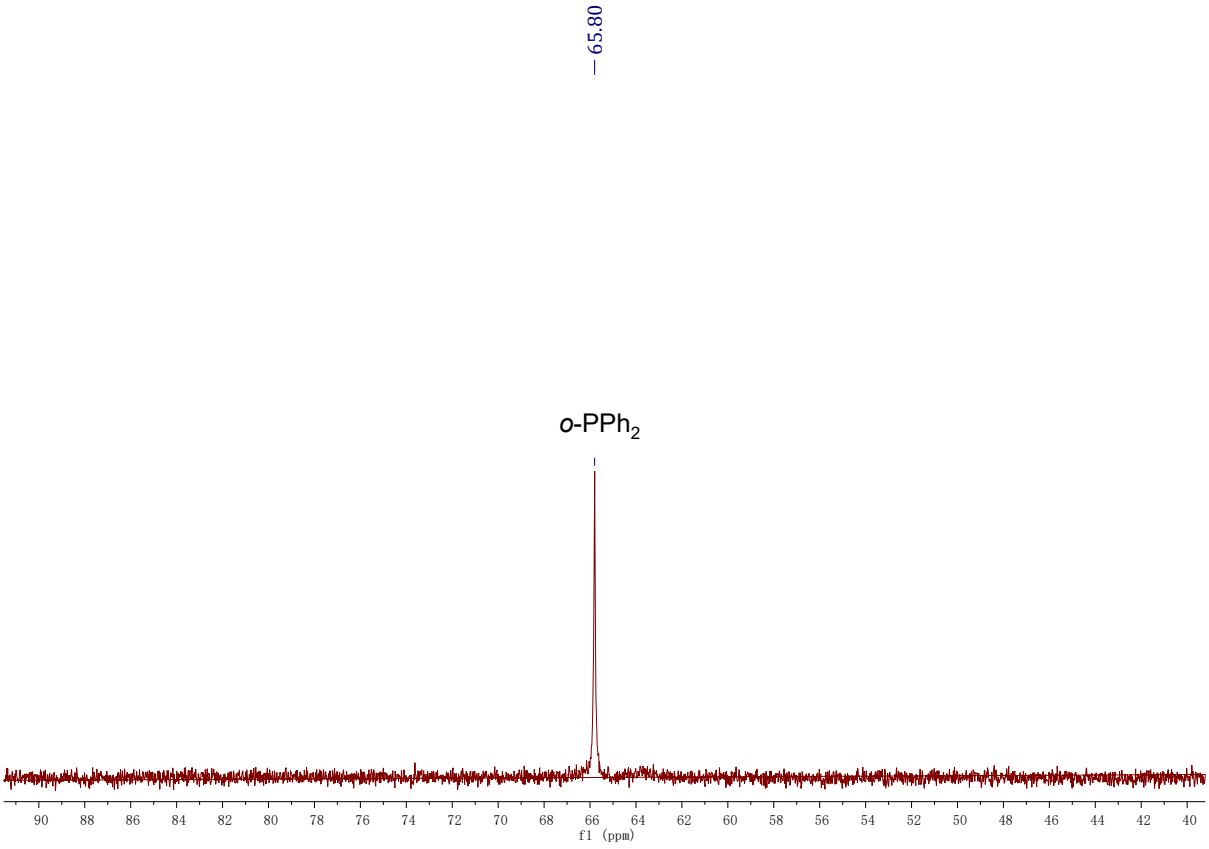

Fig. S9 ^{31}P{^{1}H} NMR spectrum of **11** in $CDCl_3$.

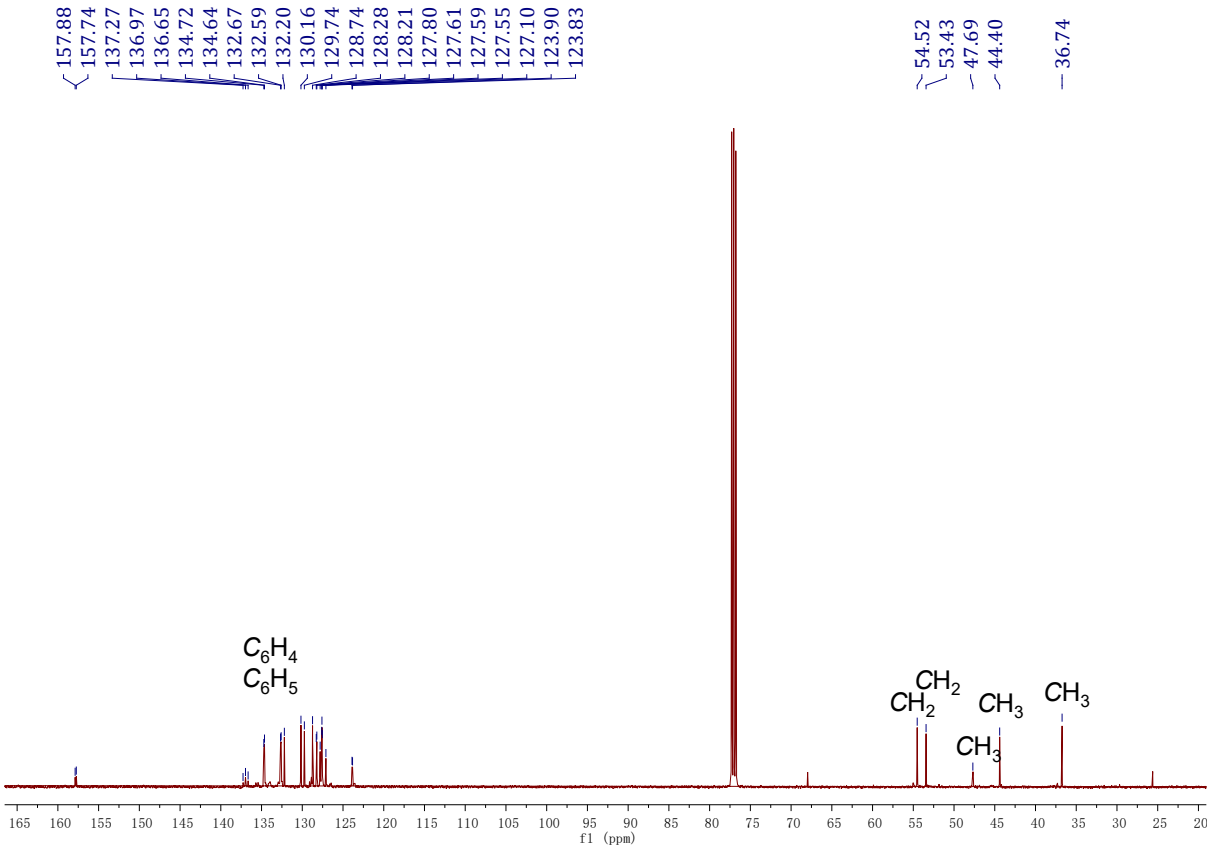

Fig. S10 $^{13}C\{^{1}H\}$ NMR spectrum of **11** in $CDCl_3$.

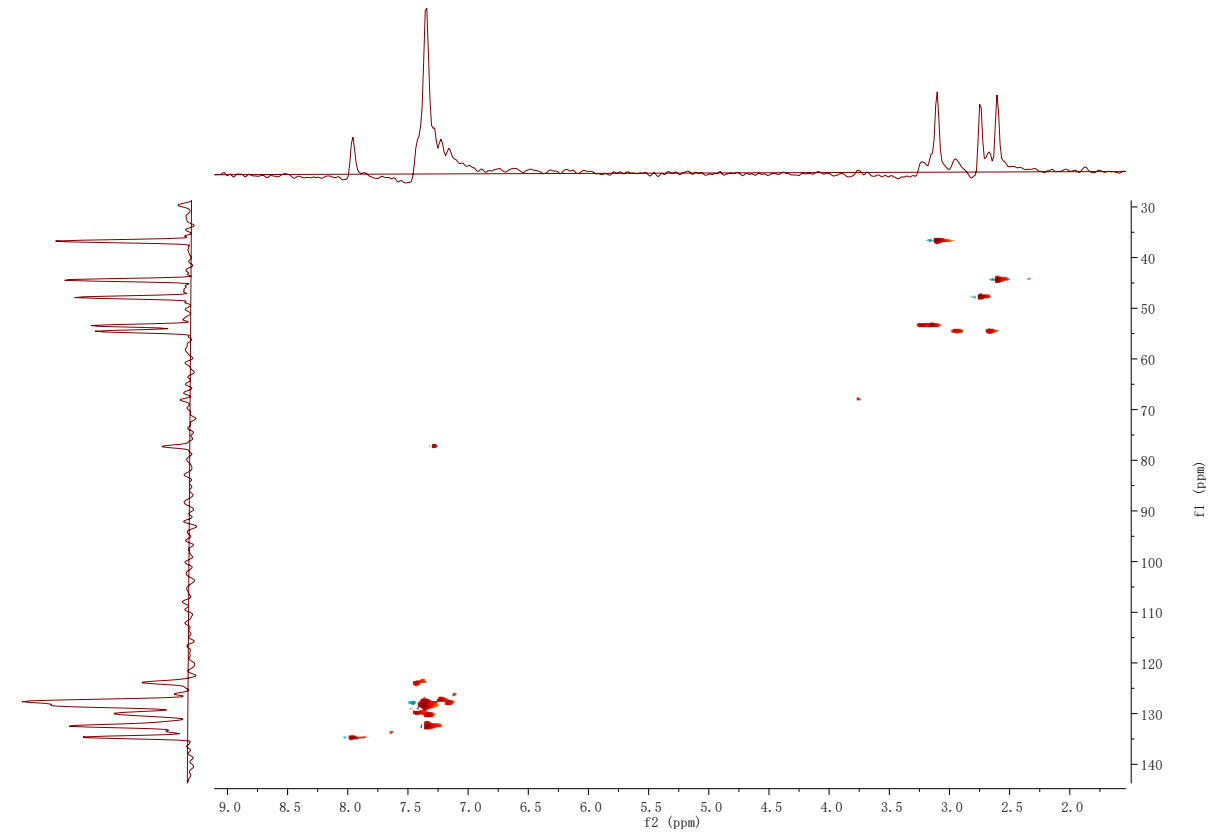

Fig. S11 ^{1}H-^{13}C HSQC NMR spectrum of **11** in $CDCl_3$.

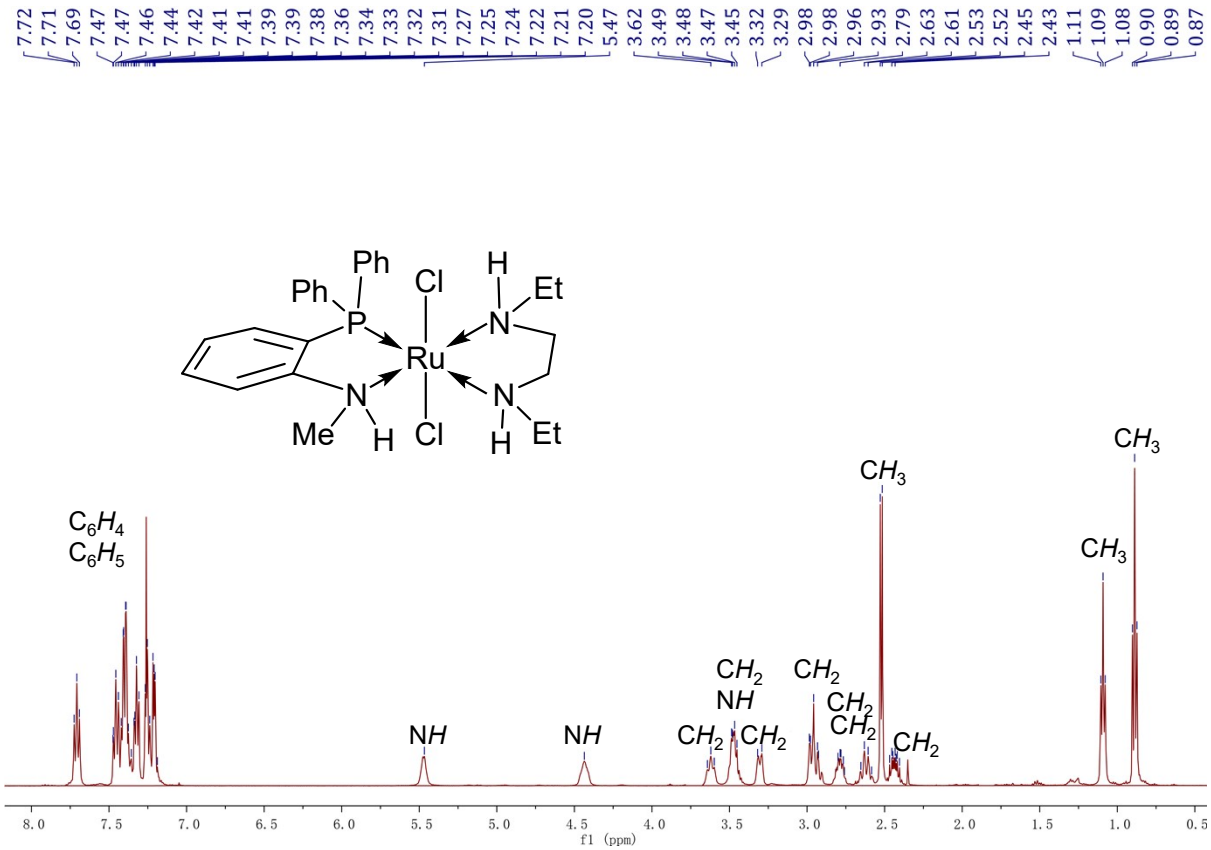

Fig. S12 ^{1}H NMR spectrum of **12** in $CDCl_3$.

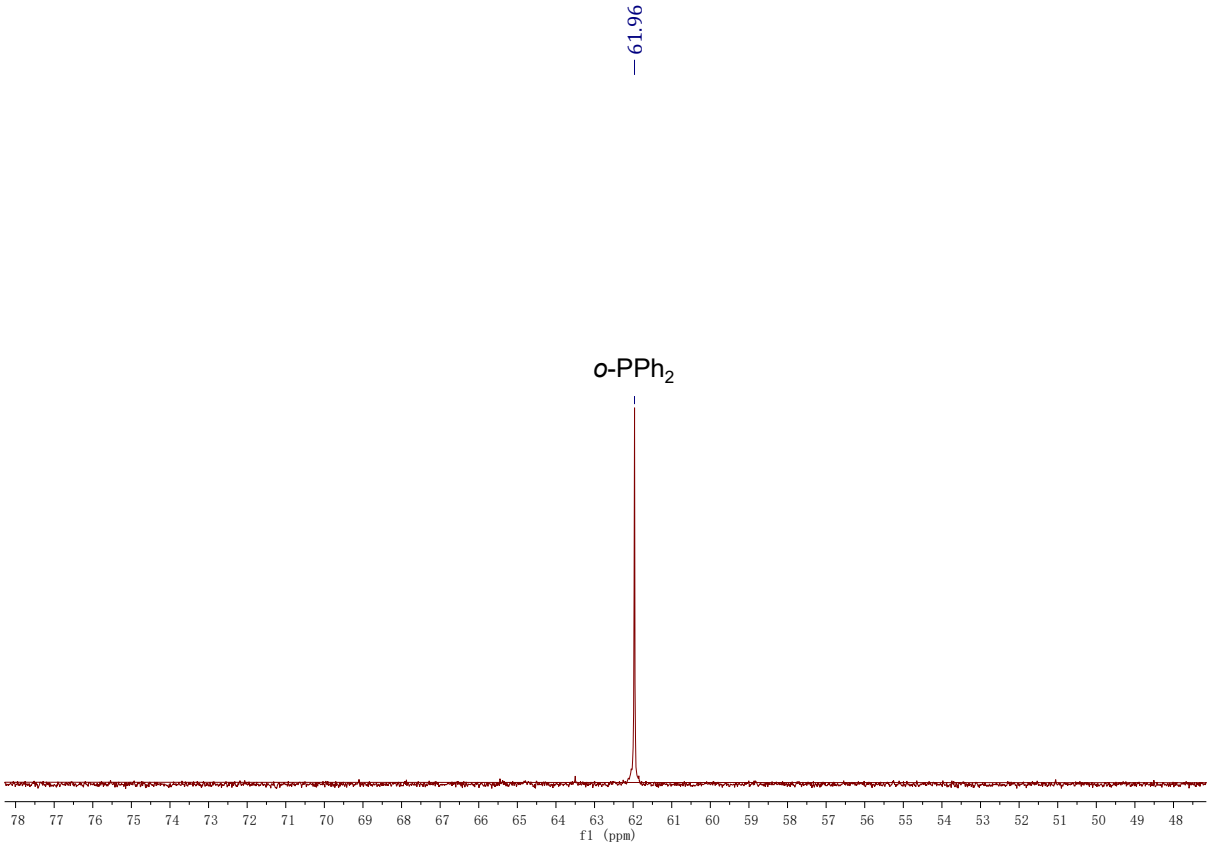

Fig. S13 ^{31}P{^{1}H} NMR spectrum of **12** in $CDCl_3$.

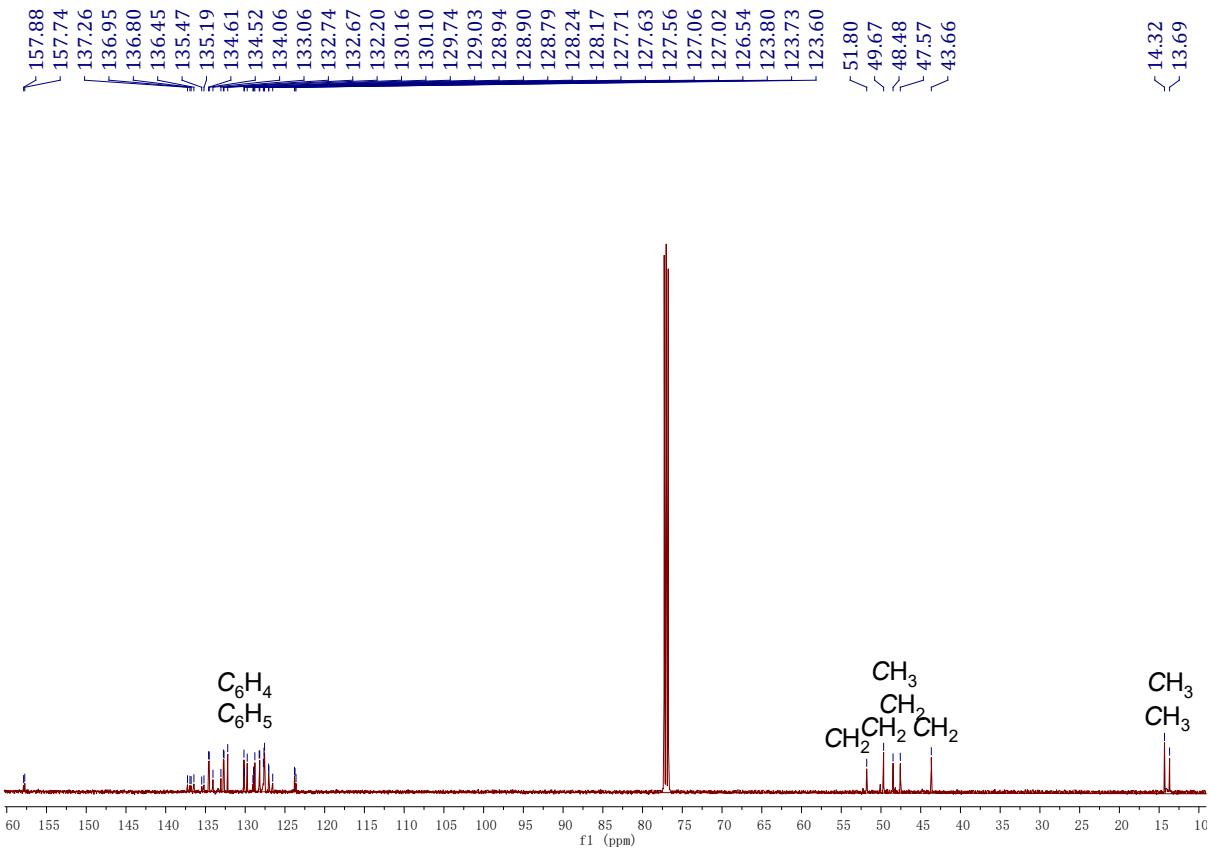

Fig. S14 $^{13}C\{^{1}H\}$ NMR spectrum of **12** in $CDCl_3$.

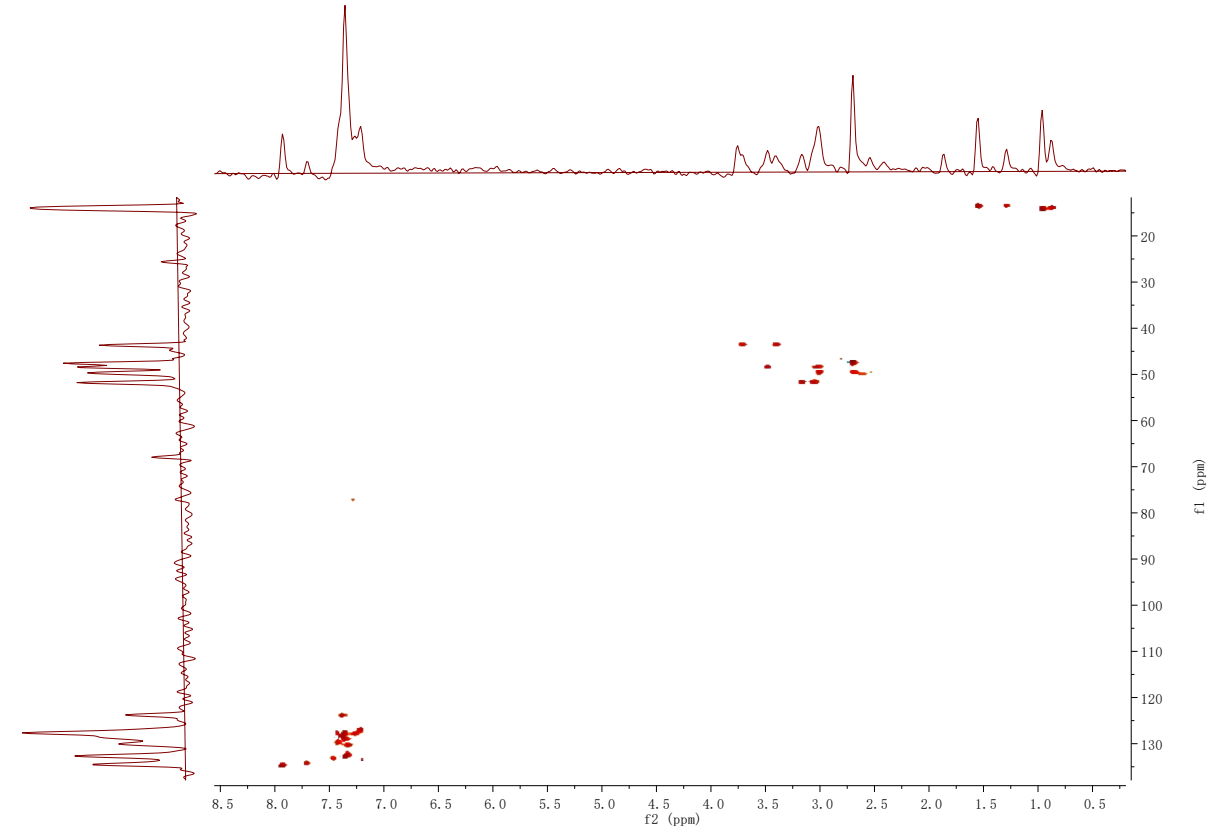

Fig. S15 ^{1}H-^{13}C HSQC NMR spectrum of **12** in $CDCl_3$.

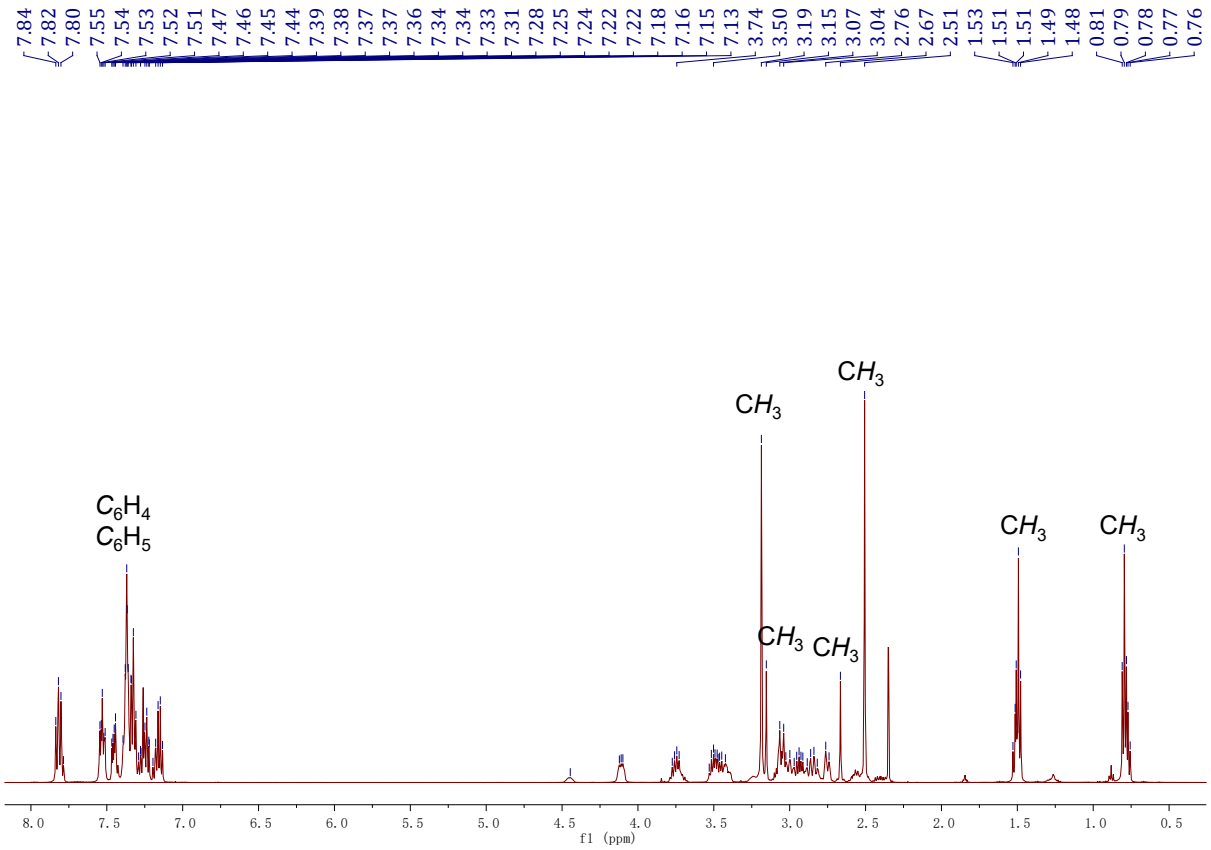

Fig. S16 ^{1}H NMR spectrum of **13** in $CDCl_3$.

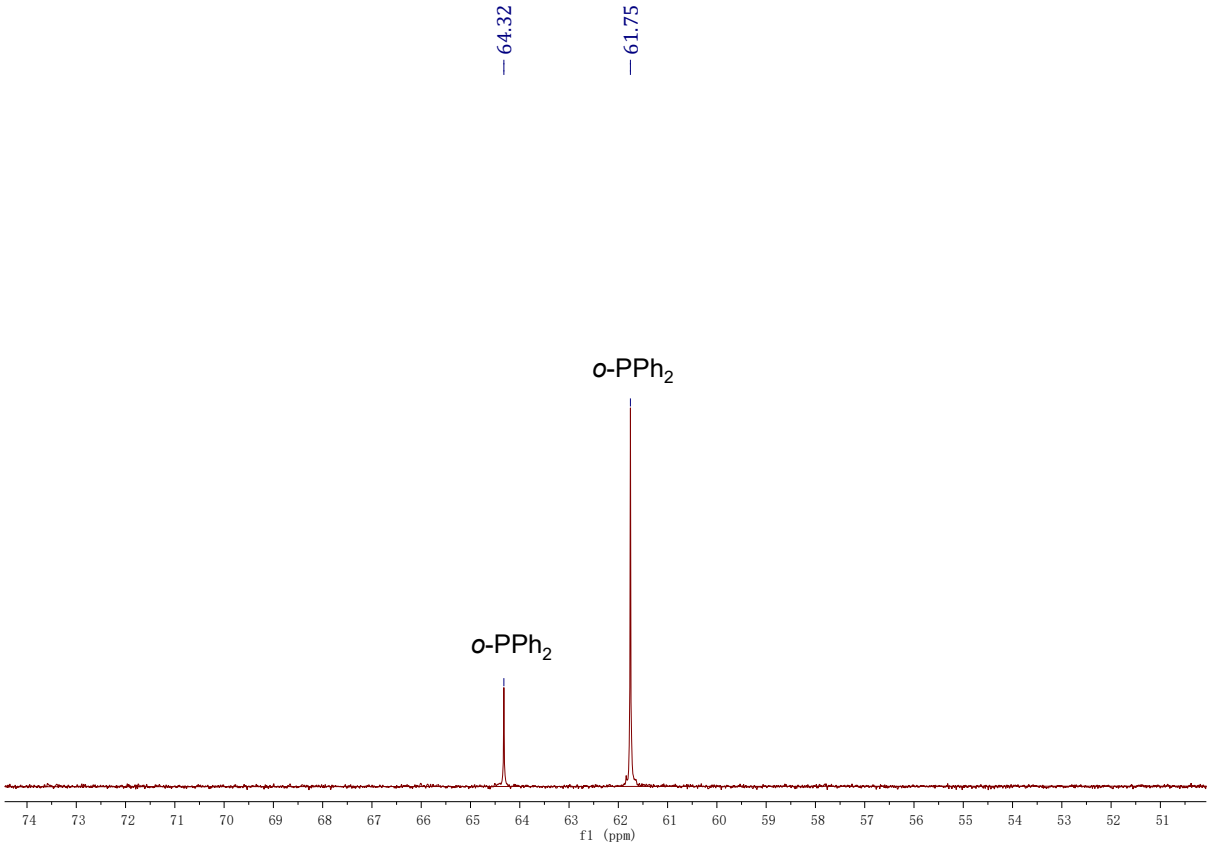

Fig. S17 ^{31}P{^{1}H} NMR spectrum of **13** in $CDCl_3$.

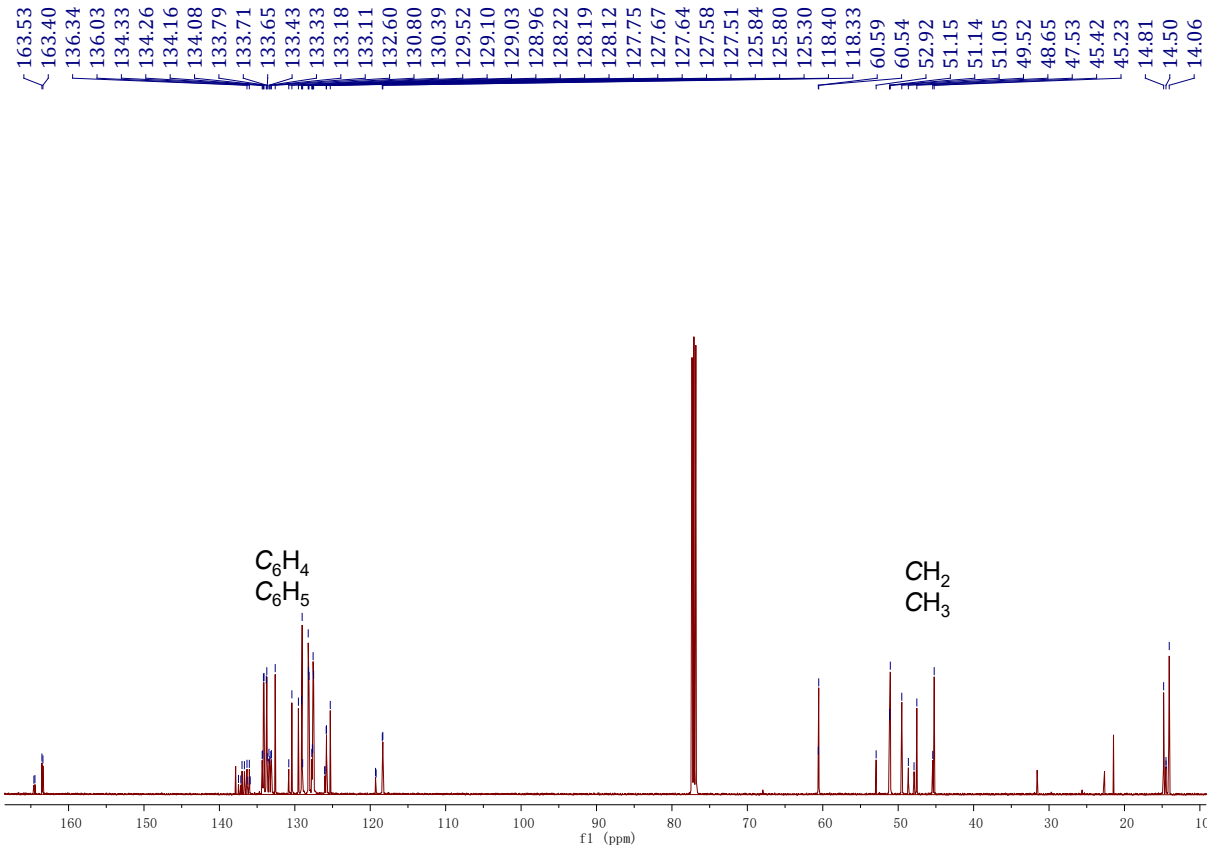

Fig. S18 $^{13}C\{^{1}H\}$ NMR spectrum of **13** in $CDCl_3$.

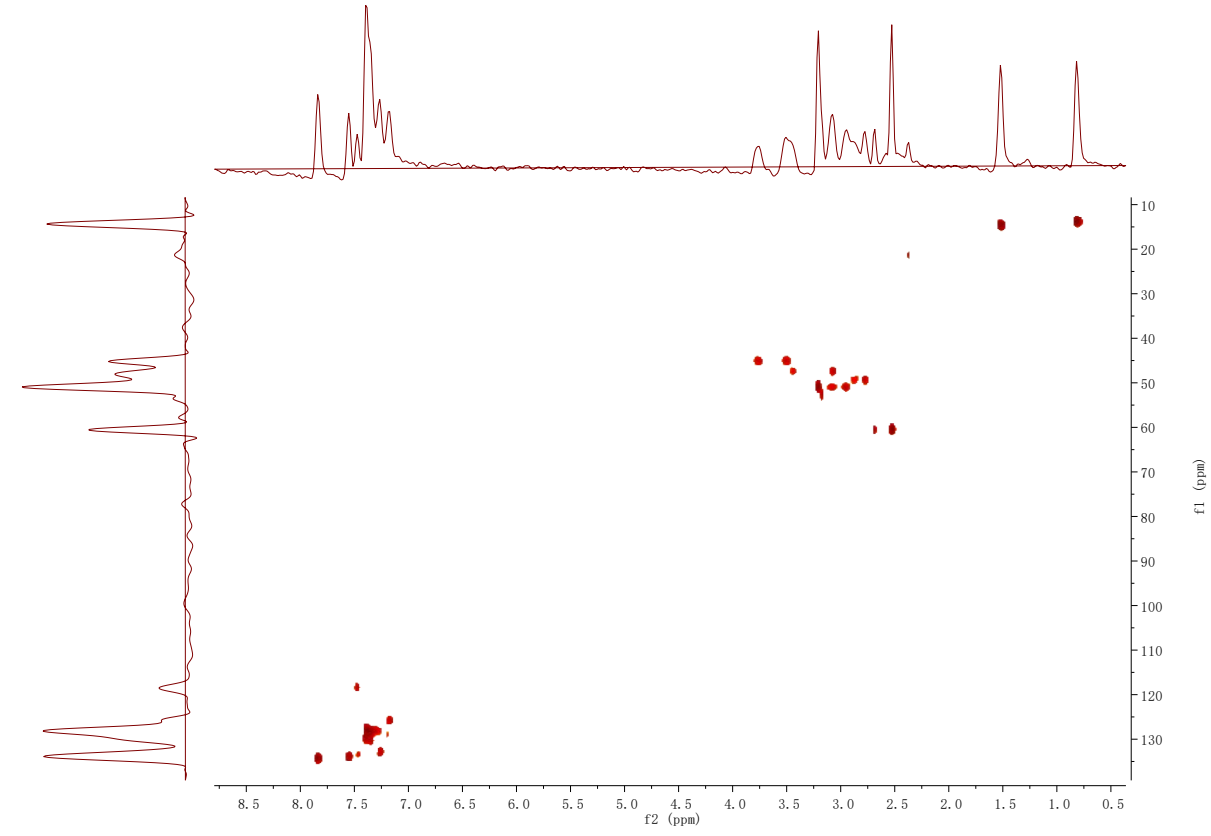

Fig. S19 ^{1}H-^{13}C HSQC NMR spectrum of **13** in $CDCl_3$.

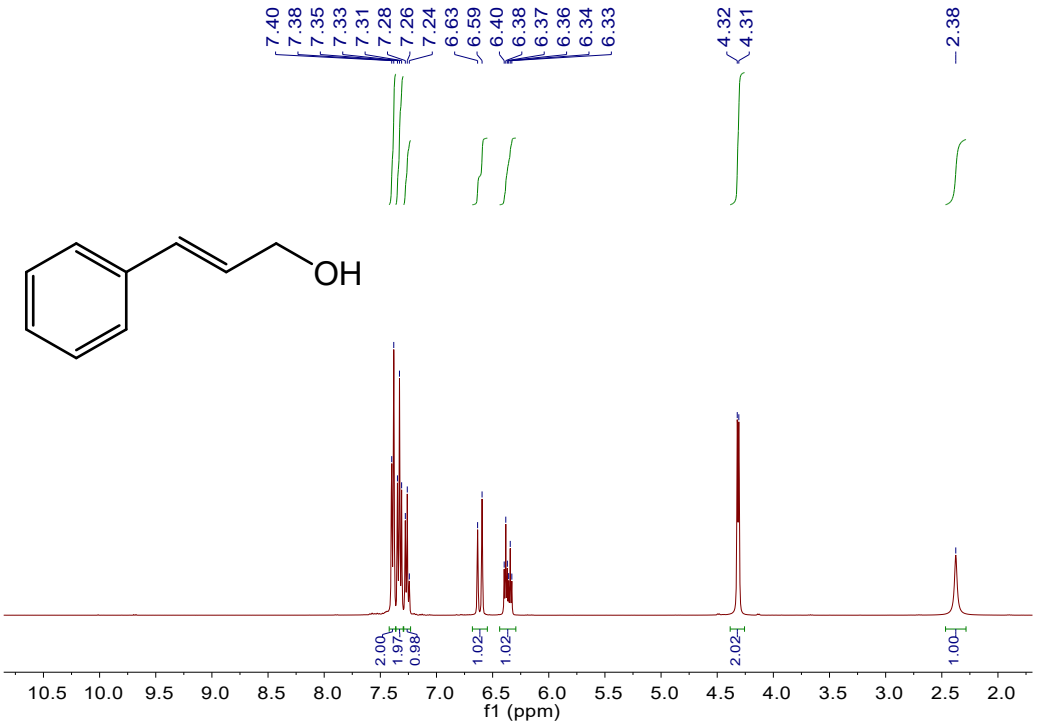

Fig. S20 ^{1}H NMR spectrum of cinnamyl alcohol.[7] ^{1}H NMR (400 MHz, $CDCl_3$, 298 k, ppm): δ = 2.38 (br, 1 H), 4.32 (d, J_{HH} = 5.6 Hz, 2 H), 6.37 (m, 1 H), 6.61 (d, J_{HH} = 16.0 Hz, 1 H), 7.24-7.40 (m, 6 H).

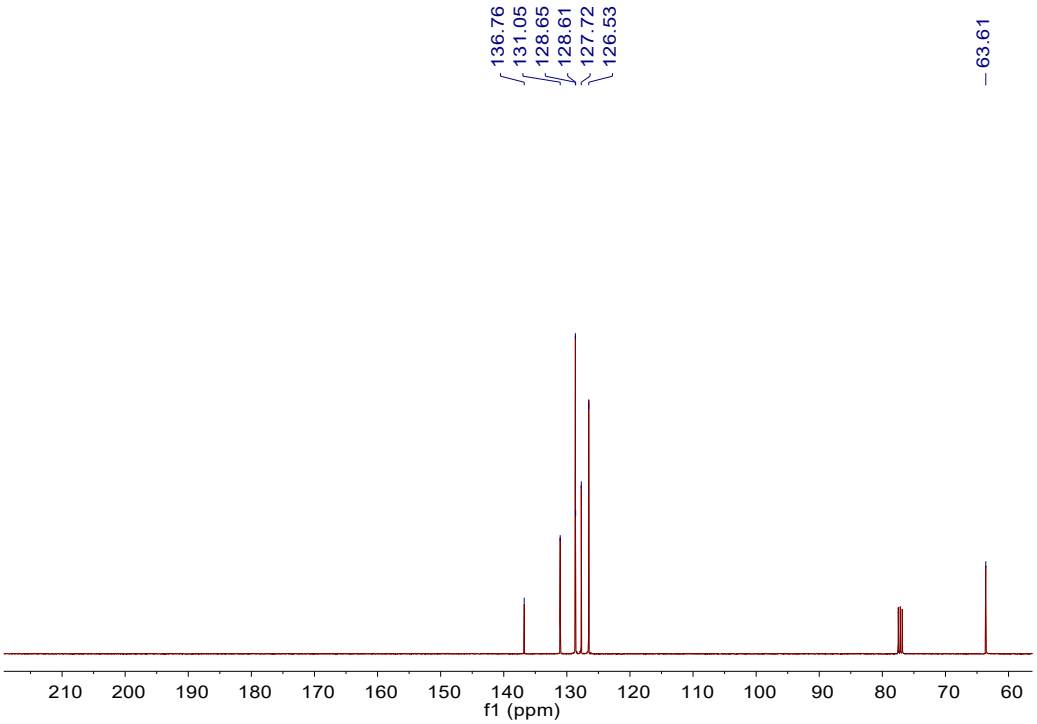

Fig. S21 ^{13}C{^{1}H} NMR spectrum of cinnamyl alcohol. ^{13}C{^{1}H} NMR (100 MHz, $CDCl_3$, 298 k, ppm): δ = 63.61, 126.53, 127.72, 128.61, 128.65, 131.05, 136.76.

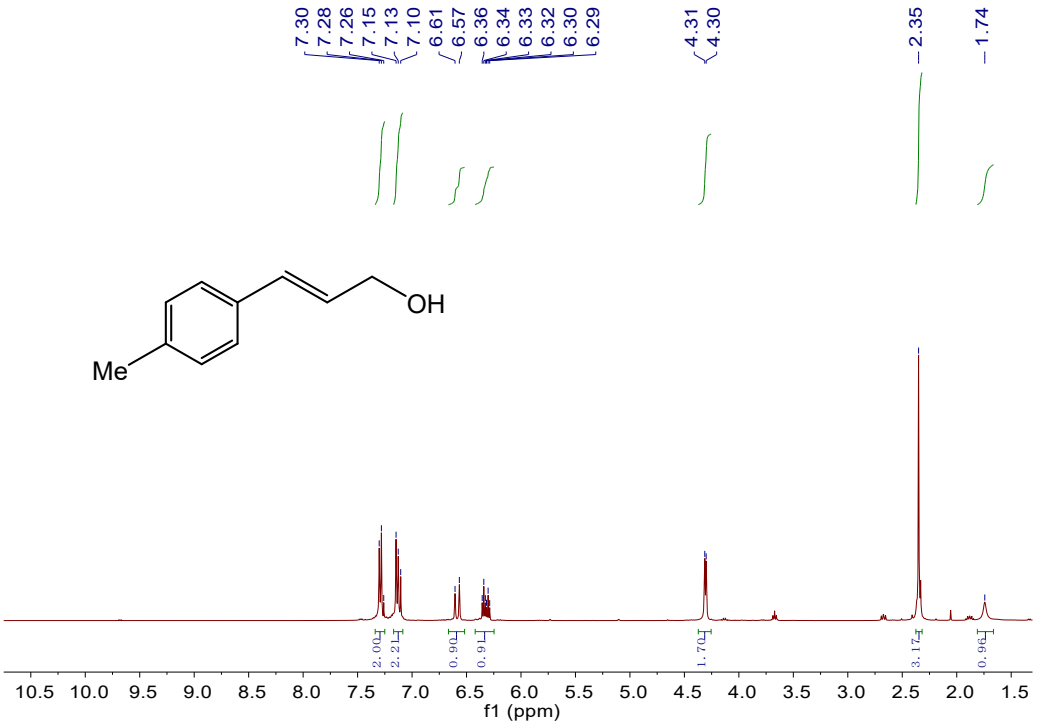

Fig. S22 ^{1}H NMR spectrum of **15a**.[7] ^{1}H NMR (400 MHz, $CDCl_3$, 298 k, ppm): δ = 1.74 (br, 1 H), 2.35 (s, 3 H), 4.32 (d, J_{HH} = 5.2 Hz, 2 H), 6.29-6.36 (m, 1 H), 6.59 (d, J_{HH} = 15.6 Hz, 1 H), 7.10-7.15 (m, 2 H), 7.29 (d, J_{HH} = 8.0 Hz, 2 H).

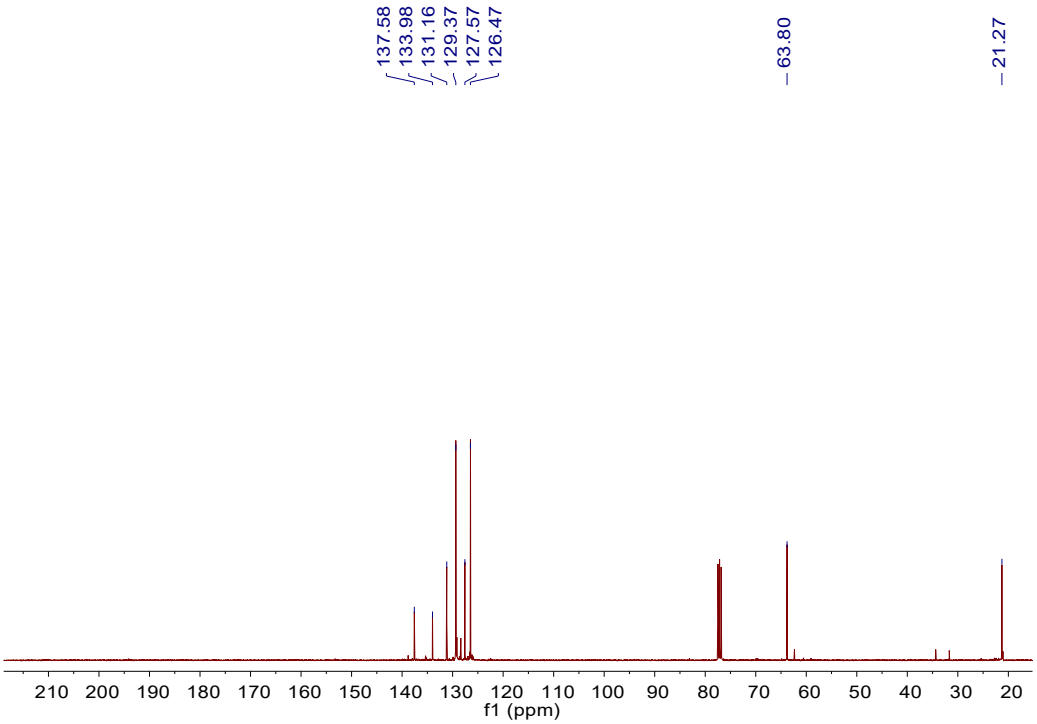

Fig. S23 ^{13}C{^{1}H} NMR spectrum of **15a**. ^{13}C{^{1}H} NMR (100 MHz, $CDCl_3$, 298 k, ppm): δ = 21.27, 63.80, 126.47, 127.57, 129.37, 131.16, 133.98, 137.58.

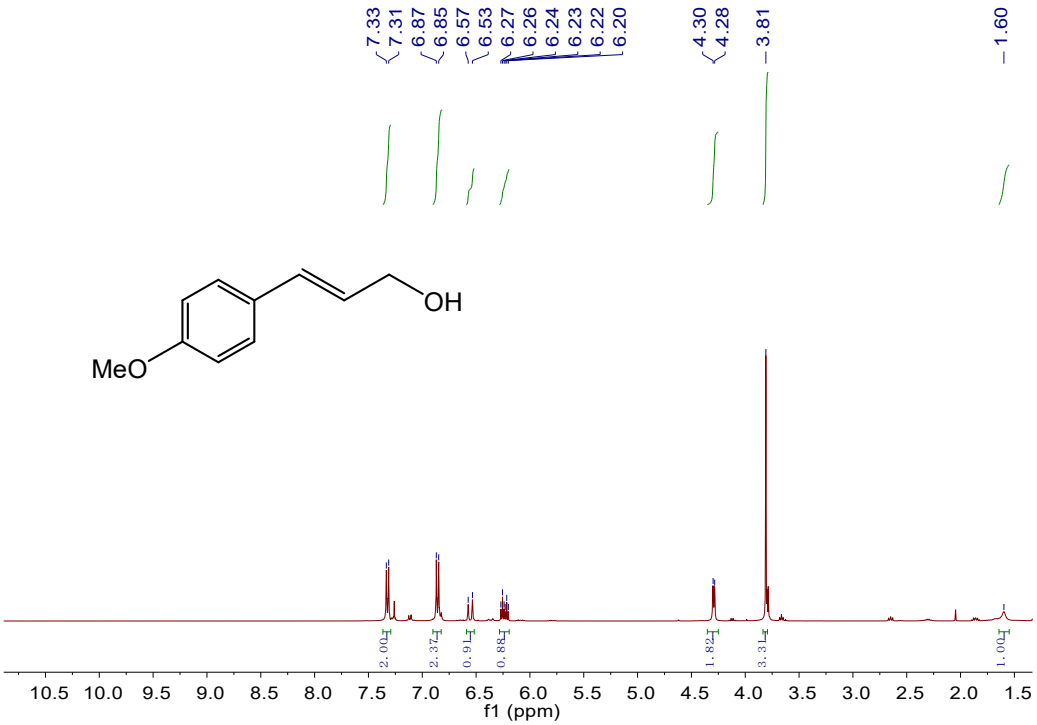

Fig. S24 ^{1}H NMR spectrum of **15b**.[7] ^{1}H NMR (400 MHz, $CDCl_3$, 298 k, ppm): δ = 1.60 (br, 1 H), 3.31 (s, 3 H), 4.29 (d, J_{HH} = 6.0 Hz, 2 H), 6.20-6.27 (m, 1 H), 6.55 (d, J_{HH} = 16.0 Hz, 1 H), 6.86 (d, J_{HH} = 8.8 Hz, 2 H), 7.32 (d, J_{HH} = 8.8 Hz, 2 H).

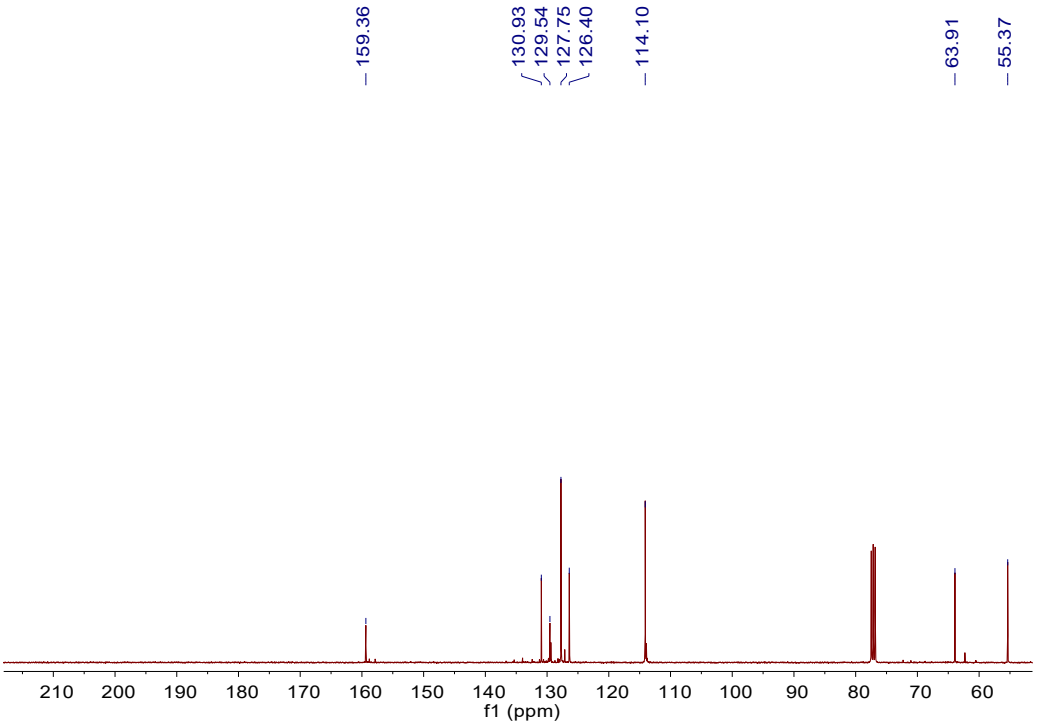

Fig. S25 ^{13}C{^{1}H} NMR spectrum of **15b**. ^{13}C{^{1}H} NMR (100 MHz, $CDCl_3$, 298 k, ppm): δ = 55.37, 63.91, 114.10, 126.40, 127.75, 129.54, 130.93, 159.36.

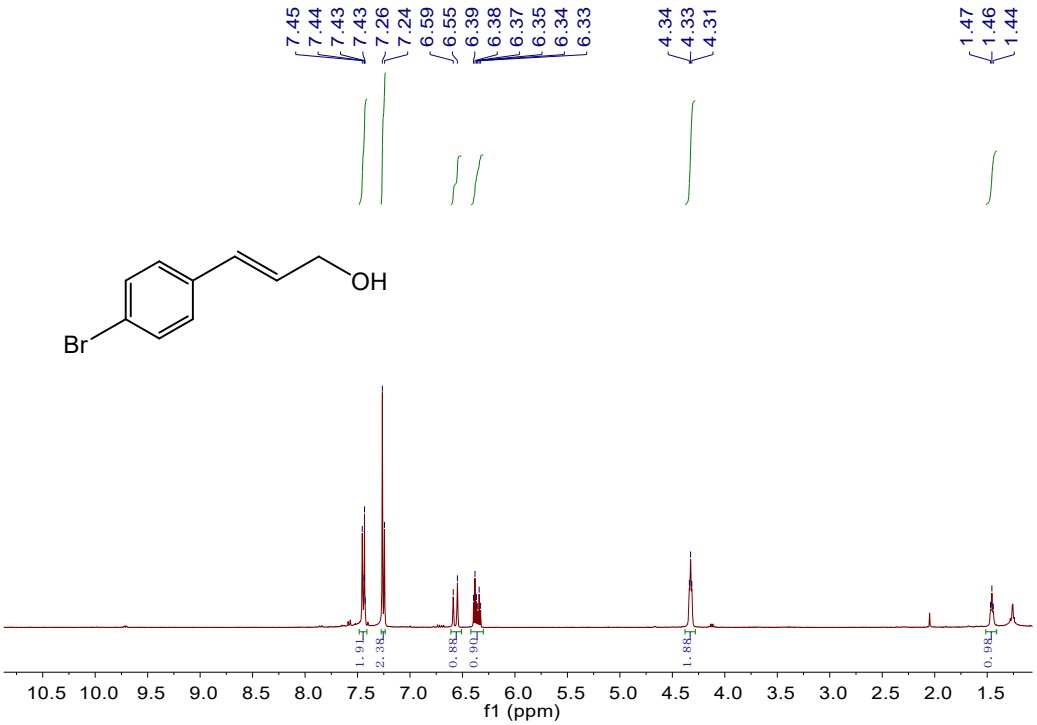

Fig. S26 ^{1}H NMR spectrum of **15c**.[7] ^{1}H NMR (400 MHz, $CDCl_3$, 298 k, ppm): δ = 1.46 (t, J_{HH} = 5.2 Hz, 1 H), 4.33 (t, J_{HH} = 4.8 Hz, 2 H), 6.33-6.39 (m, 1 H), 6.57 (d, J_{HH} = 16.0 Hz, 1 H), 7.24-7.26 (m, 2 H), 7.43-7.45 (m, 2 H).

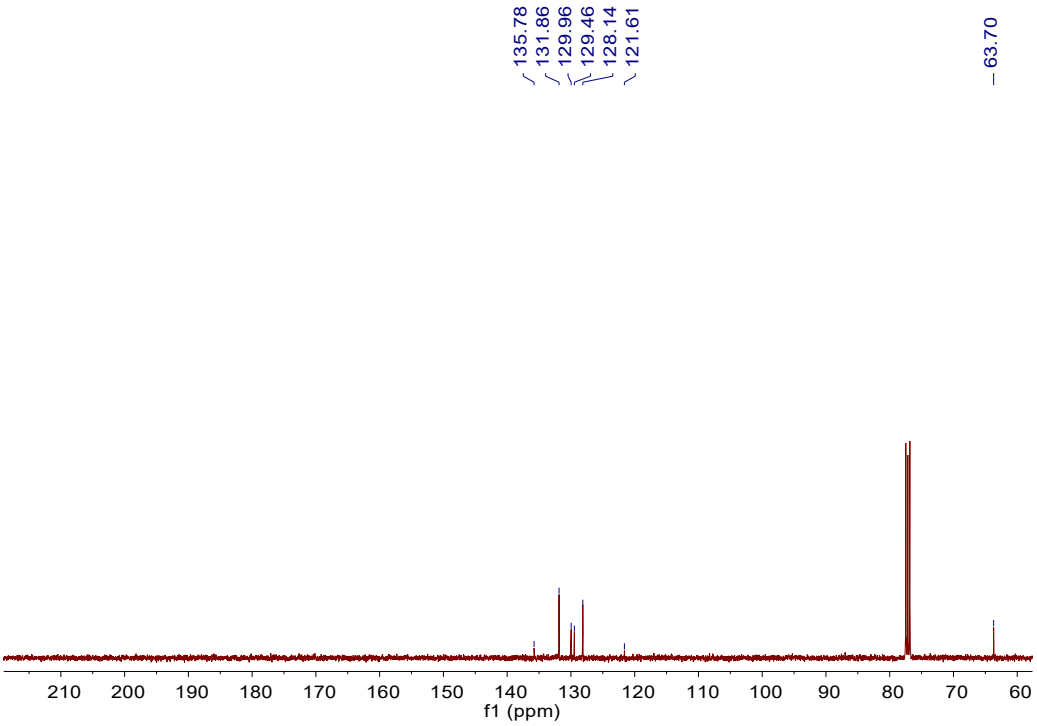

Fig. S27 ^{13}C{^{1}H} NMR spectrum of **15c**. ^{13}C{^{1}H} NMR (100 MHz, $CDCl_3$, 298 k, ppm): δ = 63,70, 121.61, 128.14, 129.46, 129.96, 131.86, 135.78.

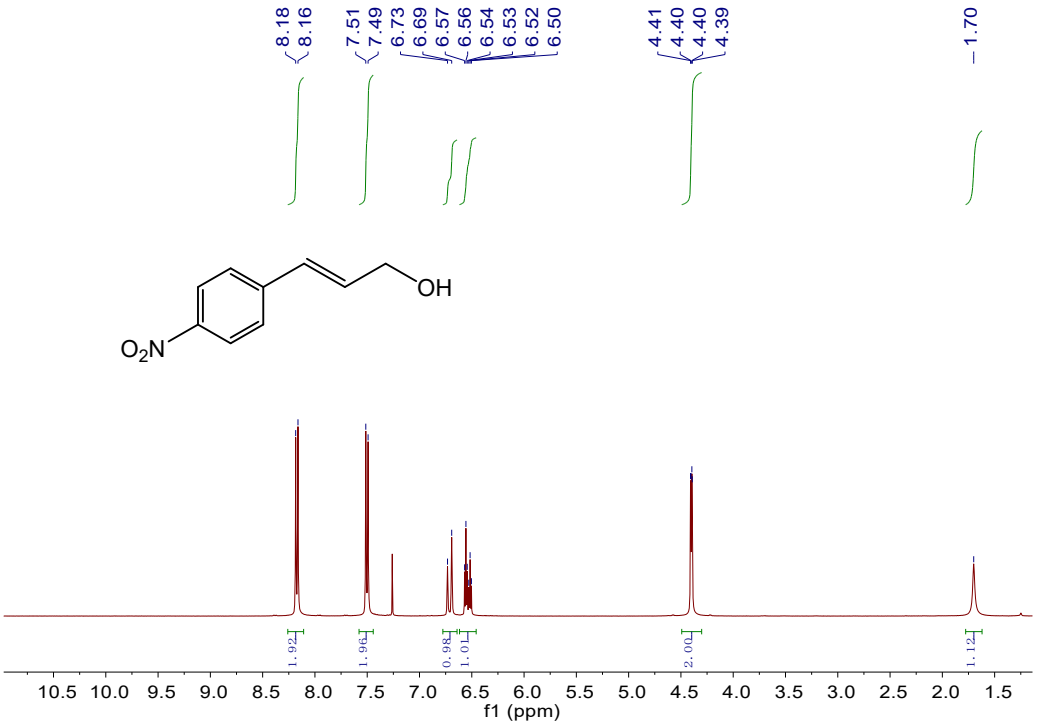

Fig. S28 ^{1}H NMR spectrum of **15d**.[8] ^{1}H NMR (400 MHz, $CDCl_3$, 298 k, ppm): δ = 1.70 (br, 1 H), 4.40 (dd, J_{HH} = 1.6, 3.6 Hz, 2 H), 6.50-6.57 (m, 1 H), 6.71 (d, J_{HH} = 1.6 Hz, 1 H), 7.50 (d, J_{HH} = 8.8 Hz, 2 H), 8.17 (d, J_{HH} = 8.8 Hz, 2 H).

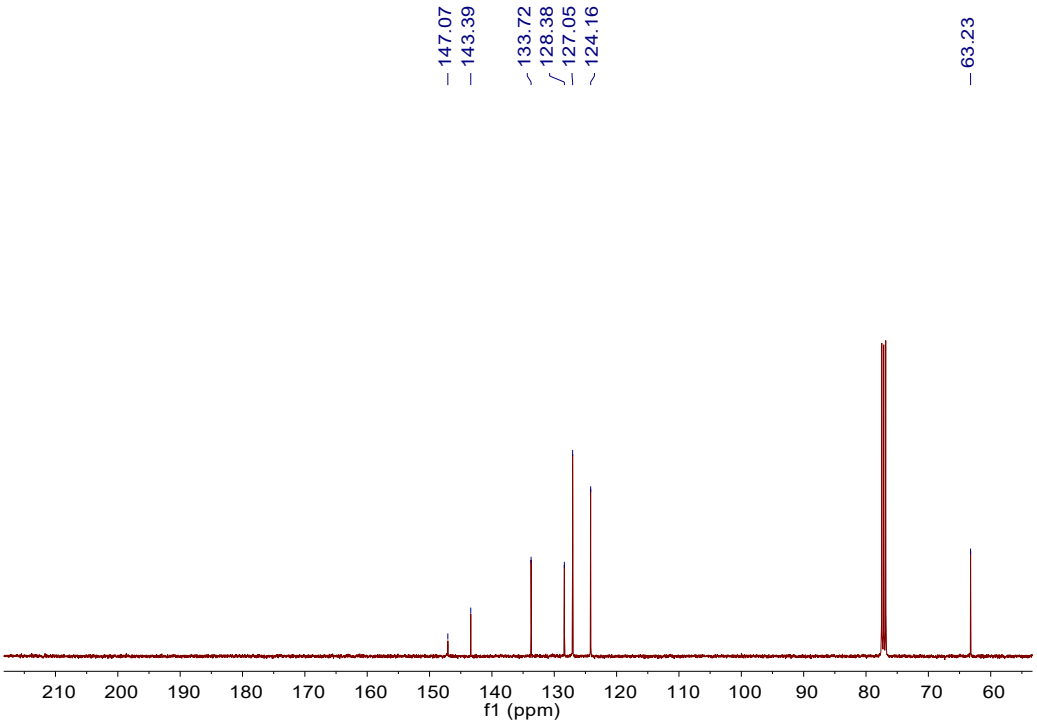

Fig. S29 ^{13}C{^{1}H} NMR spectrum of **15d**. ^{13}C{^{1}H} NMR (100 MHz, $CDCl_3$, 298 k, ppm): δ = 63.23, 124.16, 127.05, 128.38, 133.72, 143.39, 147.07.

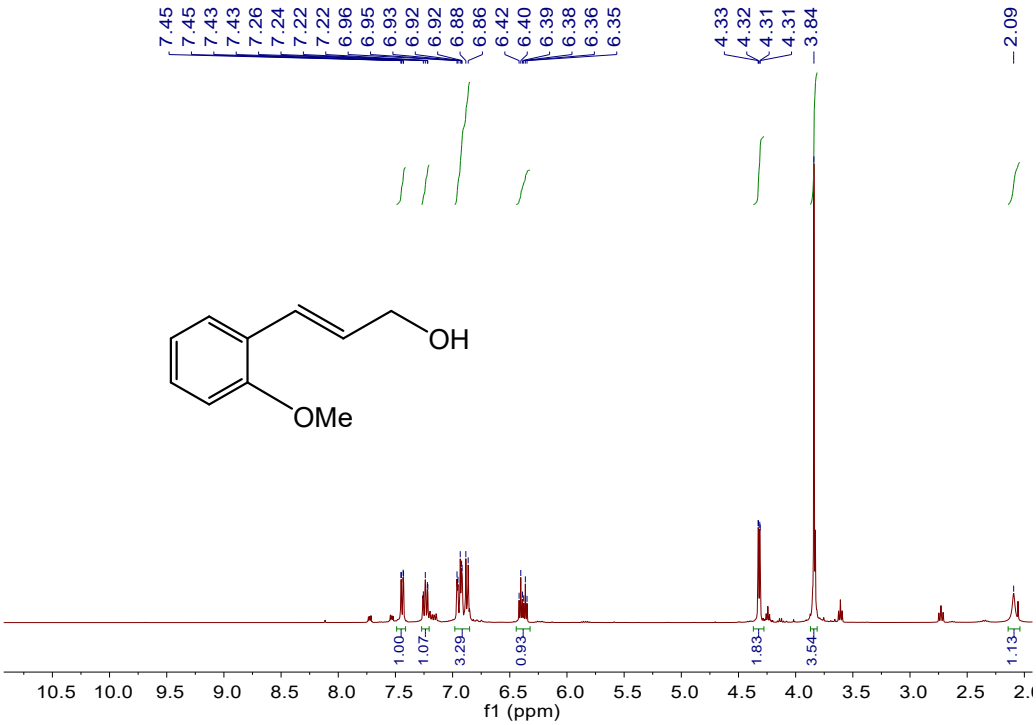

Fig. S30 ^{1}H NMR spectrum of **15e**.[8] ^{1}H NMR (400 MHz, $CDCl_3$, 298 k, ppm): δ = 2.09 (br, 1 H), 3.84 (s ,3 H), 4.32 (dd, J_{HH} = 1.2, 6.0 Hz, 2 H), 6.35-6.42 (m, 1 H), 6.86-6.96 (m, 3 H), 7.22-7.26 (m, 1 H), 7.44 (dd, J_{HH} = 1.6, 7.6 Hz, 1 H).

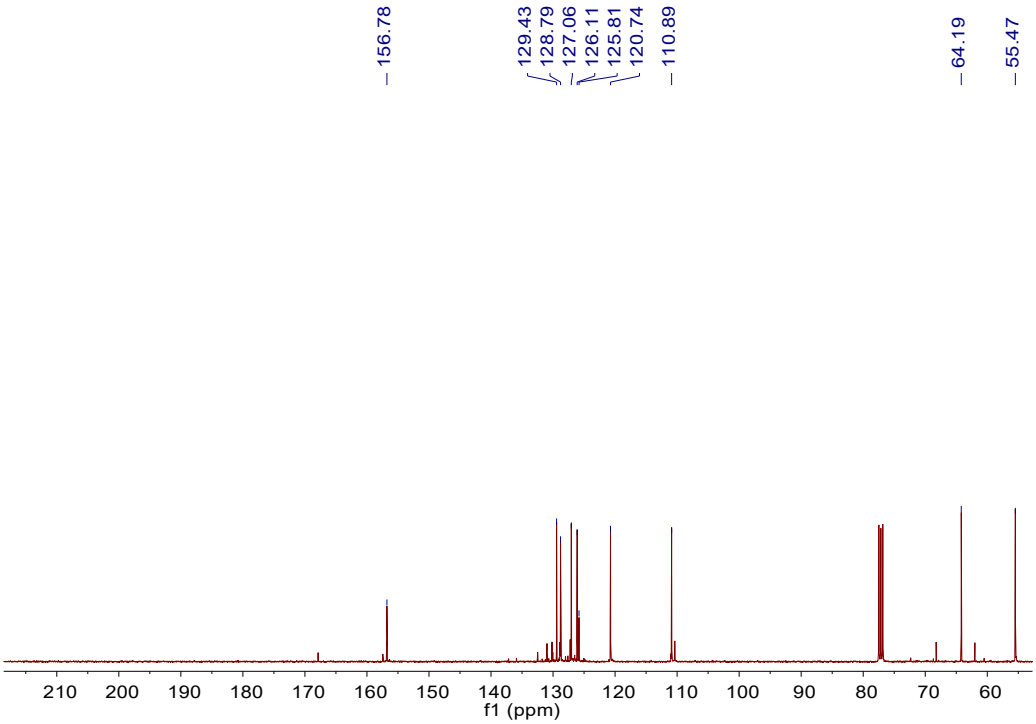

Fig. S31 ^{13}C{^{1}H} NMR spectrum of **15e**. ^{13}C{^{1}H} NMR (100 MHz, $CDCl_3$, 298 k, ppm): δ = 55.47, 64.19, 110.89, 120.74, 125.81, 126.11, 127.06, 128.79, 129.43, 156.78.

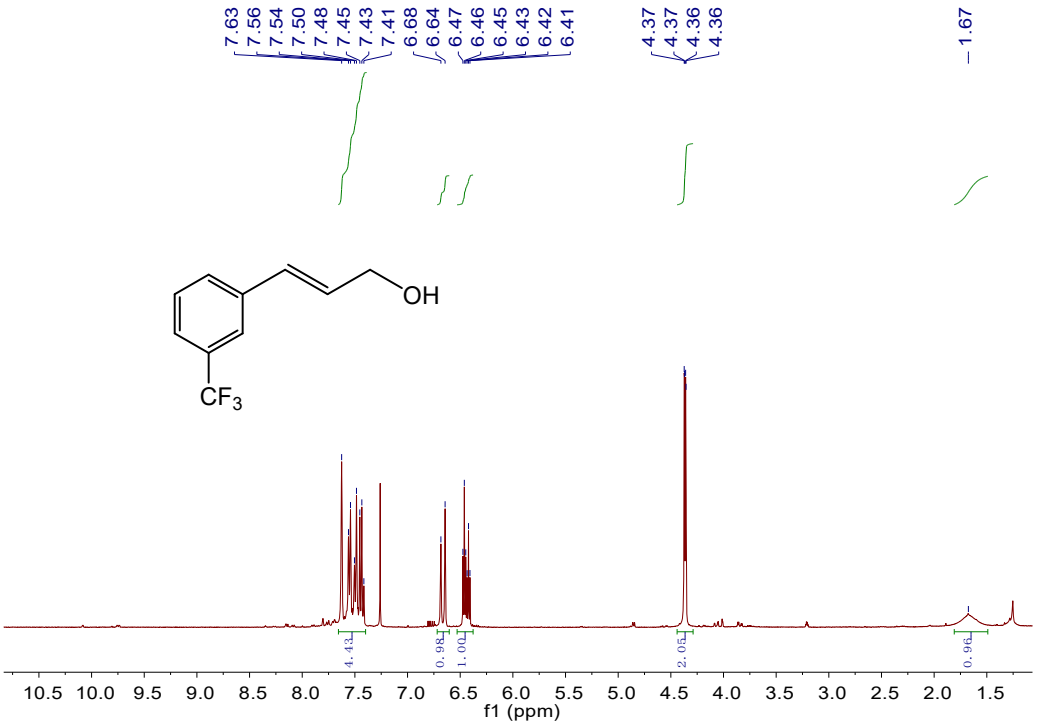

Fig. S32 ^{1}H NMR spectrum of **15f**.[7] ^{1}H NMR (400 MHz, $CDCl_3$, 298 k, ppm): δ = 1.67 (br, 1 H), 4.36 (dd, J_{HH} = 1.6, 5.2 Hz, 2 H), 6.41-6.47 (m, 1 H), 6.66 (d, J_{HH} = 16.0 Hz, 1 H), 7.41-7.64 (m, 4 H).

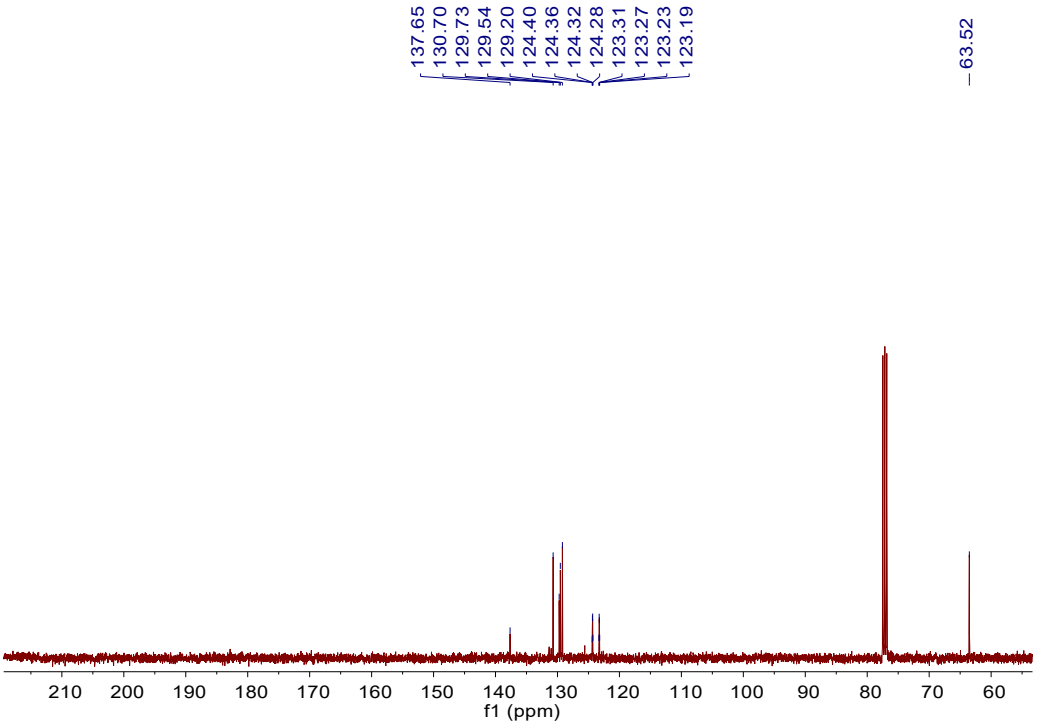

Fig. S33 ^{13}C{^{1}H} NMR spectrum of **15f**. ^{13}C{^{1}H} NMR (100 MHz, $CDCl_3$, 298 k, ppm): δ = 63.52, 123.25 (q, J_{FC} = 3.8 Hz), 124.34 (q, J_{FC} = 3.8 Hz), 129.20, 129.54, 129.73, 130.70, 137.65.

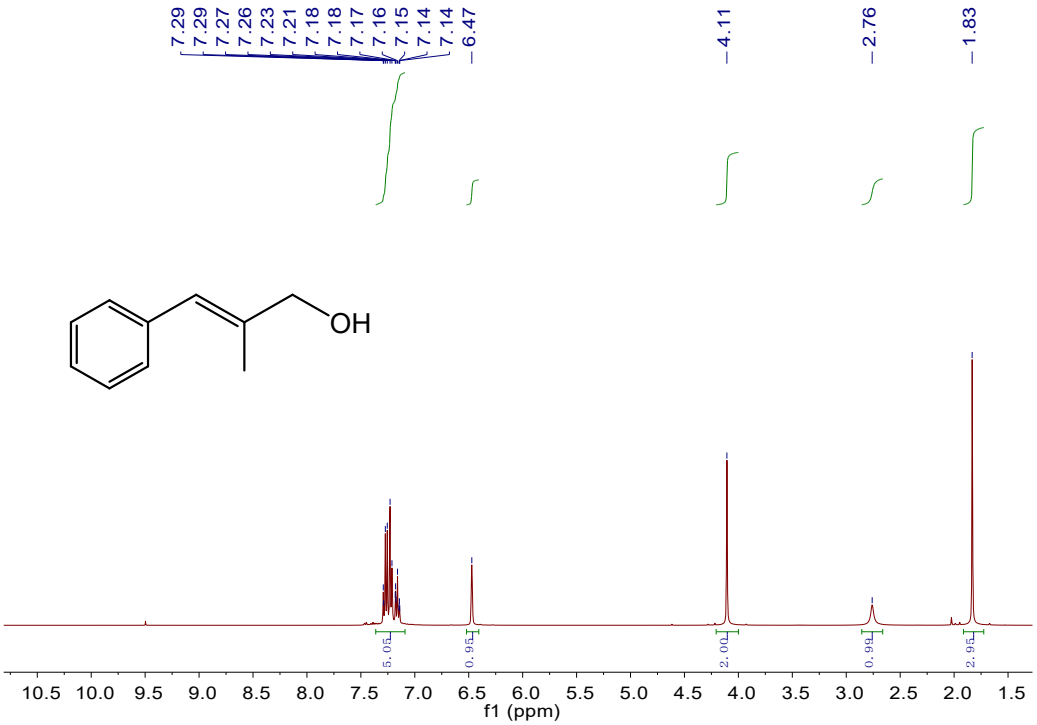

Fig. S34 ^{1}H NMR spectrum of **15g**.[7] ^{1}H NMR (400 MHz, $CDCl_3$, 298 k, ppm): δ = 1.83 (s, 3 H), 2.76 (br, 1 H), 4.11 (s, 2 H), 6.47 (s, 1 H), 7.14-7.29 (m, 5 H).

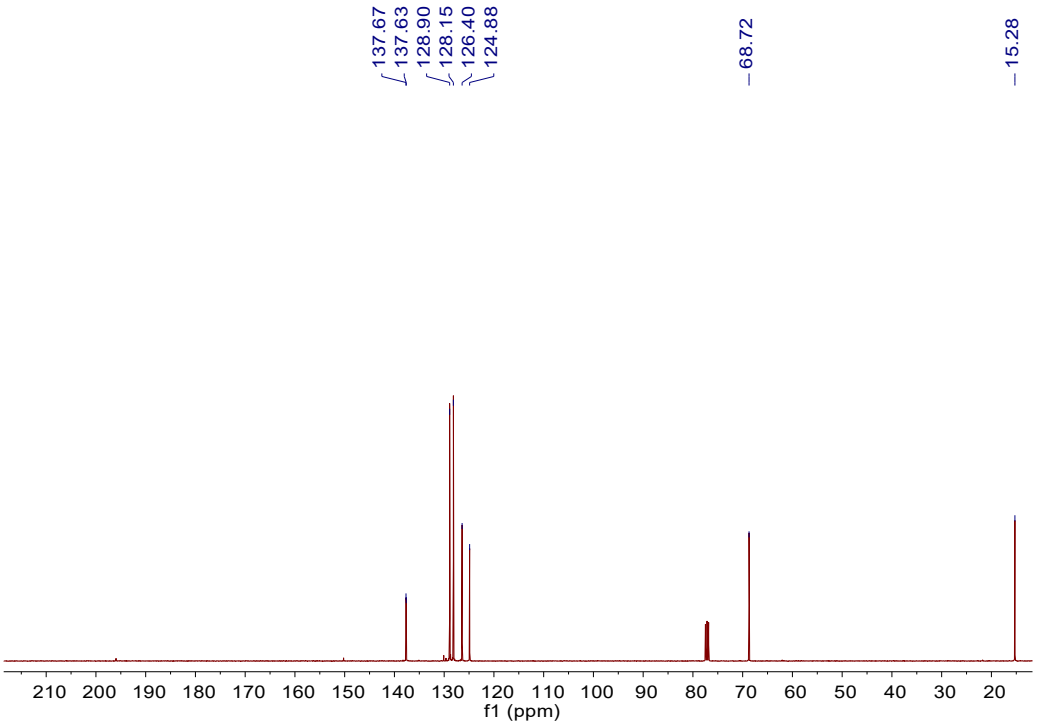

Fig. S35 ^{13}C{^{1}H} NMR spectrum of **15g**. ^{13}C{^{1}H} NMR (100 MHz, $CDCl_3$, 298 k, ppm): δ = 15.28, 68.72, 124.88, 126.40, 128.15, 128.90, 137.63, 137.67.

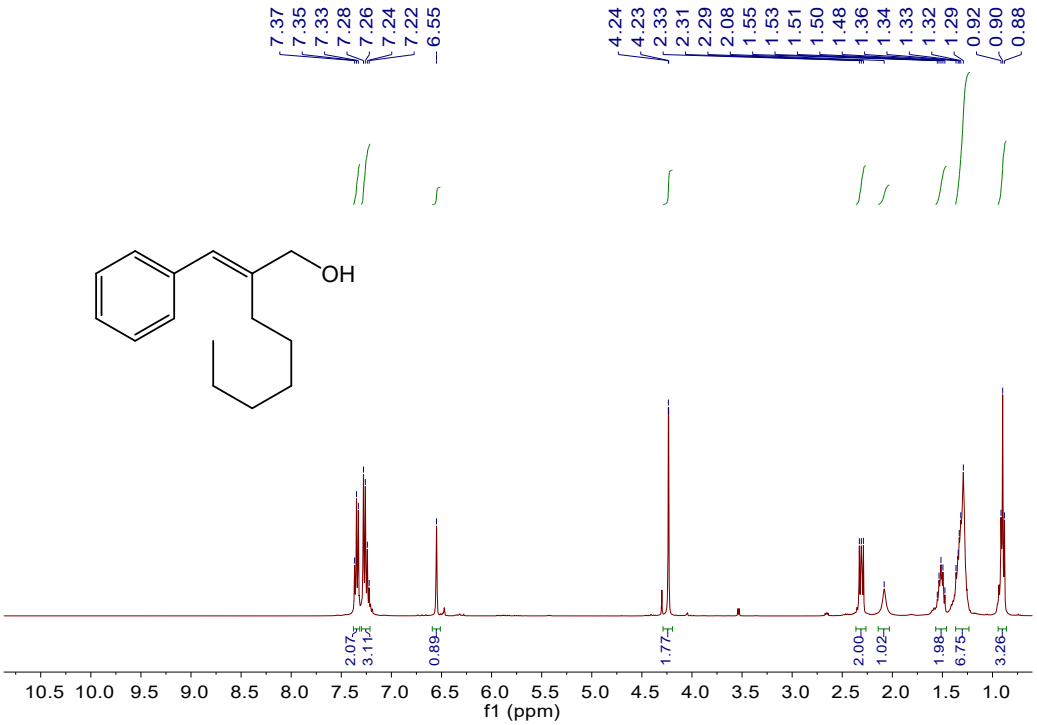

Fig. S36 ^{1}H NMR spectrum of **15h**.[9] ^{1}H NMR (400 MHz, $CDCl_3$, 298 k, ppm): δ = 0.90 (t, J_{HH} = 10.0 Hz, 3 H), 1.29-1.36 (m, 6 H), 1.48-1.55 (m, 2 H), 2.08 (br, 1 H), 2.31 (t, J_{HH} = 8.0 Hz, 2 H), 2.23 (d, J_{HH} = 0.8 Hz, 2 H), 6.55 (s, 1 H), 7.22-7.28 (m, 3 H), 7.35 (t, J_{HH} = 7.2 Hz, 2 H).

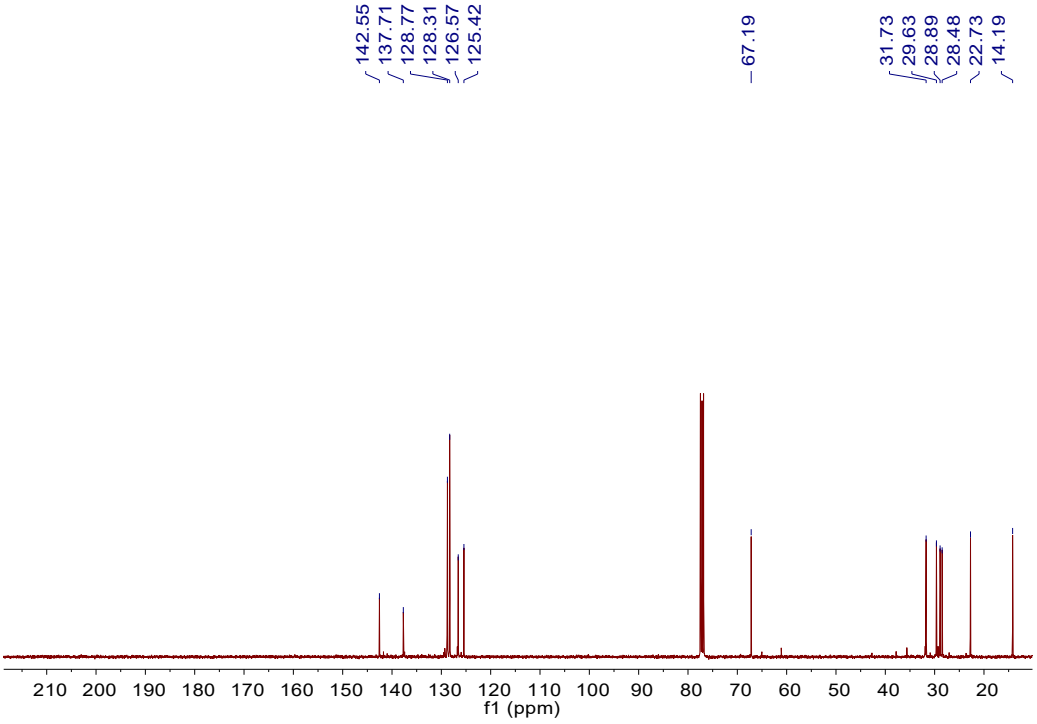

Fig. S37 ^{13}C{^{1}H} NMR spectrum of **15h**. ^{13}C{^{1}H} NMR (100 MHz, $CDCl_3$, 298 k, ppm): δ = 14.19, 22.73, 28.48, 28.89, 29.63, 31.73, 67.19, 125.42, 126.57, 128.31, 128.77, 137.71, 142.55.

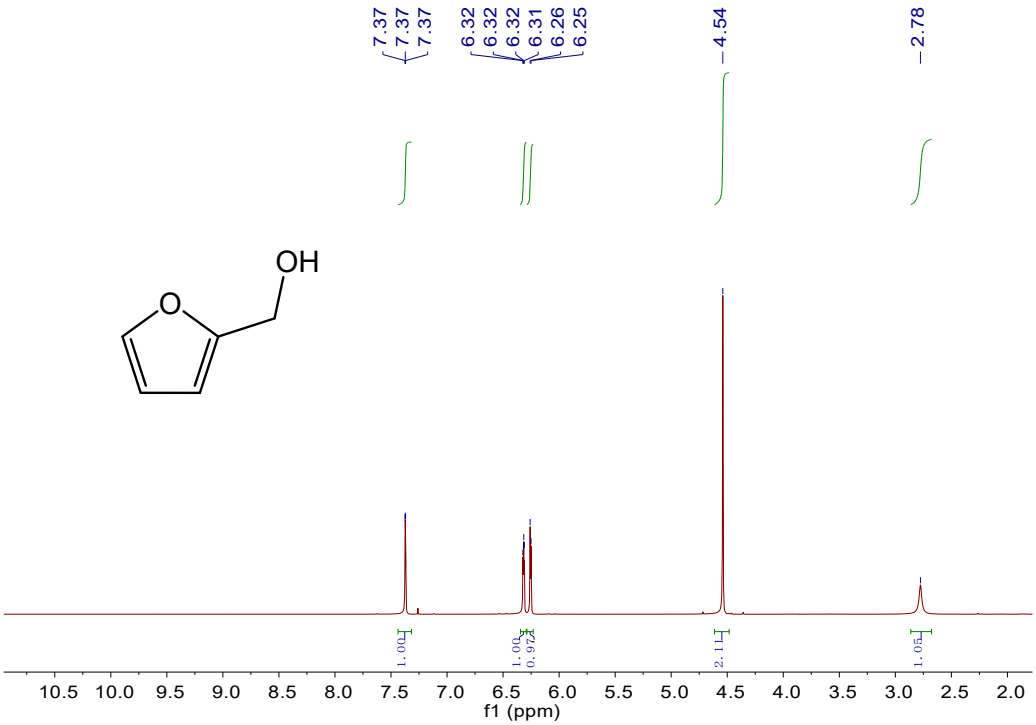

Fig. S38 ^{1}H NMR spectrum of **15i**.[10] ^{1}H NMR (400 MHz, $CDCl_3$, 298 k, ppm): δ = 2.78 (br, 1 H), 4.54 (s, 2 H), 6.25 (d, J_{HH} = 2.8 Hz, 1 H), 6.32 (dd, J_{HH} = 1.2, 2.0 Hz, 1 H), 7.37 (m, 1 H).

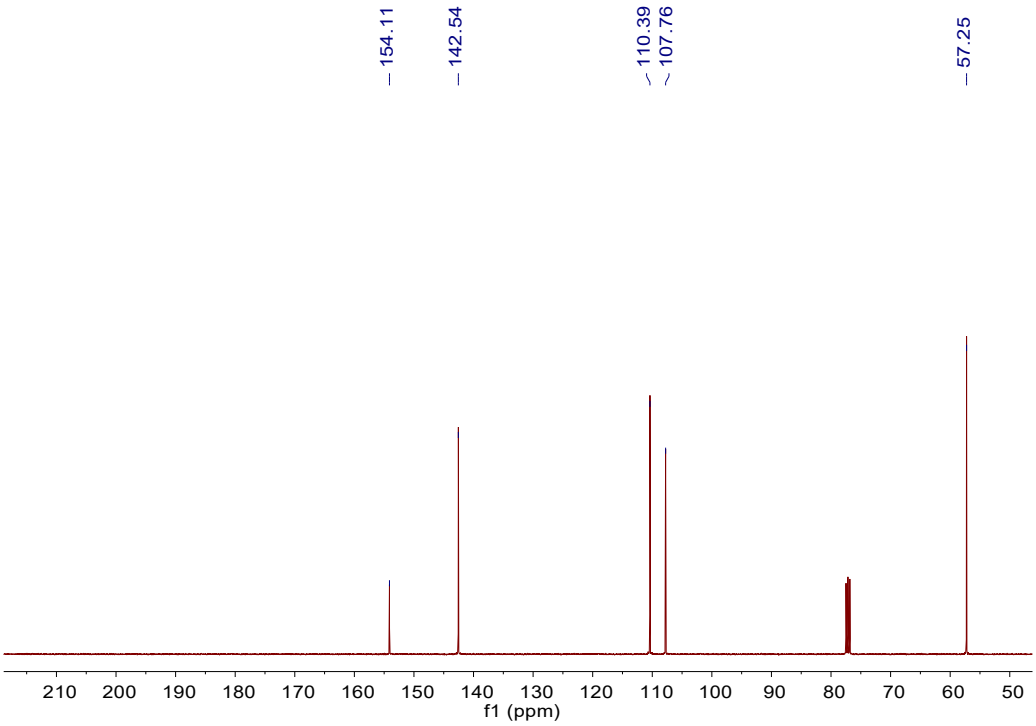

Fig. S39 ^{13}C{^{1}H} NMR spectrum of **15i**. ^{13}C{^{1}H} NMR (100 MHz, $CDCl_3$, 298 k, ppm): δ = 57.25, 107.76, 110.39, 142.54, 154.11.

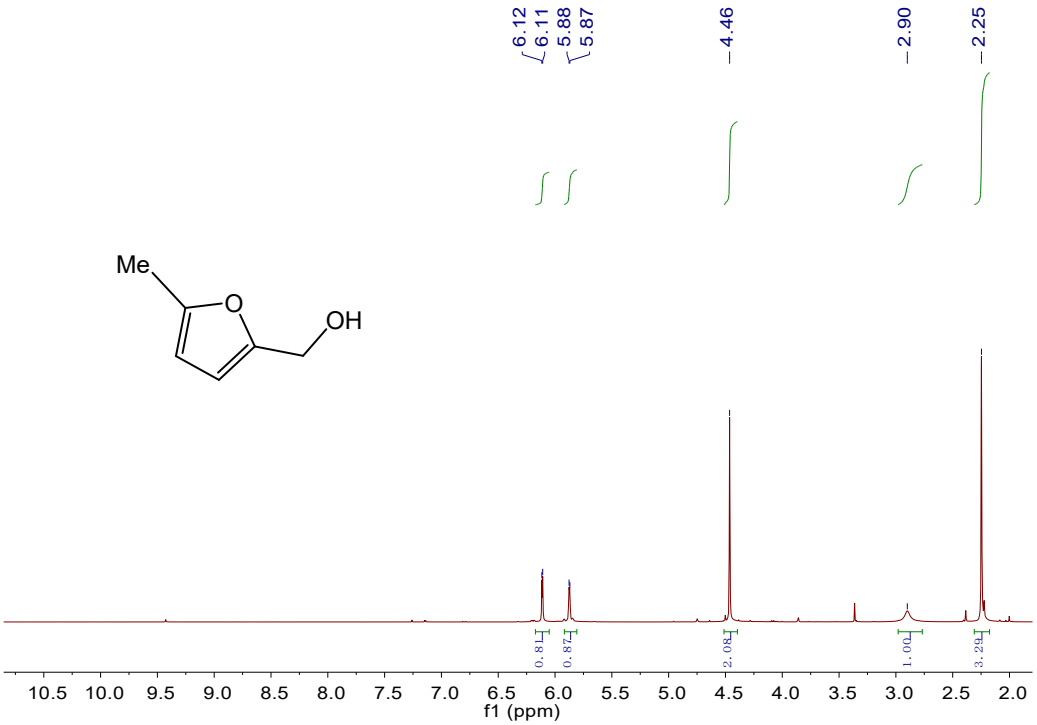

Fig. S40 ^{1}H NMR spectrum of **15j**.[11] ^{1}H NMR (400 MHz, $CDCl_3$, 298 k, ppm): δ = 2.25 (s, 3 H), 2.90 (br, 1 H), 4.46 (s, 2 H), 5.87 (d, J_{HH} = 2.4 Hz, 1 H), 6.11 (dd, J_{HH} = 2.8 Hz, 1 H).

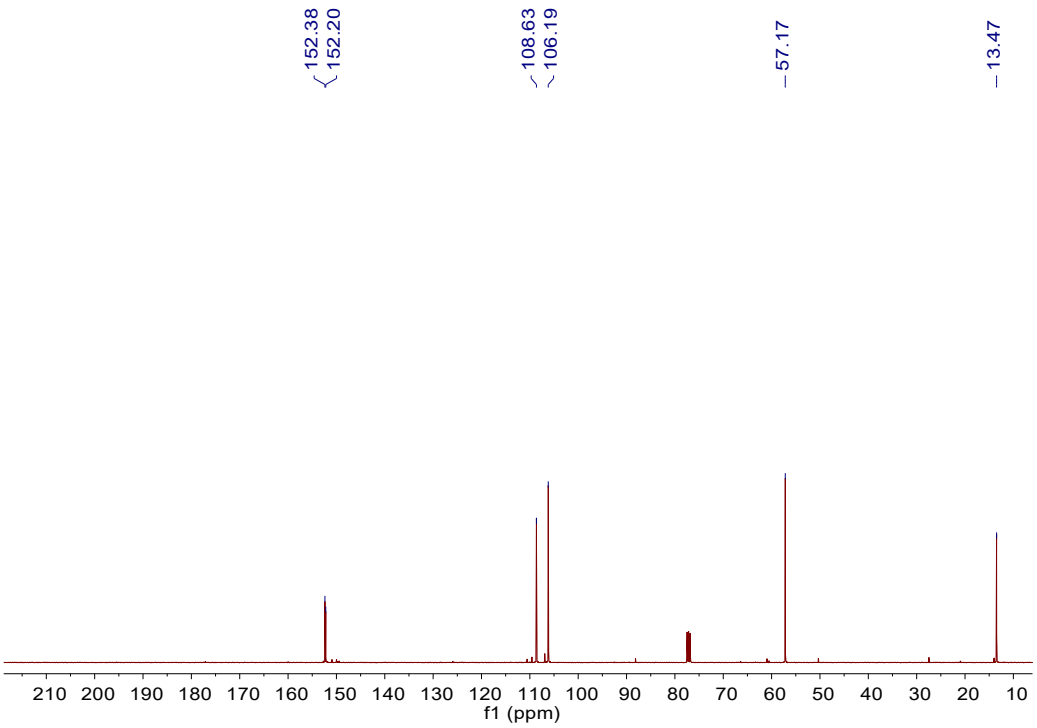

Fig. S41 ^{13}C{^{1}H} NMR spectrum of **15j**. ^{13}C{^{1}H} NMR (100 MHz, $CDCl_3$, 298 k, ppm): δ = 13.47, 57.17, 106.19, 108.63, 152.20, 152.38.

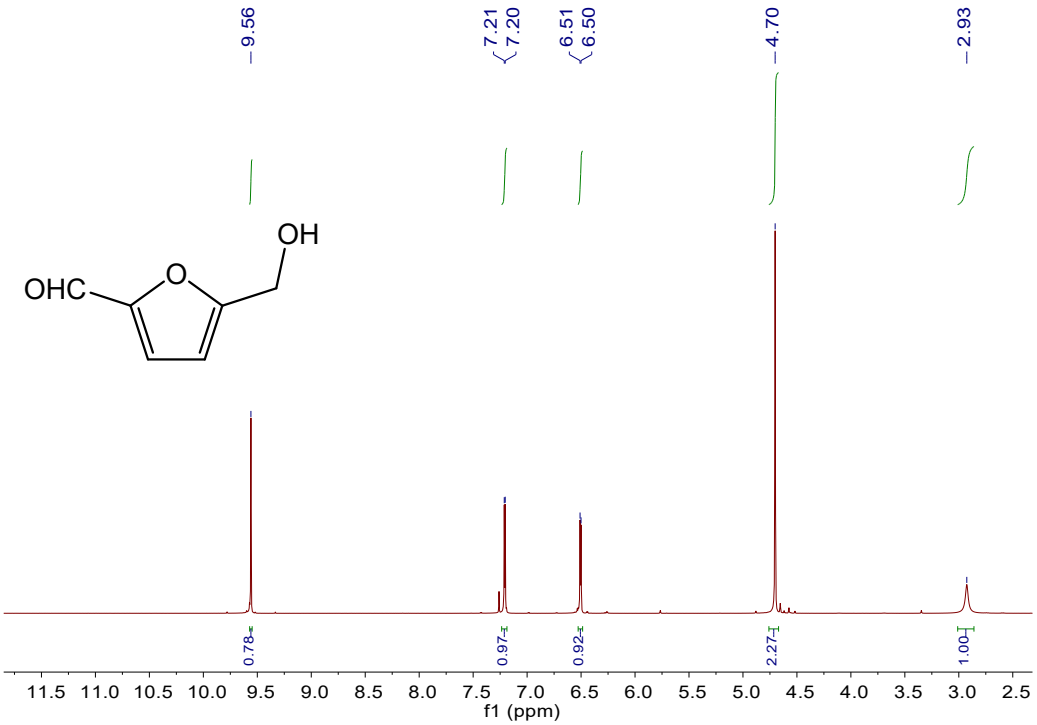

Fig. S42 ^{1}H NMR spectrum of **15k**.[10] ^{1}H NMR (400 MHz, $CDCl_3$, 298 k, ppm): δ = 2.93 (br, 1 H), 4.70 (s, 2 H), 6.51 (d, J_{HH} = 3.2 Hz, 1 H), 7.21 (d, J_{HH} = 3.6 Hz, 1 H), 9.56 (s, 1 H).

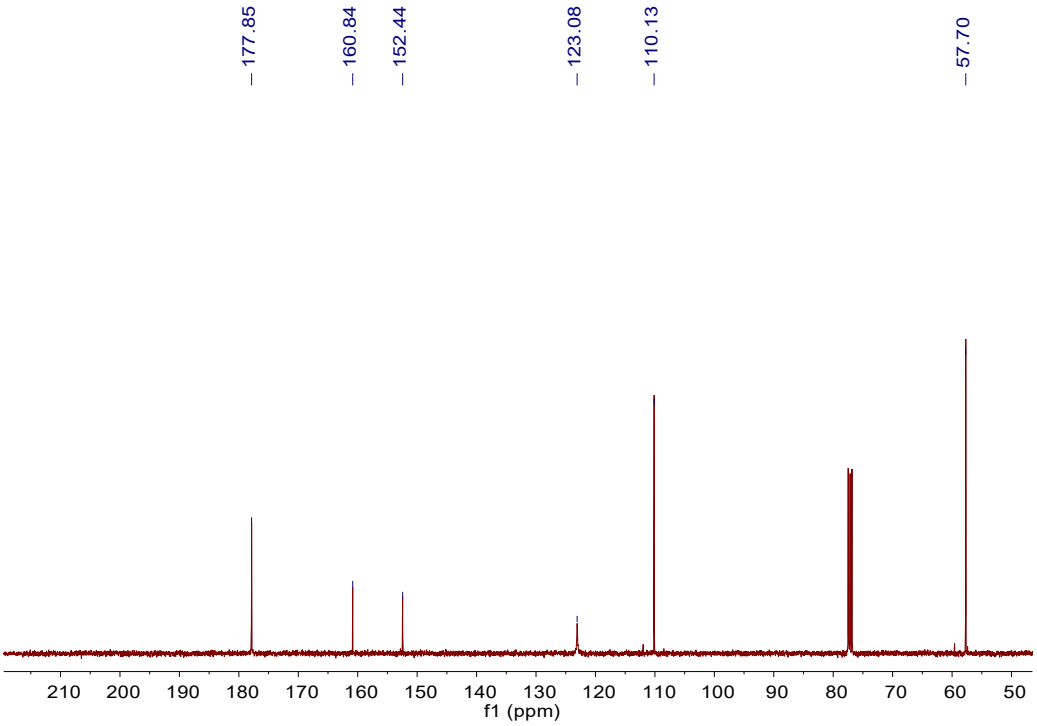

Fig. S43 ^{13}C{^{1}H} NMR spectrum of **15k**. ^{13}C{^{1}H} NMR (100 MHz, $CDCl_3$, 298 k, ppm): δ = 57.70, 110.13, 123.08, 152.44, 160.84, 177.85.

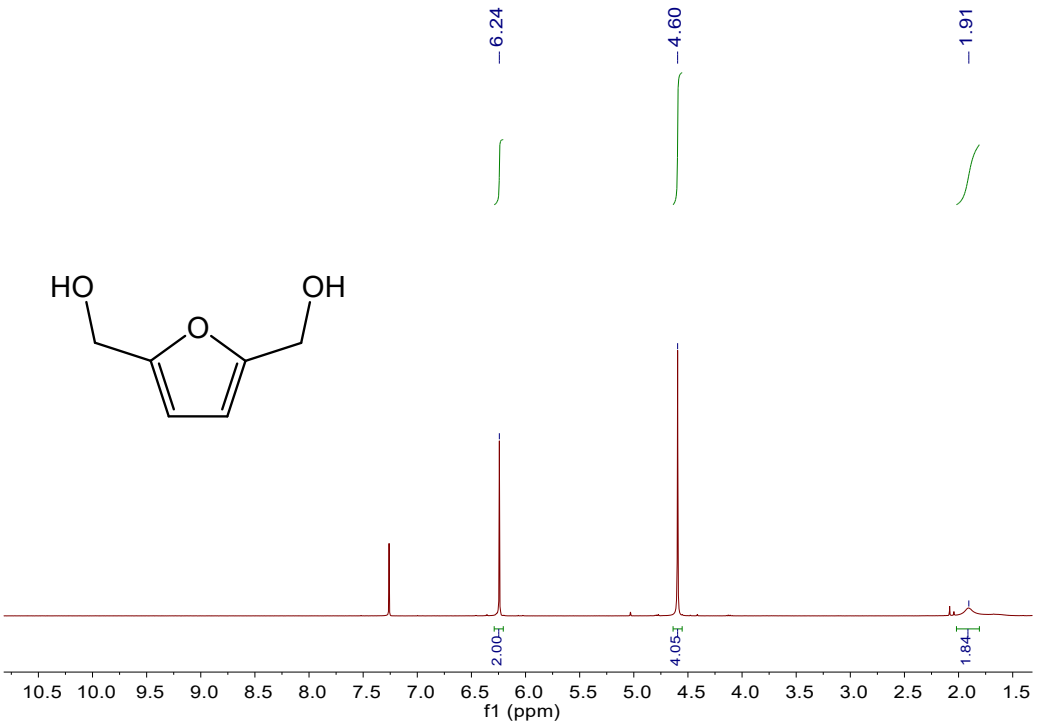

Fig. S44 ^{1}H NMR spectrum of **15l**.[10] ^{1}H NMR (400 MHz, $CDCl_3$, 298 k, ppm): δ = 1.91 (br, 2 H), 4.60 (s, 4 H), 6.24 (s, 2 H).

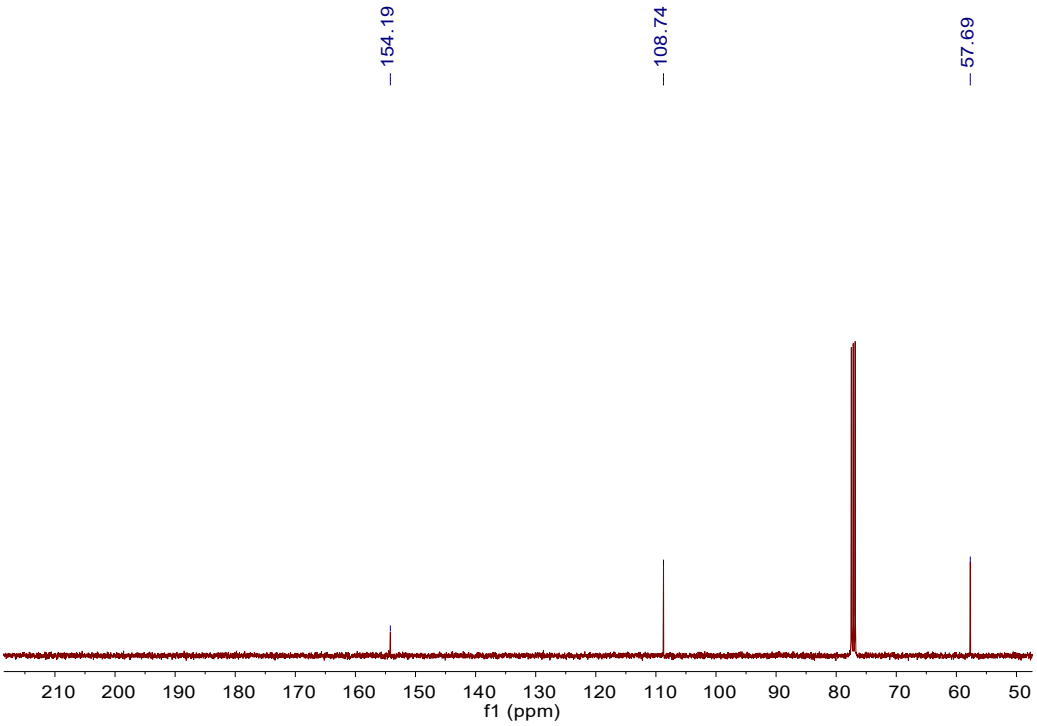

Fig. S45 ^{13}C{^{1}H} NMR spectrum of **15l**. ^{13}C{^{1}H} NMR (100 MHz, $CDCl_3$, 298 k, ppm): δ = 57.69, 108.74, 154.19.

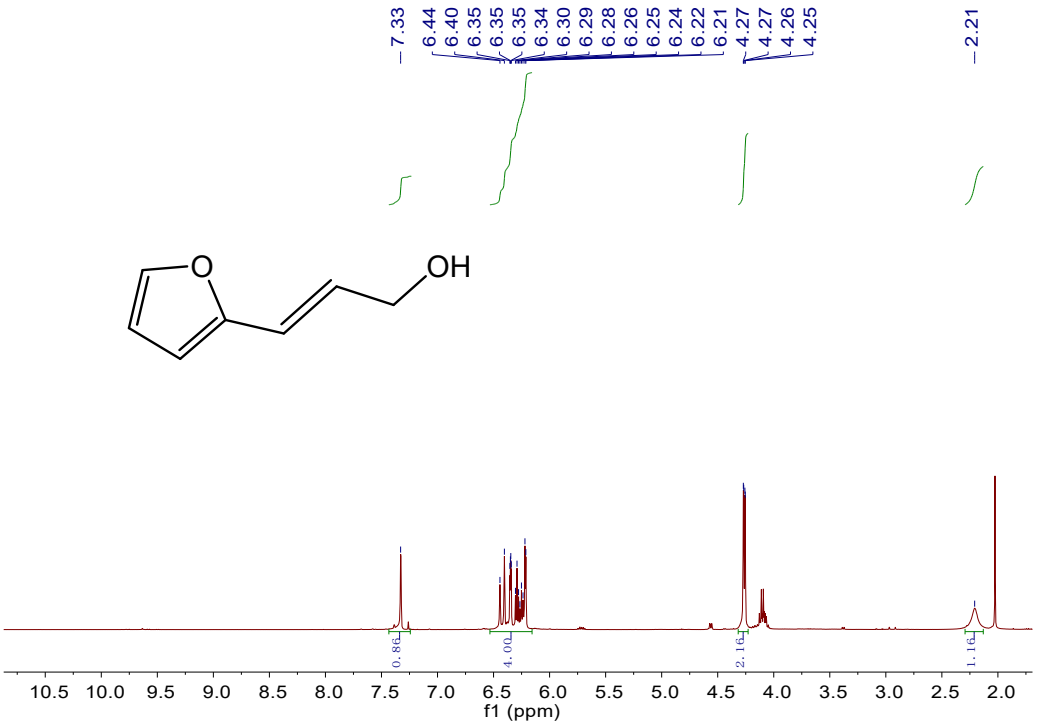

Fig. S46 ^{1}H NMR spectrum of **15m**.[7] ^{1}H NMR (400 MHz, $CDCl_3$, 298 k, ppm): δ = 2.21 (br, 1 H), 4.26 (dd, , J_{HH} = 1.2, 4.0 Hz, 2 H), 6.21-6.44 (m, 4 H), 7.33 (s, 1 H).

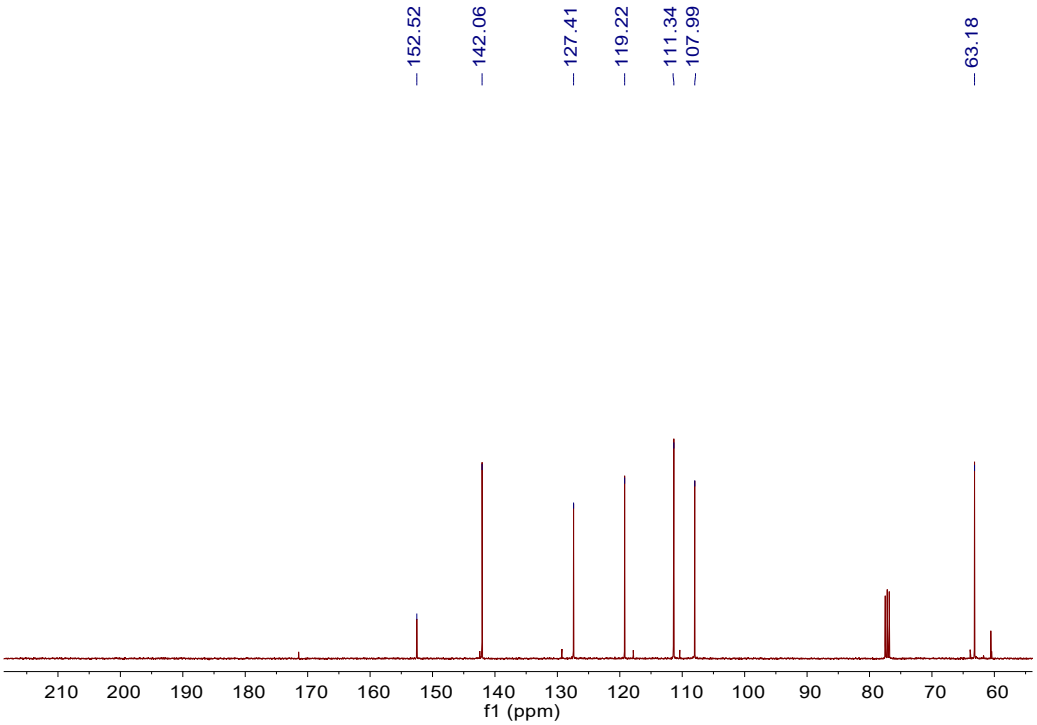

Fig. S47 ^{13}C{^{1}H} NMR spectrum of **15m**. ^{13}C{^{1}H} NMR (100 MHz, $CDCl_3$, 298 k, ppm): δ = 63.18, 107.99, 111.34, 119.22, 127.41, 142.06, 152.52.

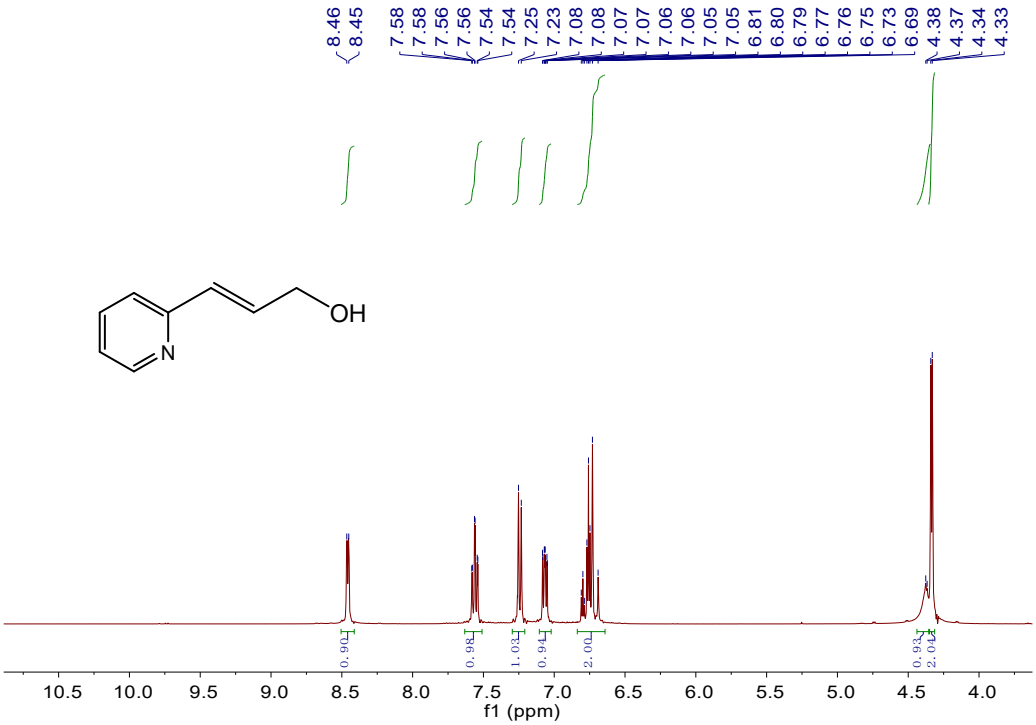

Fig. S48 ^{1}H NMR spectrum of **15n**.[12] ^{1}H NMR (400 MHz, $CDCl_3$, 298 k, ppm): δ = 4.33 (d, J_{HH} = 4.4 Hz, 2 H), 4.37 (d, J_{HH} = 3.6 Hz, 1 H), 6.69-6.81 (m, 2 H), 7.05-7.08 (m, 1 H), 7.24 (d, J_{HH} = 7.6 Hz, 1 H), 7.54-7.58 (m, 1 H), 8.46 (d, J_{HH} = 4.8 Hz, 1 H).

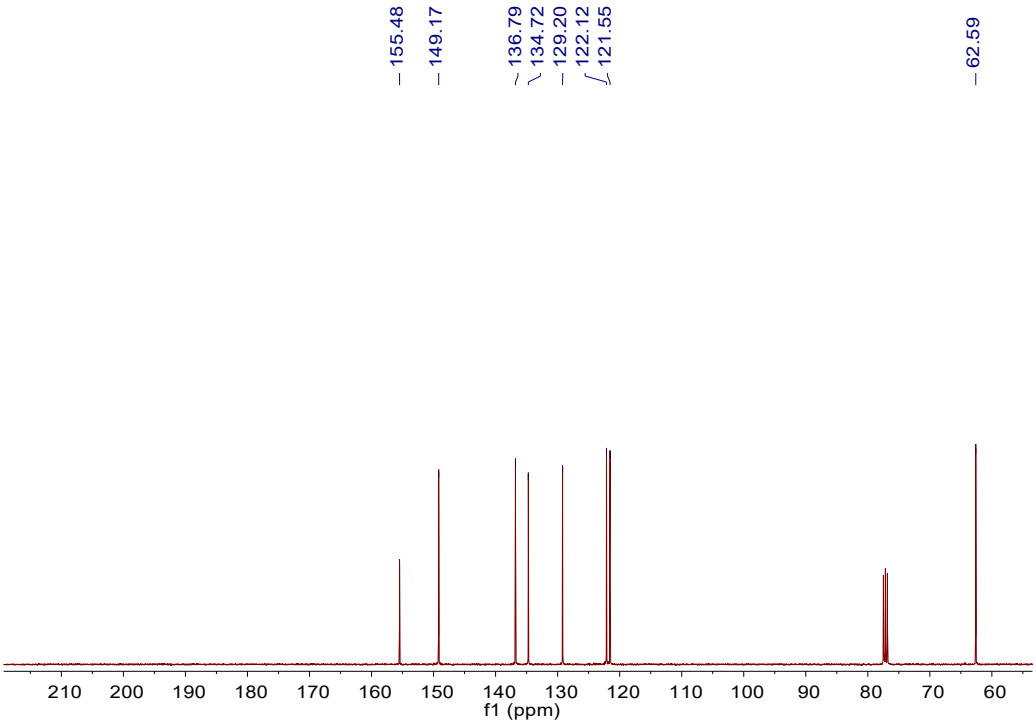

Fig. S49 ^{13}C{^{1}H} NMR spectrum of **15n**. ^{13}C{^{1}H} NMR (100 MHz, $CDCl_3$, 298 k, ppm): δ = 62.59, 121.55, 122.12, 129.20, 134.72, 136.79, 149.17, 155.48.

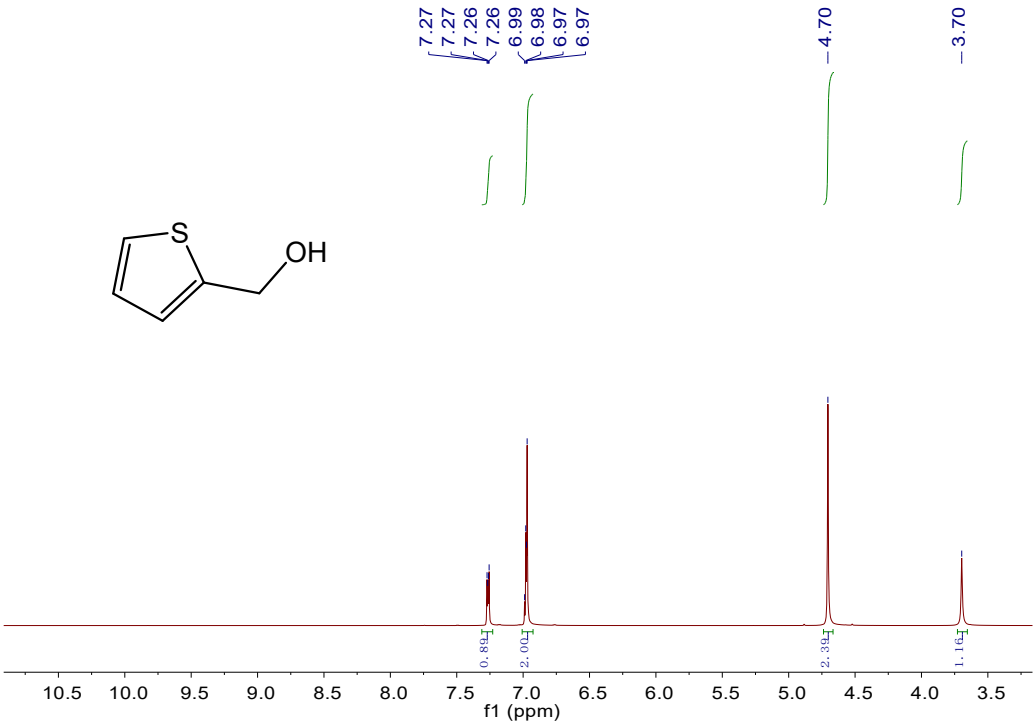

Fig. S50 ^{1}H NMR spectrum of **15q**.[7] ^{1}H NMR (400 MHz, $CDCl_3$, 298 k, ppm): δ = 3.70 (s, 1 H), 4.70 (s, 2 H), 6.97-6.99 (m, 2 H), 7.27 (dd, J_{HH} = 2.0, 2.4 Hz, 1 H).

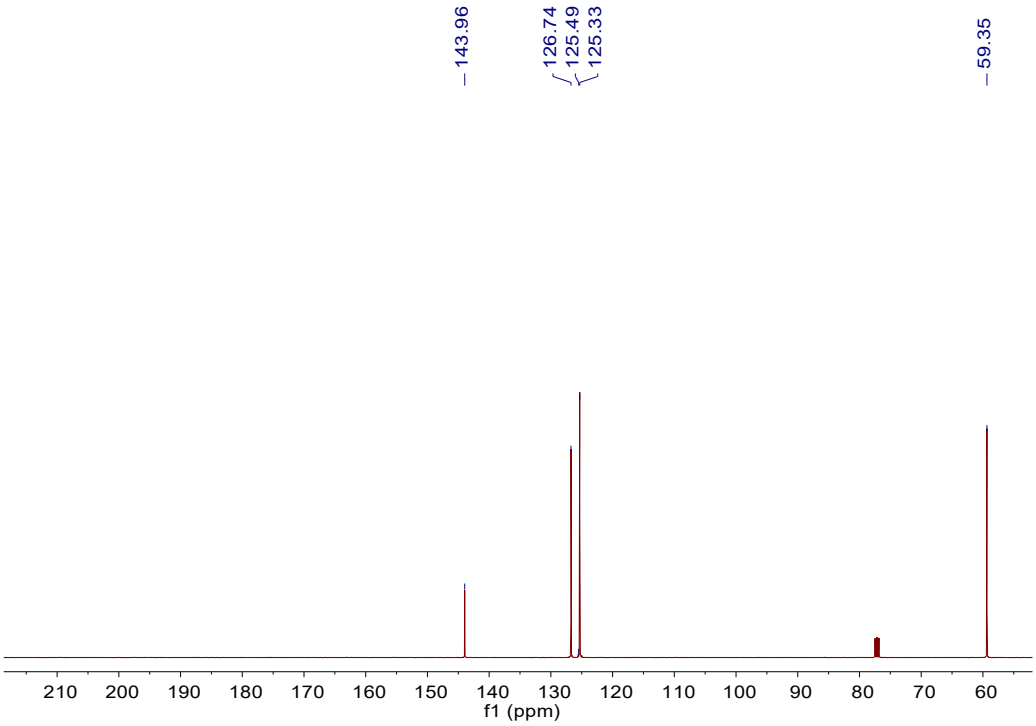

Fig. S51 ^{13}C{^{1}H} NMR spectrum of **15q**. ^{13}C{^{1}H} NMR (100 MHz, $CDCl_3$, 298 k, ppm): δ = 59.35, 125.33, 125.49, 126.74, 143.96.

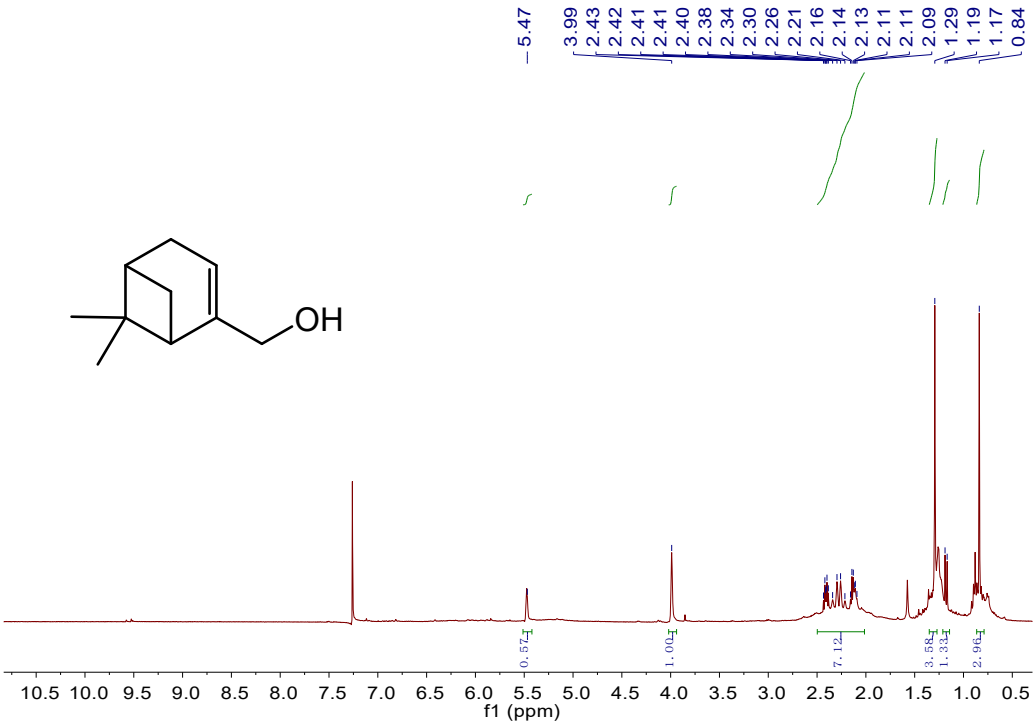

Fig. S52 ^{1}H NMR spectrum of **15r**.[13] ^{1}H NMR (400 MHz, $CDCl_3$, 298 k, ppm): δ = 0.84 (s, 3 H), 1.18 (d, J_{HH} = 8.8 Hz, 1 H), 1.29 (s, 3 H), 2.09-2.43 (m, 7 H), 3.99 (s, 1 H), 5.47 (s, 1 H).

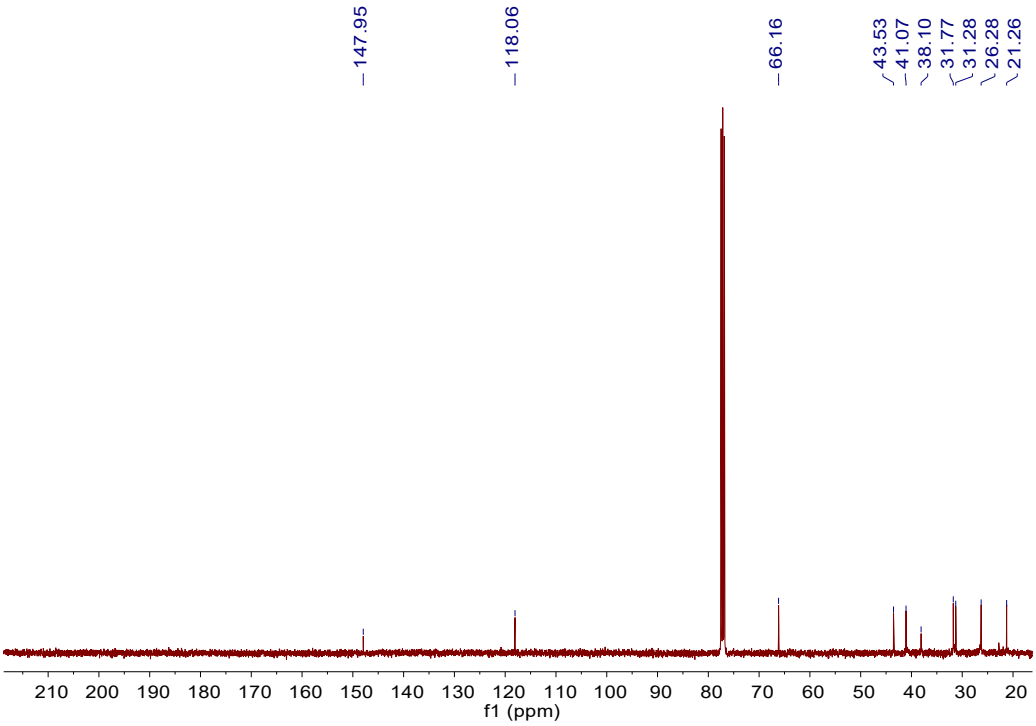

Fig. S53 ^{13}C{^{1}H} NMR spectrum of **15r**. ^{13}C{^{1}H} NMR (100 MHz, $CDCl_3$, 298 k, ppm): δ = 21.26, 26.28, 31.28, 31.77, 38.10, 41.07, 43.53, 66.16, 118.06, 147.95.

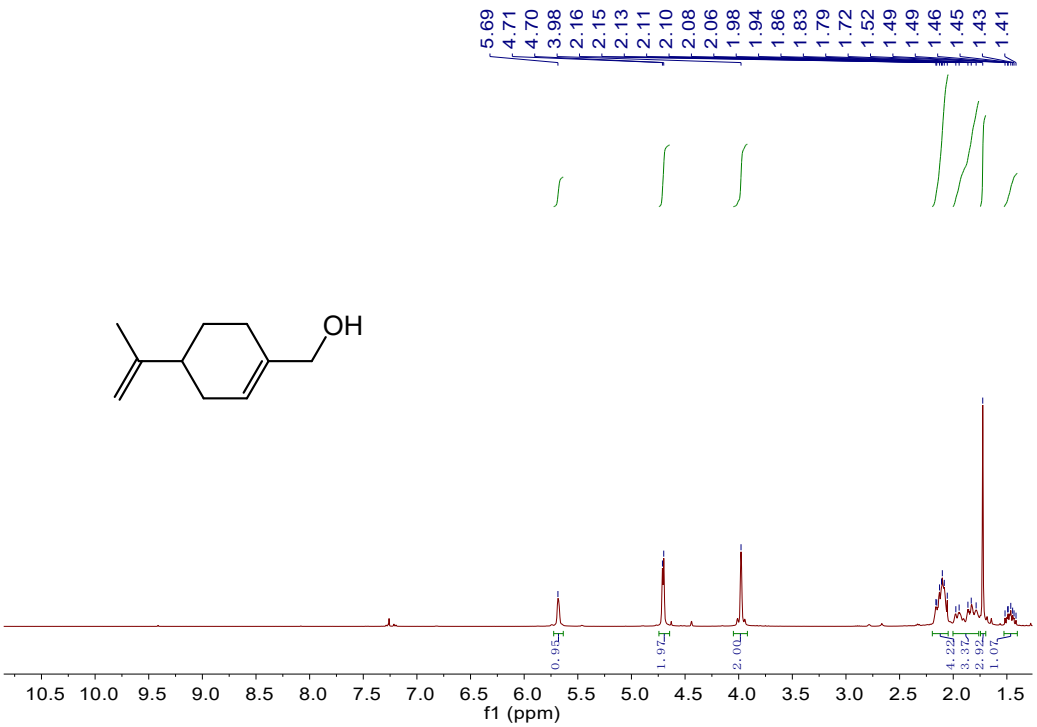

Fig. S54 ^{1}H NMR spectrum of **15s**.[9] ^{1}H NMR (400 MHz, $CDCl_3$, 298 k, ppm): δ = 1.41-1.52 (m, 1 H), 1.72 (s, 3 H), 1.79-1.98 (m, 3 H), 2.06-2.16 (m, 4 H), 3.98 (s, 2 H), 4.71 (d, J_{HH} = 4.8 Hz, 2 H), 5.69 (s, 1 H).

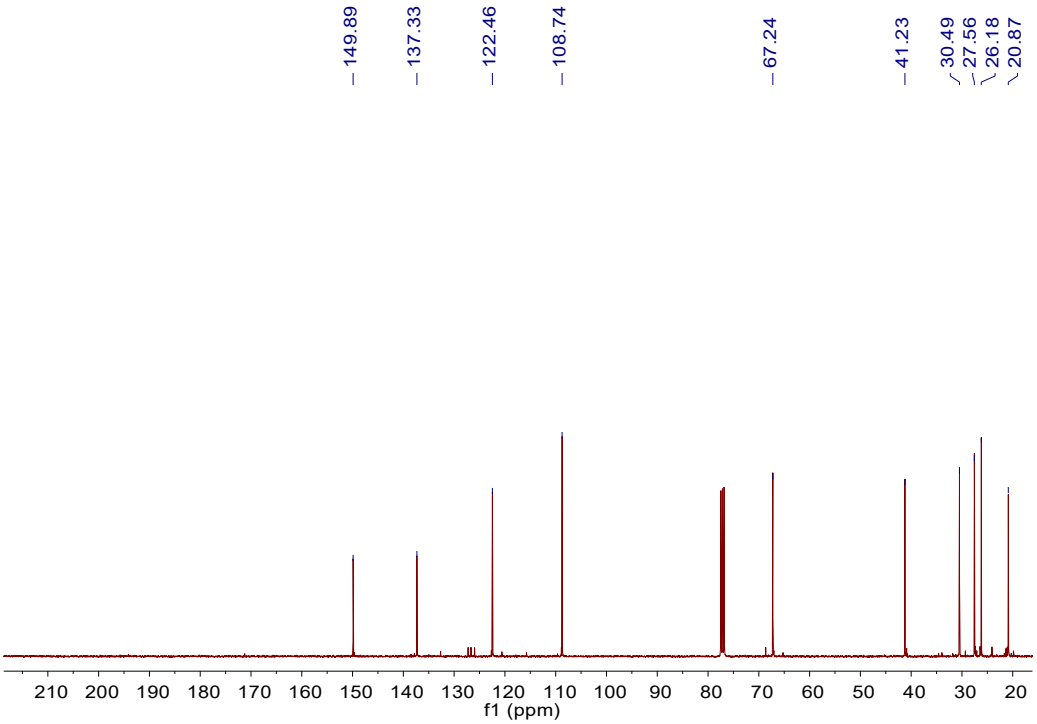

Fig. S55 ^{13}C{^{1}H} NMR spectrum of **15s**. ^{13}C{^{1}H} NMR (100 MHz, $CDCl_3$, 298 k, ppm): δ = 20.87, 26.18, 27.56, 30.49, 41.23, 67.24, 108.74, 122.46, 137.33, 149.89.

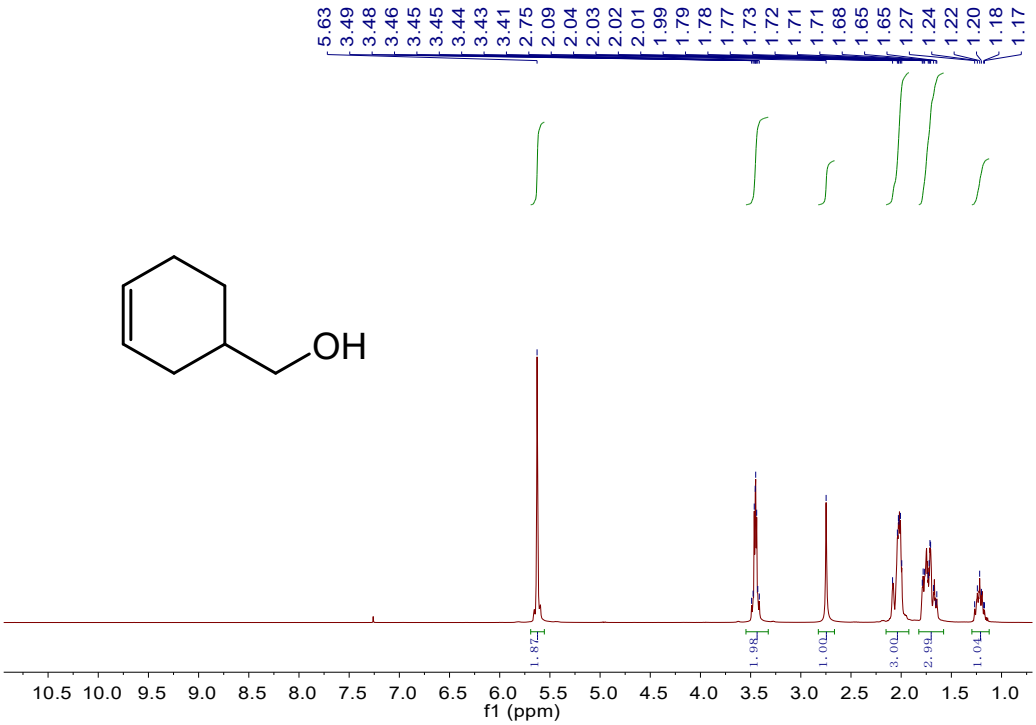

Fig. S56 ^{1}H NMR spectrum of **15t**.[9] ^{1}H NMR (400 MHz, $CDCl_3$, 298 k, ppm): δ = 1.17-1.27 (m, 1 H), 1.65-1.79 (m, 3 H), 1.99-2.09 (m, 3 H), 2.75 (s, 1 H), 3.41-3.49 (m, 2 H), 5.63 (s, 2 H).

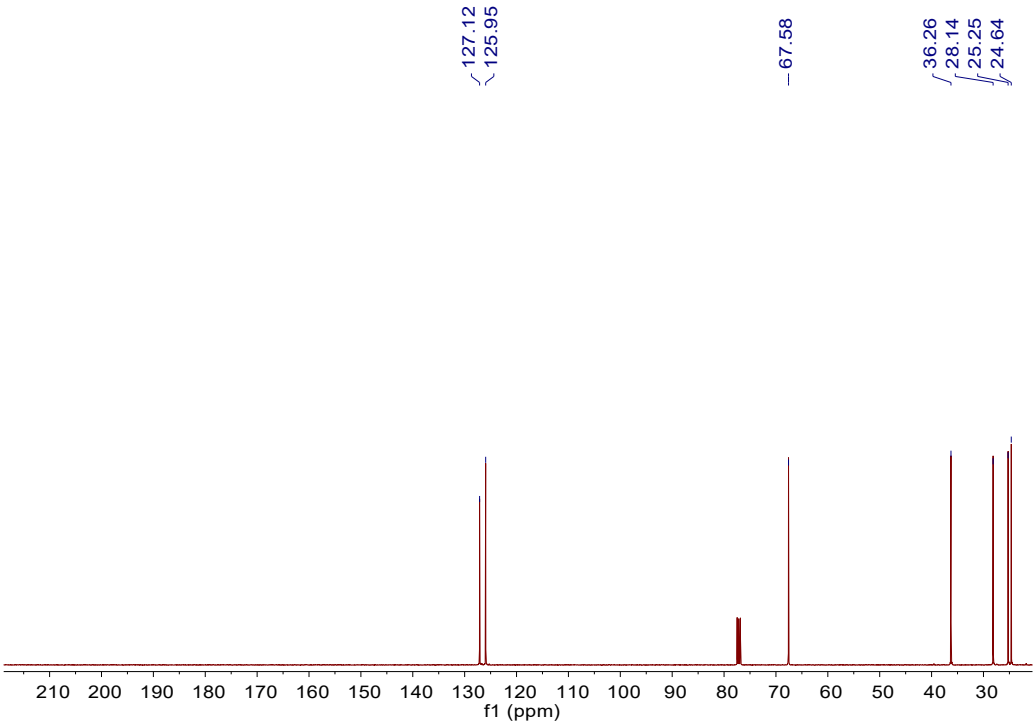

Fig. S57 ^{13}C{^{1}H} NMR spectrum of **15t**. ^{13}C{^{1}H} NMR (100 MHz, $CDCl_3$, 298 k, ppm): δ = 24.64, 25.25, 28.14, 36.26, 67.58, 125.95, 127.12.

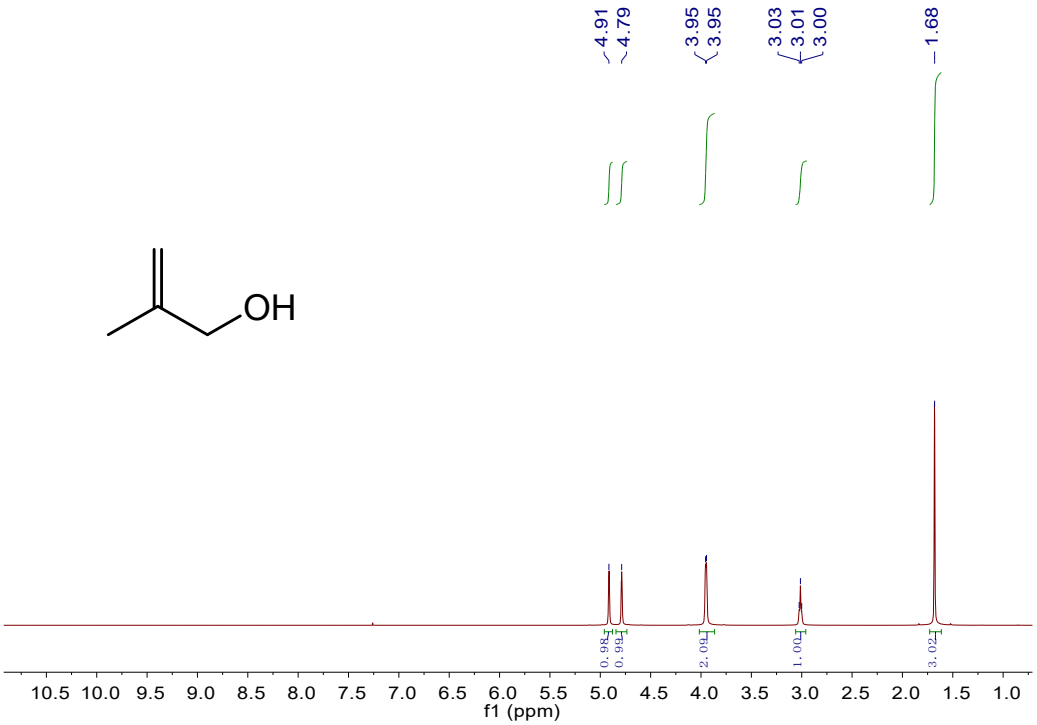

Fig. S58 ^{1}H NMR spectrum of **15u**.[14] ^{1}H NMR (400 MHz, $CDCl_3$, 298 k, ppm): δ = 1.68 (s, 3 H), 3.01 (t, J_{HH} = 4.8 Hz, 1 H), 3.95 (d, J_{HH} = 3.6 Hz, 2 H), 4.79 (s, 1 H), 4.91 (s, 1 H).

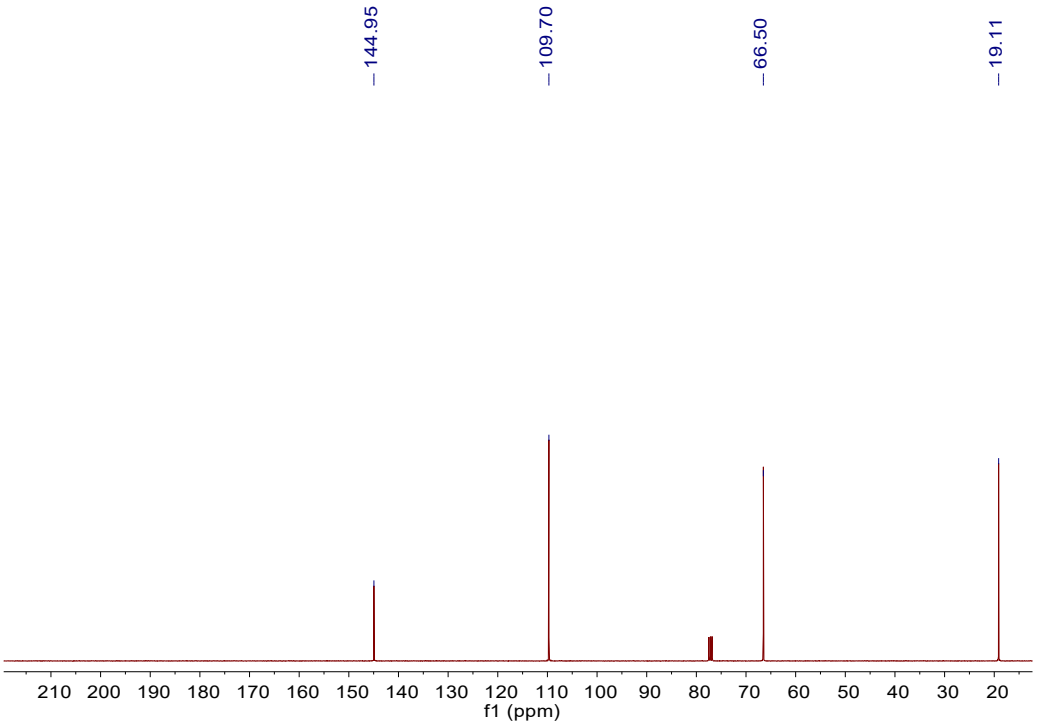

Fig. S59 ^{13}C{^{1}H} NMR spectrum of **15u**. ^{13}C{^{1}H} NMR (100 MHz, $CDCl_3$, 298 k, ppm): δ = 19.11, 66.50, 109.70, 144.95.

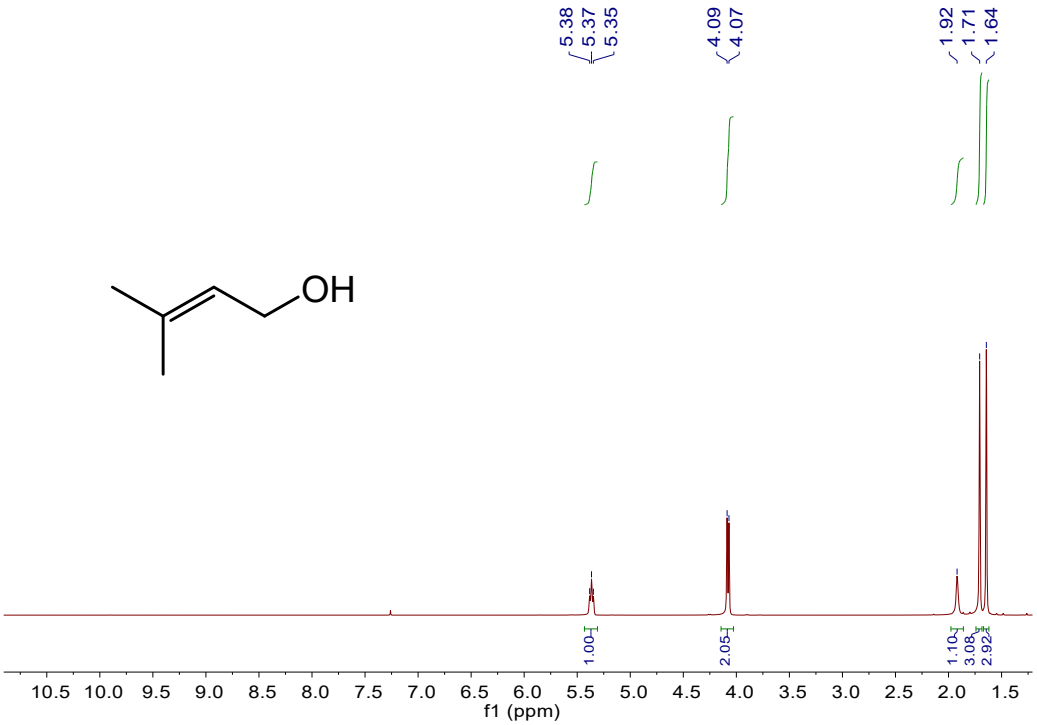

Fig. S60 ^{1}H NMR spectrum of **15v**.[15] ^{1}H NMR (400 MHz, $CDCl_3$, 298 k, ppm): δ = 1.64 (s, 3 H), 1.71 (s, 3 H), 1.92 (br, 1 H), 4.08 (d, J_{HH} = 6.8 Hz, 2 H), 5.37 (t, J_{HH} = 7.2 Hz, 1 H).

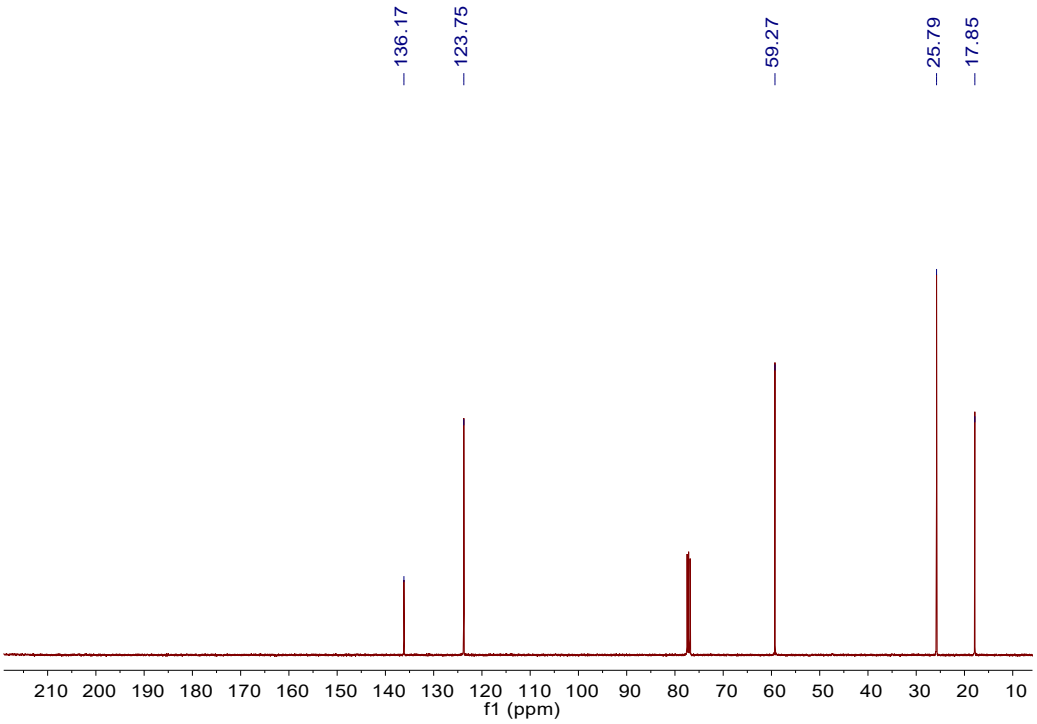

Fig. S61 ^{13}C{^{1}H} NMR spectrum of **15v**. ^{13}C{^{1}H} NMR (100 MHz, $CDCl_3$, 298 k, ppm): δ = 17.85, 25.79, 59.27, 123.75, 136.17.

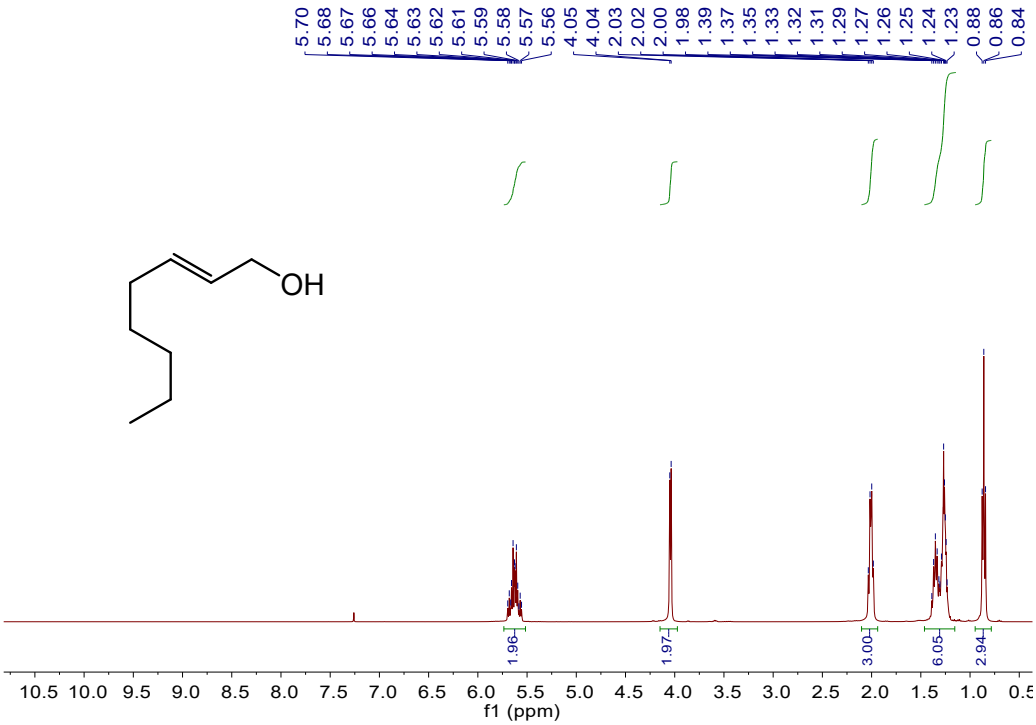

Fig. S62 ^{1}H NMR spectrum of **15w**.[16] ^{1}H NMR (400 MHz, $CDCl_3$, 298 k, ppm): δ = 0.86 (t, J_{HH} = 6.8 Hz, 3 H), 1.23-1.39 (m, 6 H), 2.01 (q, J_{HH} = 6.8 Hz, 3 H), 5.56-5.70 (m, 2 H).

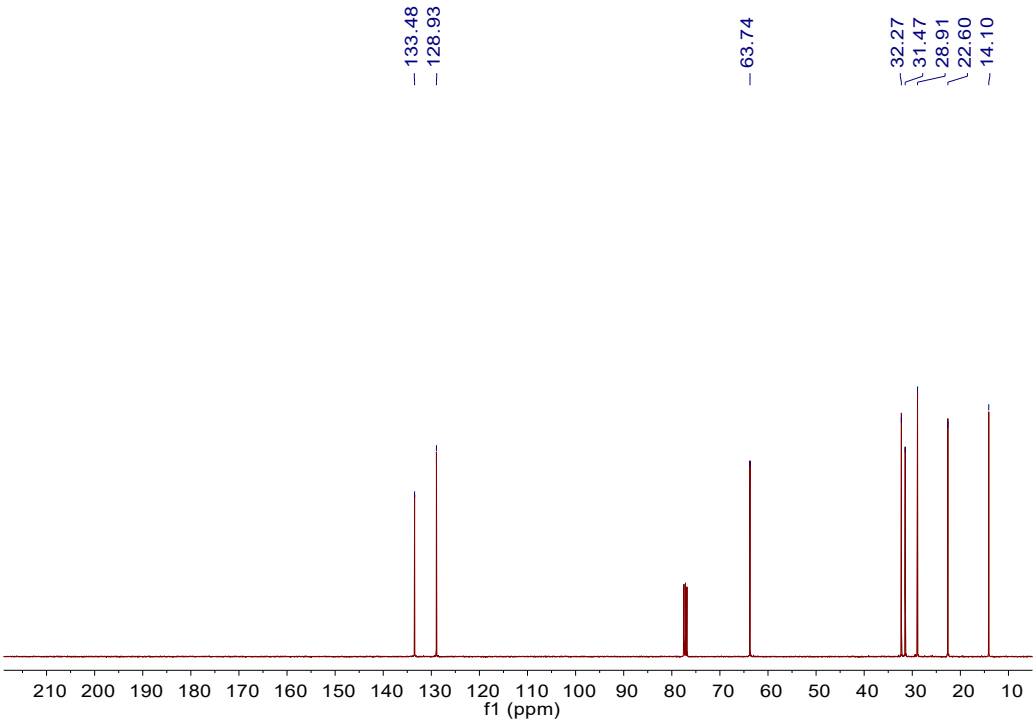

Fig. S63 ^{13}C{1H} NMR spectrum of **15w**. ^{13}C{^{1}H} NMR (100 MHz, $CDCl_3$, 298 k, ppm): δ = 14.10, 22.60, 28.91, 31.47, 32.27, 63.74, 128.93, 133.48.

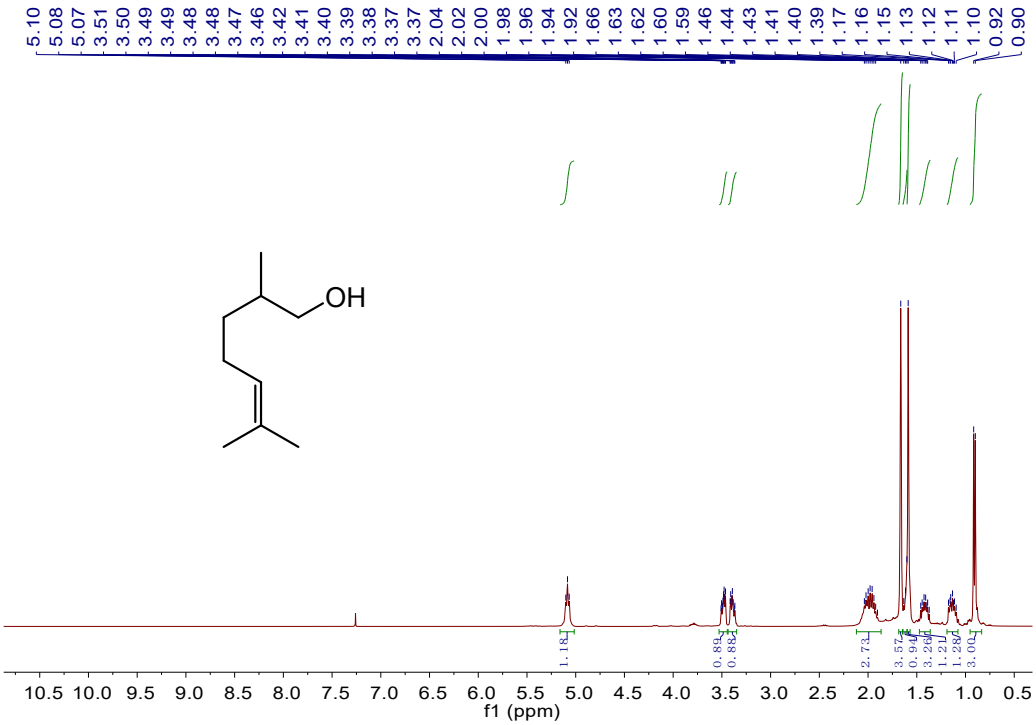

Fig. S64 ^{1}H NMR spectrum of **15x**.[15] ^{1}H NMR (400 MHz, $CDCl_3$, 298 k, ppm): δ = 0.91 (d, J_{HH} = 6.8 Hz, 3 H), 1.10-1.17 (m, 1 H), 1.37-1.46 (m, 1 H), 1.59 (s, 3 H), 1.60-1,63 (m, 1 H), 1.66 (s, 3 H), 1.90-2.04 (m, 3 H), 3.37-3.42 (m, 1 H), 3.46-3.51 (m, 1 H), 5.08 (t, J_{HH} = 7.2 Hz, 1 H).

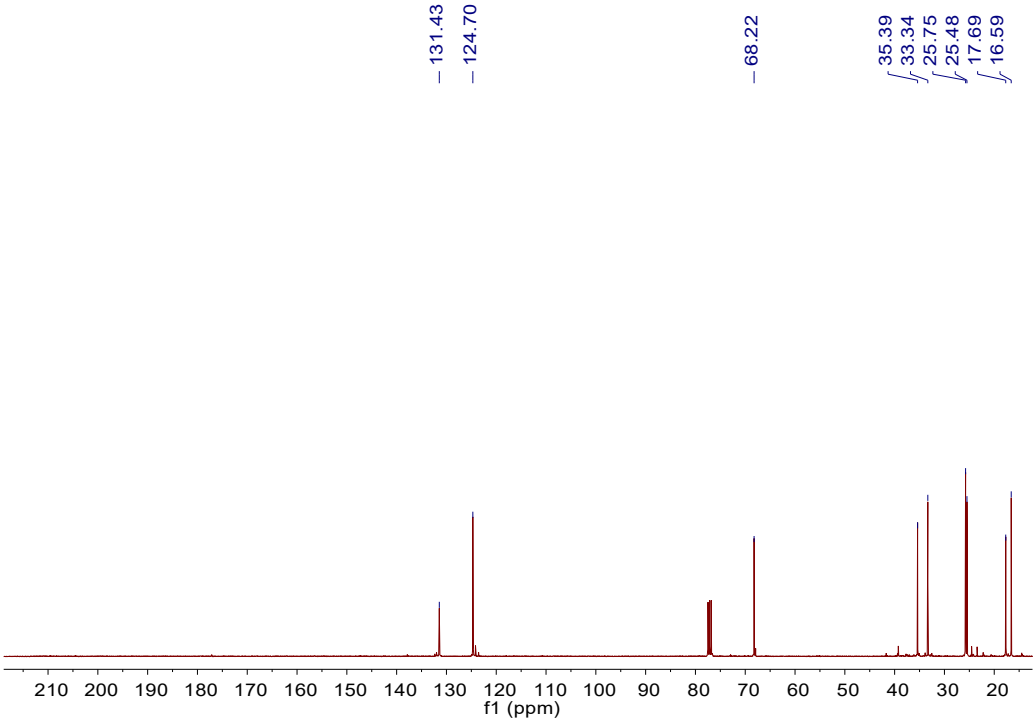

Fig. S65 ^{13}C{1H} NMR spectrum of **15x**. ^{13}C{^{1}H} NMR (100 MHz, $CDCl_3$, 298 k, ppm): δ = 16.59, 17.69, 25.48, 25.75, 33.34, 35.39, 68.22, 124.70, 131.43.

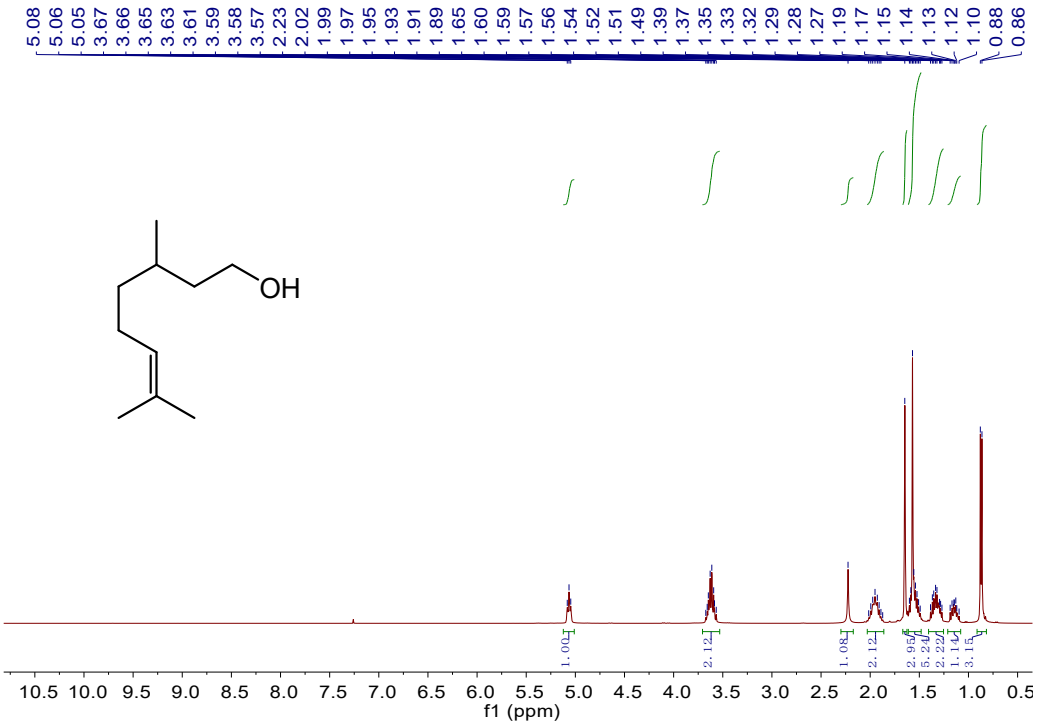

Fig. S66 ^{1}H NMR spectrum of **15y**.[7] ^{1}H NMR (400 MHz, $CDCl_3$, 298 k, ppm): δ = 0.87 (d, J_{HH} = 6.4 Hz, 3 H), 1.10-1.19 (m, 1 H), 1.27-1.39 (m, 2 H), 1.49-1.60 (m, 5 H), 1.65 (s, 3 H), 1.87-2.02 (m, 2 H), 2.23 (s, 1 H), 3.57-3.67 (m, 2 H), 5.06 (t, J_{HH} = 6.8 Hz, 1 H).

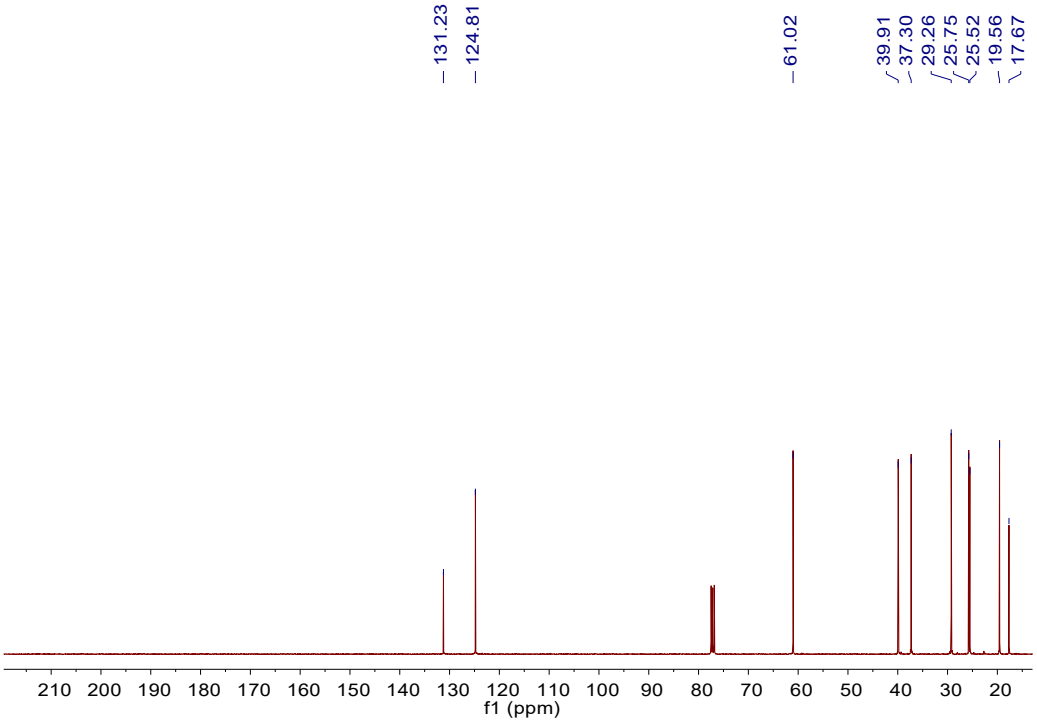

Fig. S67 ^{13}C{1H} NMR spectrum of **15y**. ^{13}C{^{1}H} NMR (100 MHz, $CDCl_3$, 298 k, ppm): δ = 17.67, 19.56, 25.52, 25.75, 29.26, 37.30, 39.91, 61.02, 124.81, 131.23.

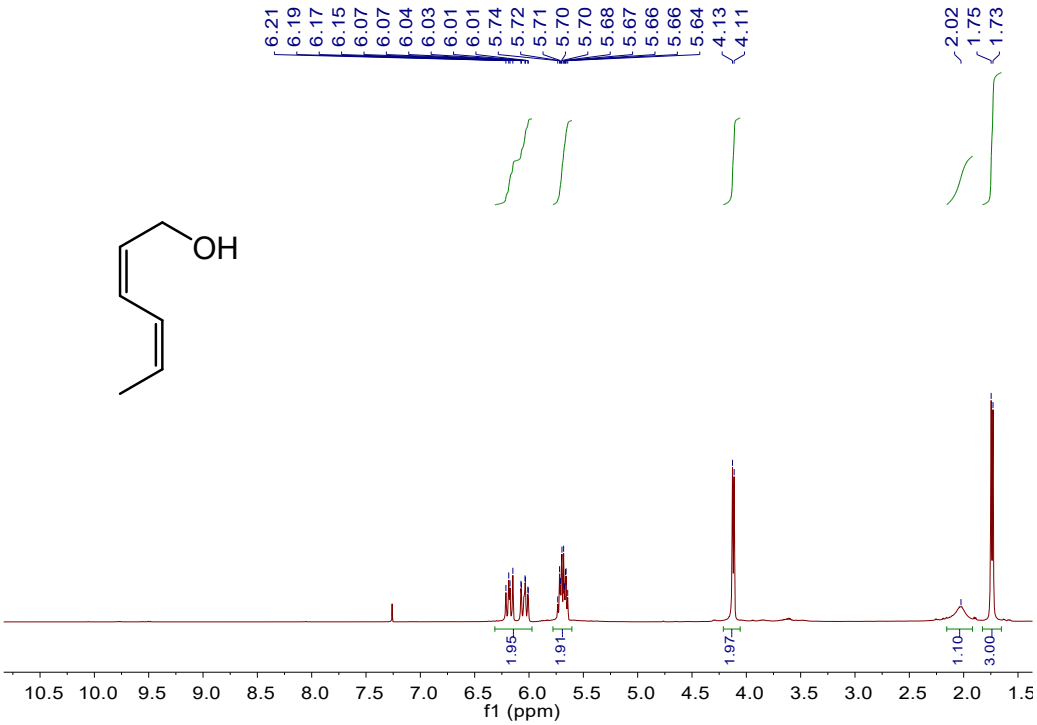

Fig. S68 ^{1}H NMR spectrum of **15z**.[17] ^{1}H NMR (400 MHz, $CDCl_3$, 298 k, ppm): δ = 1.74 (d, J_{HH} = 6.8 Hz, 3 H), 2.02 (br, 1 H), 4.12 (d, J_{HH} = 6.0 Hz, 2 H), 5.64-5.74 (m, 2 H), 6.01-6.21 (m, 2 H).

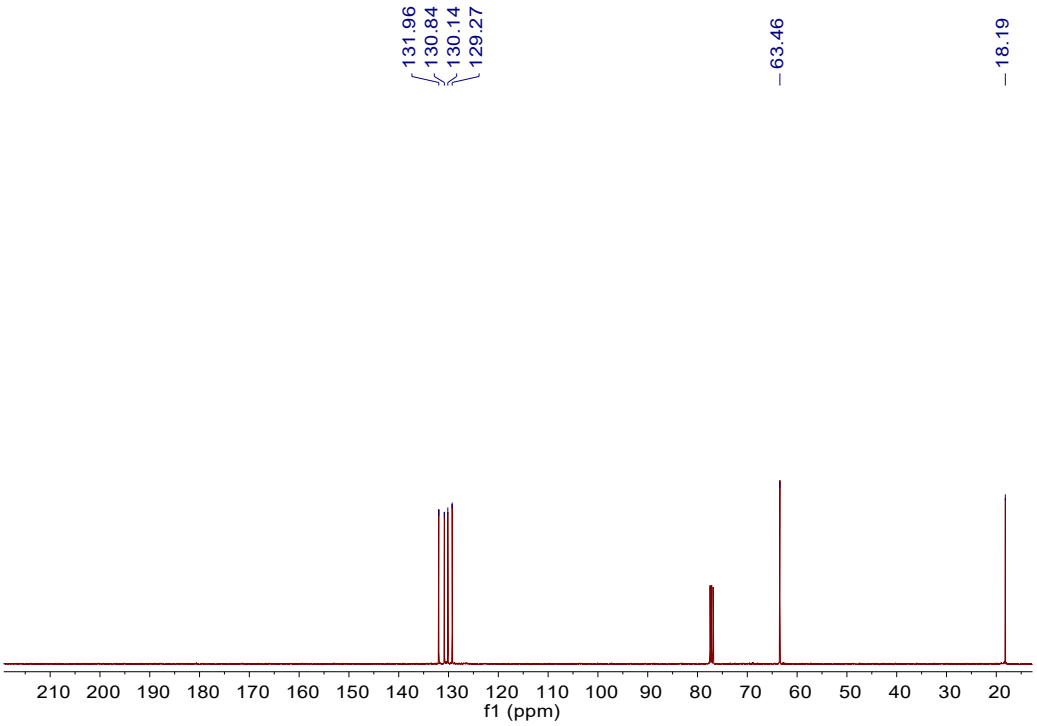

Fig. S69 ^{13}C{^{1}H} NMR spectrum of **15z**. ^{13}C{^{1}H} NMR (100 MHz, $CDCl_3$, 298 k, ppm): δ = 18.19, 63.46, 129.27, 130.14, 130.84, 131.96.

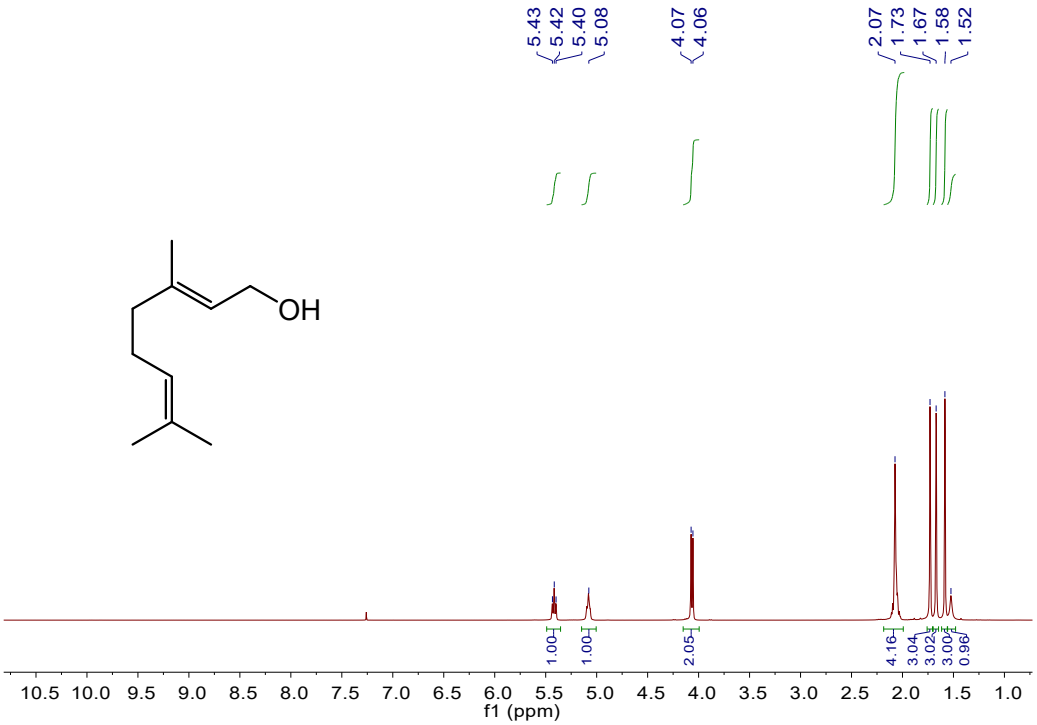

Fig. S70 ^{1}H NMR spectrum of **15aa**.[7] ^{1}H NMR (400 MHz, $CDCl_3$, 298 k, ppm): δ = 1.52 (s, 1 H), 1.58 (s, 3 H), 1.67 (s, 3 H), 1.73 (s, 3 H), 2.07 (s, 4 H), 4.06 (d, J_{HH} = 7.2 Hz, 2 H), 5.08 (br, 1 H), 5.43 (t, J_{HH} = 6.4 Hz, 2 H).

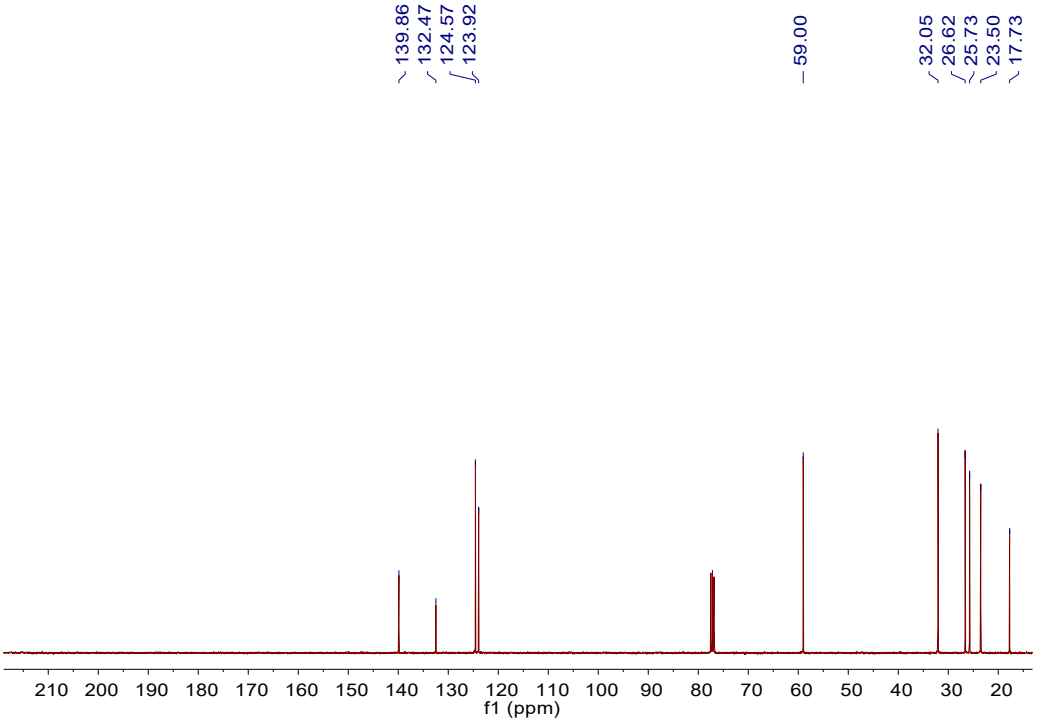

Fig. S71 ^{13}C{^{1}H} NMR spectrum of **15aa**. ^{13}C{^{1}H} NMR (100 MHz, $CDCl_3$, 298 k, ppm): δ = 17.73, 23.50, 25.73, 26.62, 32.05, 59.00, 123.92, 124.57, 132.47, 139.86.

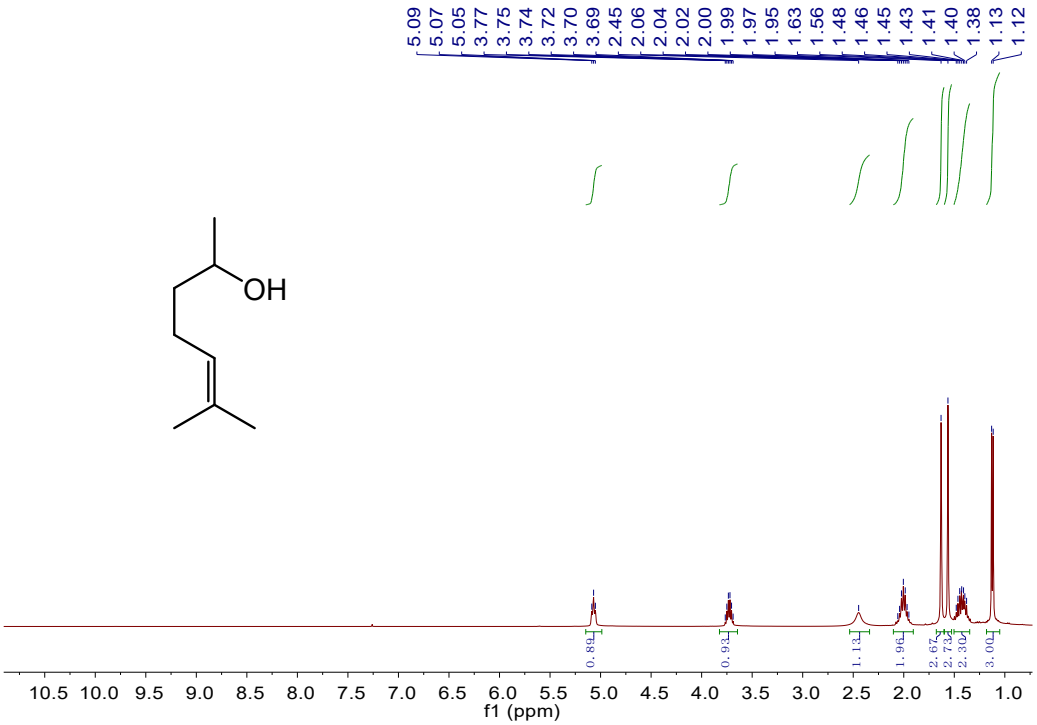

Fig. S72 ^{1}H NMR spectrum of **15ac**.[18] ^{1}H NMR (400 MHz, $CDCl_3$, 298 k, ppm): δ = 1.13 (d, J_{HH} = 6.4 Hz, 3 H), 1.38-1.48 (m, 2 H), 1.56 (s, 3 H), 1.63 (s, 3 H), 1.95-2.06 (m, 2 H), 2.45 (br, 1 H), 3.69-3.77 (m, 1 H), 5.07 (t, J_{HH} = 7.2 Hz, 1 H).

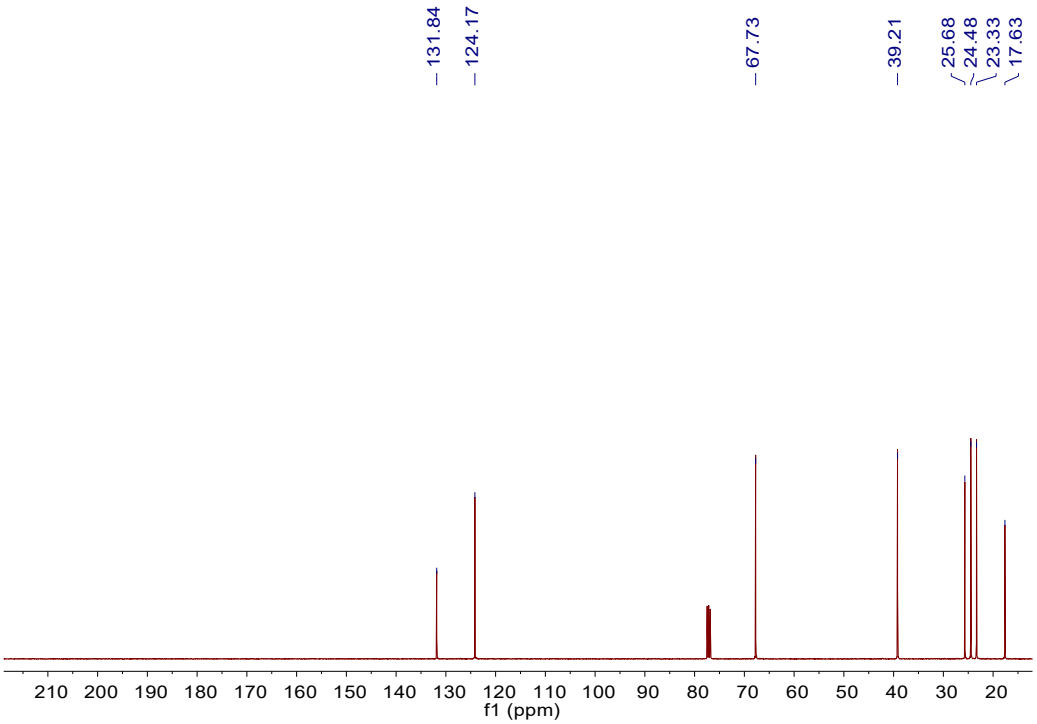

Fig. S73 ^{13}C{^{1}H} NMR spectrum of **15ac**. ^{13}C{^{1}H} NMR (100 MHz, $CDCl_3$, 298 k, ppm): δ = 17.63, 23.33, 24.48, 25.68, 39.21, 67.73, 124.17, 131.84.

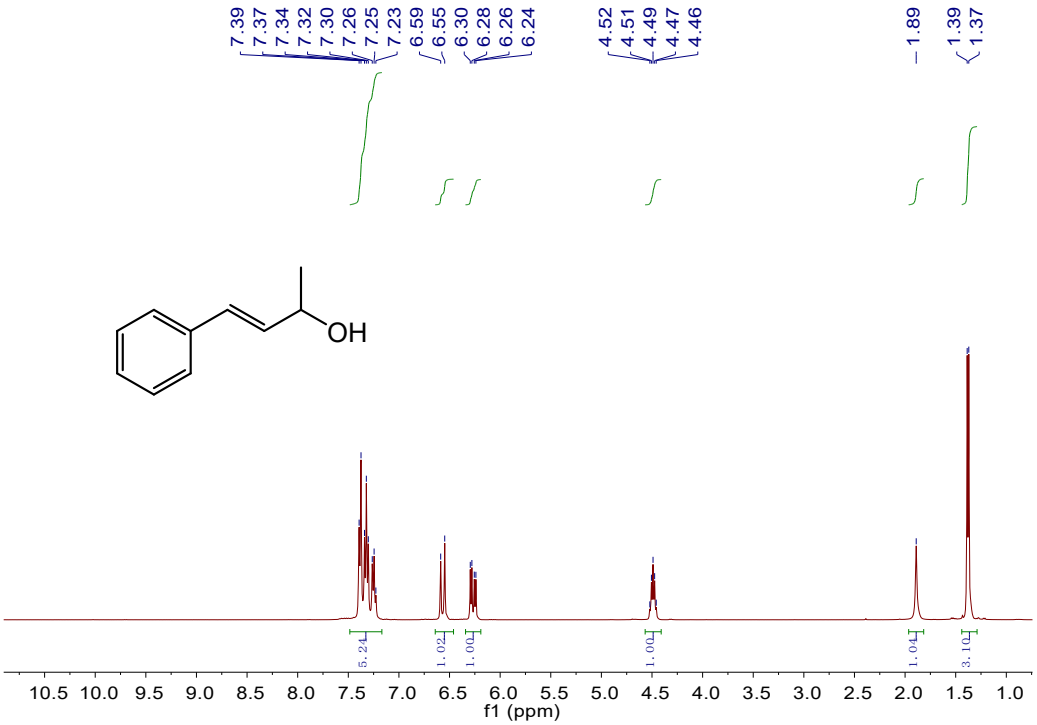

Fig. S74 ^{1}H NMR spectrum of **15ad**.[9] ^{1}H NMR (400 MHz, $CDCl_3$, 298 k, ppm): δ = 1.38 (d, J_{HH} = 6.4 Hz, 3 H), 1.89 (s, 1 H), 4.49 (m, 1 H), 6.27 (dd, J_{HH} = 6.4, 9.6 Hz, 1 H), 6.57 (d, J_{HH} = 15.6 Hz, 1 H), 7.23-7.39 (m, 5 H).

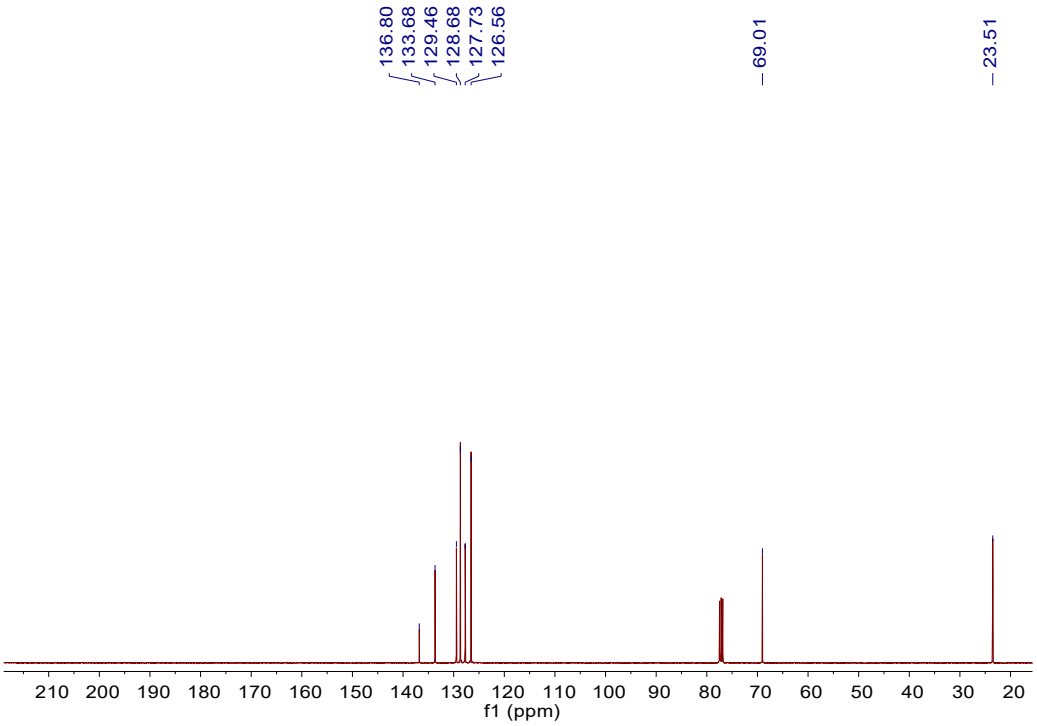

Fig. S75 $^{13}C\{^{1}H\}$ NMR spectrum of **15ad**. $^{13}C\{^{1}H\}$ NMR (100 MHz, $CDCl_3$, 298 k, ppm): δ = 23.51, 69.01, 126.56, 127.73, 128.68, 129.46, 133.68, 136.80.

VII. GC spectra

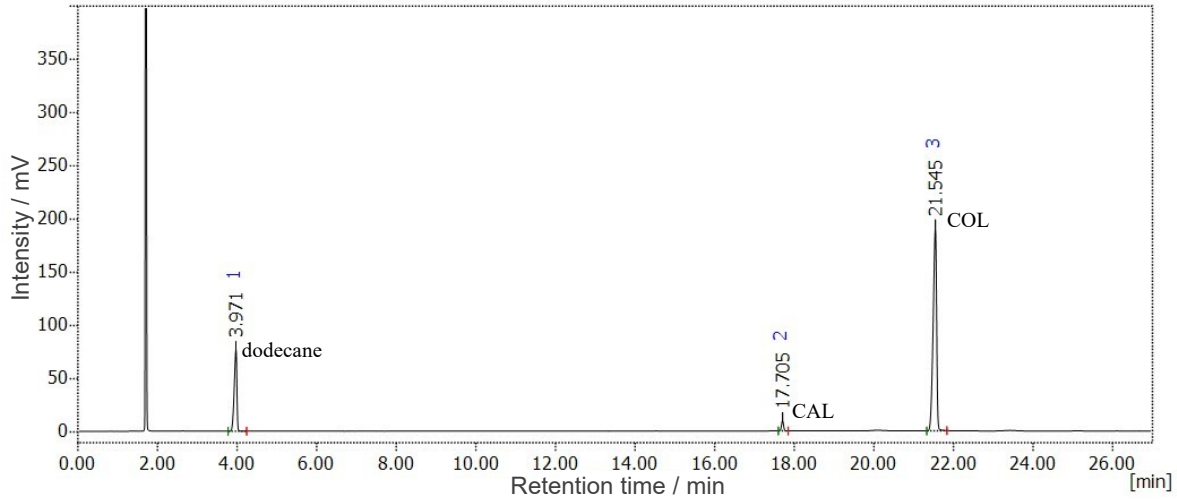

Fig. S76 GC analysis result for catalytic hydrogenation of cinnamaldehyde by **12** (Entry 1, Table 1).

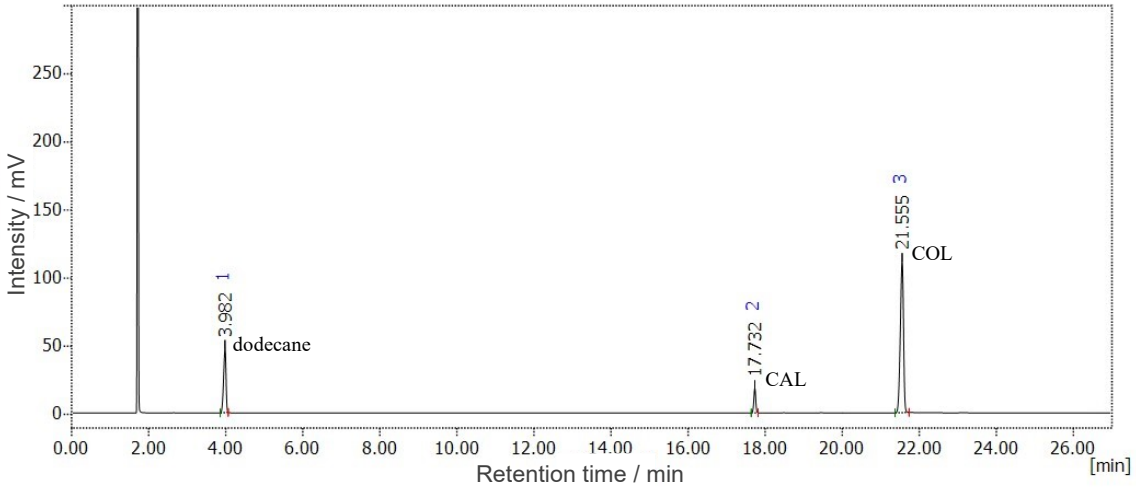

Fig. S77 GC analysis result for catalytic hydrogenation of cinnamaldehyde by **12** (Entry 5, Table 1).

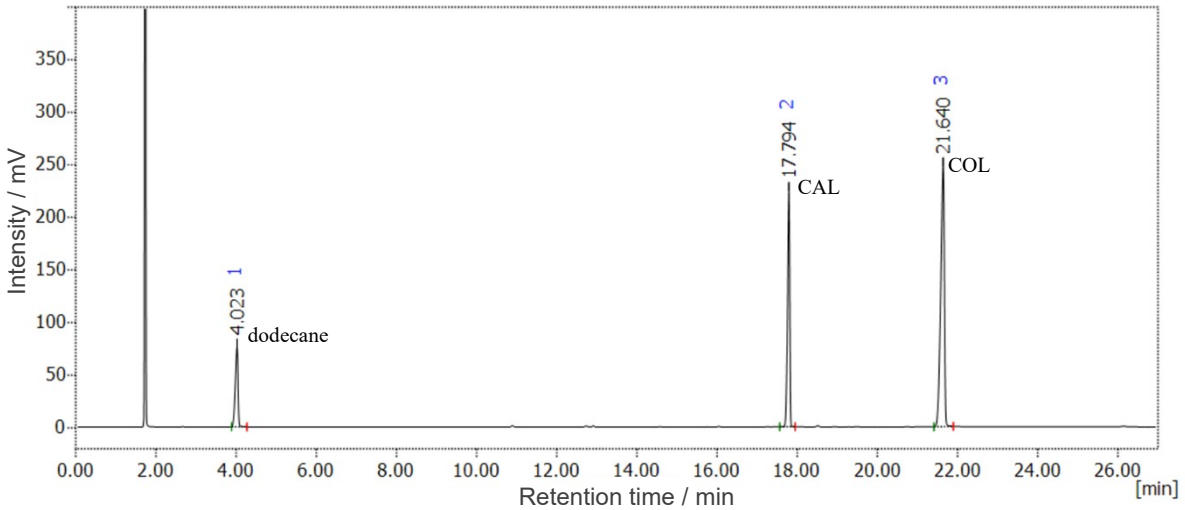

Fig. S78 GC analysis result for catalytic hydrogenation of cinnamaldehyde by **12** (Entry 6, Table 1).

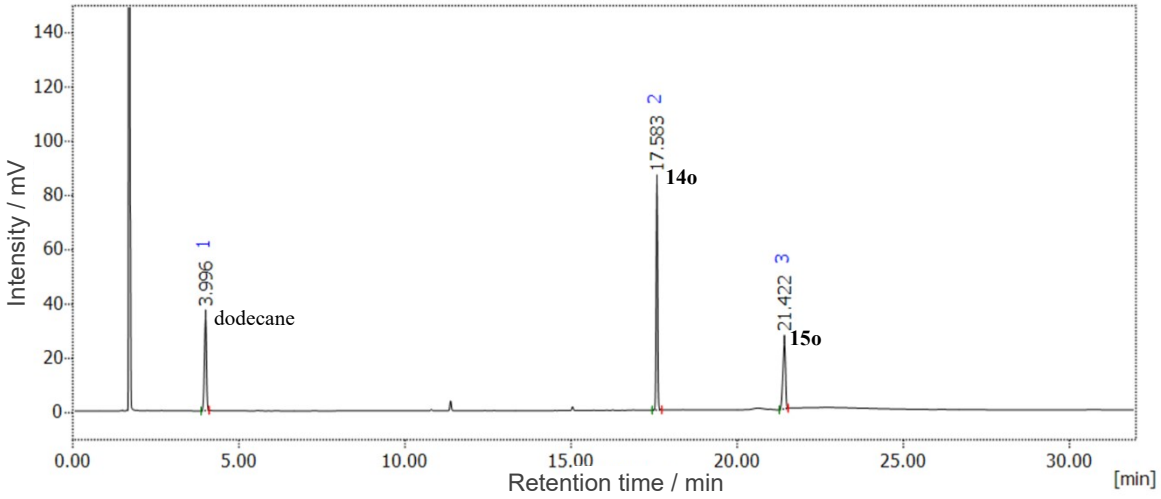

Fig. S79 GC analysis result for catalytic hydrogenation of **14o** by **12**.

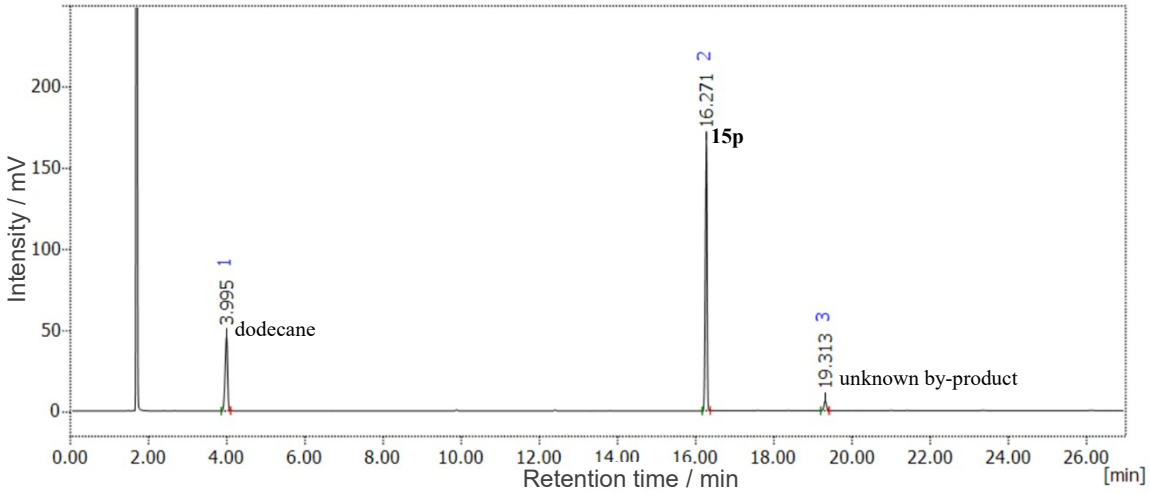

Fig. S80 GC analysis result for catalytic hydrogenation of **14p** by **12**.

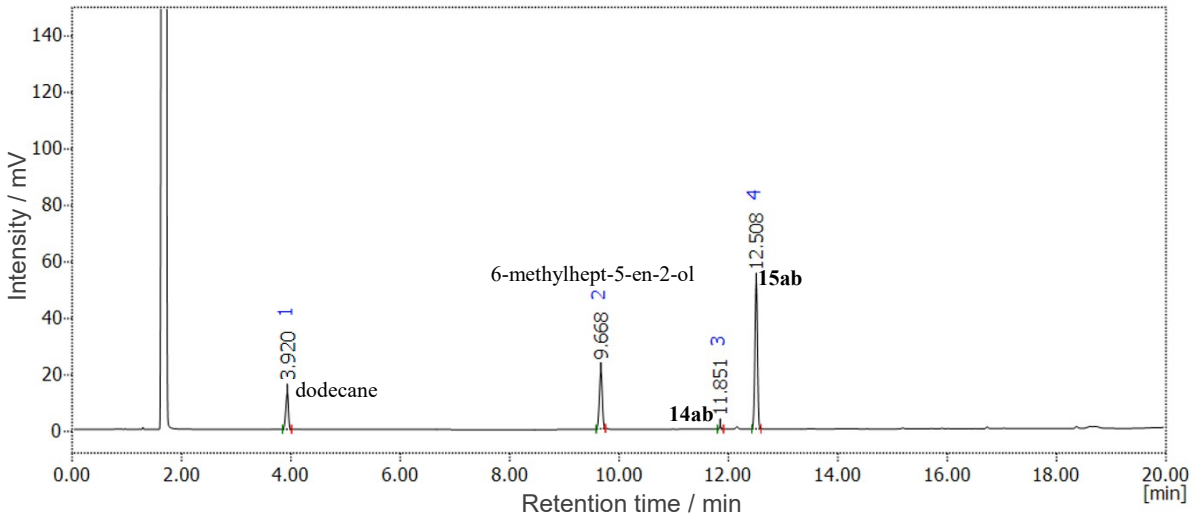

Fig. S81 GC analysis result for catalytic hydrogenation of **14ab** by **12**.

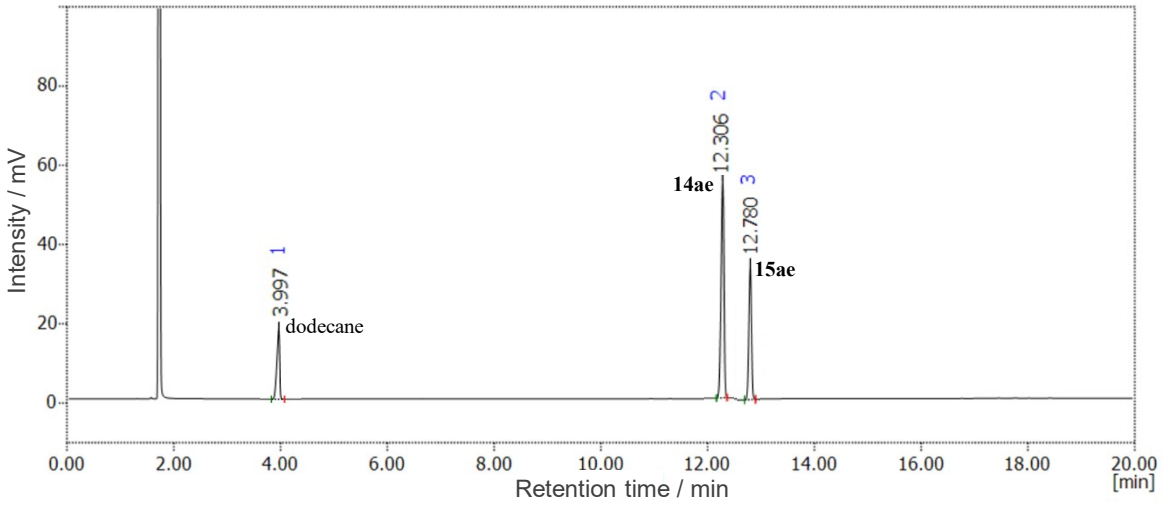

Fig. S82 GC analysis result for catalytic hydrogenation of **14ae** by **12**.

VIII. References

[1] H. Y. Wang and J. X. Gao, *Eur. J. Inorg. Chem.* 2005, ***2005***, 1665-1670.

[2] V. Richard, M. Ipouck, D. S. Merel, S. Gaillard, R. J. Whitby, B. Witulski and J. L. Renaud, *Chem. Commun.* 2014, ***50***, 593-595.

[3] I. P. Evans, A. Spencer and G. Wilkinson, *J. Chem. Soc., Dalton Trans.* 1973, ***2***, 204-209.

[4] D. C. Mudalige, S. J. Rettig, B. R. James and W. R. Cullen, *J. Chem. Soc. Chem. Commun.* 1993, ***10***, 830-832.

[5] G. M. Sheldrick, SHELXS-90, Program for structure solution. *Acta Crystallogr. Sect. A* 1990, ***46***, 467-473.

[6] G. M. Sheldrick, SHELXL-97, Program for crystal structure refinement. University of Göttingen: Göttingen, Germany, 1997.

[7] Y. Duan, Y. Zeng, Z. Cui, J Wen and X. Zhang, *J. Catal.* 2023, ***417***, 109-115.

[8] X. Wu, C. Corcoran, S. Yang and J. Xiao, *ChemSusChem* 2008, ***1***, 71-74.

[9] R. Wang, Y. Yue, J. Qi, S. Liu, A. Song, S. Zhuo and L. Xing, *J. Catal.* 2021, ***399***, 1-7.

[10] S. S. Gholap, A. A. Dakhil, P. Chakraborty, H. Li, I. Dutta, P. K. Das and K. Huang, *Chem. Comm.* 2021, ***57***, 11815-11818.

[11] A. J. Kumalaputri, G. Bottari, P. M. Erne, H. J. Heeres, and K. Barta, *ChemSusChem* 2014, ***7***, 2266-2275.

[12] P. Xu, B. Qian, Z. Qi, B. Gao, B. Hu and H. Huang, *Org. Biomol. Chem.* 2021, ***19***, 1274-1277.

[13] L. H. R. Passos, V. Martínez-Agramunt, D. G. Gusev, E. Peris and E. N. dos Santos, *ChemCatChem* 2023, ***15***, e202300394.

[14] M. Ueshima and Y. Shimasaki, *Chem. Lett.* 1992, ***7***, 1345–1348.

[15] T. Mizugaki, Y. Kanayama, K. Ebitani and K. Kaneda, *J. Org. Chem.* 1998, ***63***, 2378-2381.

[16] J. Song, Z. Xue, C. Xie, H. Wu, S. Liu, L. Zhang, and B. Han, *ChemCatChem* 2018, ***10***, 725-730.

[17] J. P. Gordon, An Asymmetric Hydrovinylation of 1,4-Substituted Linear 1,3-Dienes. The Ohio State University, American, 2018.

[18] S. G. Davies and G. Darren Smyth, J. *Chem. Soc., Perkin Trans. 1* 1996, ***20***, 2467-2477.